Université de Montréal

An RNAi Screen to Identify Factors that Control the Binding of Polycomb Group Proteins to the Chromatin Across the Cell Cycle

Par

HUANG SUNG Aurélie

Programmes de Biologie Moléculaire, Faculté de Médecine

Mémoire présenté en vue de l'obtention du grade de Maîtrise

en Biologie Moléculaire, option générale

Mars 2020

Résumé

L'établissement et le maintien du patron d'expression génique sont d'une importance critique pour l'identité cellulaire. Les protéines du groupe Polycomb (PcG) agissent sur la chromatine afin de maintenir la répression génique de ses gènes cibles à travers les cycles cellulaires de façon épigénétique. Toutefois, durant la mitose, la structure de la chromatine est grandement altérée par la répression de la transcription, la condensation de la chromatine et le relâchement de nombreux facteurs de transcription. Une question se pose alors : comment les protéines PcG peuvent-elles maintenir leur fonction à travers la mitose ? En interphase, les protéines PcG sont liées à leurs cibles sur la chromatine. Durant la mitose, la majorité des protéines PcG se libèrent de la chromatine mais une petite fraction persiste. Selon l'hypothèse du *mitotic bookmarking*, cette fraction agirait comme un ensemble de marqueurs guidant le recrutement des protéines PcG en fin de mitose pour maintenir le profil d'expression génique de la cellule. Cependant, nous ne savons pas comment ce recrutement à lieu, ni comment une fraction de protéines PcG est retenue à la chromatine. Afin de répondre à ces questions, un crible à ARN interférent a été établi pour identifier des facteurs contrôlant la liaison des protéines PcG à la chromatine à travers le cycle cellulaire. Quoiqu'une confirmation soit nécessaire, les facteurs spécifiques à l'interphase sont enrichis en protéines co-purifiant avec la protéine PcG testée et en hélicases alors que ceux spécifiques à la mitose sont enrichis en candidats liés aux protéines du groupe Trithorax (TrxG).

Mots-clés : Protéines Polycomb, Mitose, Chromatine, Chromosome, Épigénétique, Crible par ARN interférence, Drosophile.

Abstract

A critical part of cell identity is the establishment and maintenance of gene expression patterns. Polycomb group proteins (PcG) act on chromatin to maintain gene repression through cell cycles (epigenetically). However, during mitosis, chromatin structure is greatly altered by transcription repression, chromatin condensation, and the release of many transcription factors. A question then arises: how can PcG proteins maintain their function through mitosis? During interphase, PcG proteins are bound to their chromatin targets. During mitosis, most PcG proteins are released from chromatin, but a small fraction remains bound to chromatin. According to the mitotic bookmarking hypothesis, this fraction acts as a set of markers to guide the recruitment of PcG proteins at the end of mitosis to maintain the gene expression profile. However, we do not know how this recruitment takes place, nor do we know how a fraction of PcG proteins is retained on chromatin. To address these questions, an RNAi screen was established to identify factors that control the binding of PcG proteins to chromatin across the cell cycle. Although a confirmation is necessary, factors identified from interphase cells were enriched in proteins co-purifying with the tested PcG protein and in helicases while mitosis specific factors were enriched in Trithorax group (TrxG) protein related candidates.

Keywords: Polycomb Group proteins, Mitosis, Chromatin, Chromosomes, Epigenetic, RNAi screen, *Drosophila*.

Table of Content

List of Tables

List of Figures

Abbreviation

Adf1: Adh transcription Factor 1

Ago2: Argonaute 2

ANT-C: Antennapedia Complex

AP-MS: Affinity Purification-Mass Spectrometry

Asx: Additional Sex combs

BSA: Bovine Serum Albumin

BX-C: Bithorax Complex

cg: Combgap

ChIP: Chromatin Immunoprecipitation

crm: cramped

CUT&RUN: Cleavage Under Targets & Release Under Nuclease

Dcr-2: Dicer-2

ddH_2O: double-distilled water

DMSO: Dimethyl Sulfoxide

DNA: Deoxyribonucleic Acid

dNTP: deoxyribonucleotide Triphosphate

dRAF: dRing-Associated Factors

DRIP: DNA-RNA immunoprecipitation

Dsp1: Dorsal Switch Protein 1

dsRNA: Double-Stranded RNA

E(z): Enhancer of Zeste

Esc: Extra sex combs

esiRNA: endoribonuclease-prepared siRNA

fs(1)h: female sterile (1) homeotic

g/L: gram per liter

GAF: GAGA Factor

GO: Gene Ontology

grh: grainy head

H2AK118ub: Histone H2A with Ubiquitylation at Lysine 118

H3K20: Lysine 20 of Histone H3

H3K27me3: Histone H3 with trimethylation at Lysine 27

H3K36me3: Histone H3 with trimethylation at Lysine 36

H3K4me3: Histone H3 with trimethylation at Lysine 4

H3K9me2: Histone H3 with dimethylation at Lysine 9

H3S10p: Histone H3 with phosphorylation at Serine 10

HCS: High Content Screening

Hox: Homeotic

hr: hour

Jarid2: Jumonji, AT Rich interactive domain 2

KCl: Potassium Chloride

Kdm2: Lysine (K)-specific Demethylase 2

KH_2PO_4: Potassium Phosphate monobasic

$KHCO_3$: Potassium Bicarbonate

MAD: Median Absolute Deviation

MBT: Malignant Brain Tumor

MeOH: Methanol

mg/ml: milligram per milliliter

$MgCl_2$: Magnesium Chloride

min: minute

mM: millimolar

MNase: Micrococcal Nuclease

mxc: multi sex combs

Na_2HPO_4-7H2O: Sodium Phosphate dibasic Heptahydrate

NaCl: Sodium Chloride

ng/ml: nanogram per milliliter

ng: nanogram

nm: nanometer

^oC: degree Celsius

Ogt: O-glycosyltransferase

Pc: Polycomb

PcG: Polycomb Group

Pcl: Polycomblike

PCR: Polymerase Chain Reaction

PHD: Plant Homeodomain

Ph-d: Polyhomeotic Distal

Pho: Pleiohomeotic

Phol: Pleiohomeotic like

Ph-p: Polyhomeotic Proximal

PR-DUB: Polycomb Repressive Deubiquitinase

PRC1: Polycomb Repressive Complex 1

PRC2: Polycomb Repressive Complex 2

PRE: Polycomb Response Element

Psc: Posterior sex combs

psq: Pipsqueak

PTM: Post Translational Modification

QC: Quality Control

RISC: RNA-Induced Silencing Complex

RNA: Ribonucleic Acid

RNAi: RNA interference

rNTP: ribonucleotide Triphosphate

SAM: Sterile α Motif

Sce: Sex Combs Extra

Scm: Sex Combs on Midleg

SDS: Sodium Dodecyl Sulfate

sec: second

Sfmbt: Scm-related gene containing Four MBT domains

shRNA: short hairpin RNA

siRNA: small interfering RNA

SMC: Structural Maintenance of Chromosomes

Spps: Sp1-like factor for pairing-sensitive silencing

SSMD: Strictly Standardized Mean Difference

TAD: Topologically Associating Domains

z: zeste

µg: microgram

µl: microliter

µM: micromolar

Acknowledgements

I would like to thank my advisor, Dr. Nicole Francis, not only for giving me so many opportunities but also for helping me grow as a person.

I would like to thank the Francis lab members, past and present, for the formative experience.

I would also like to express my gratitude to Dr.Lécuyer for providing me with reagents, Juan-Carlos Padilla and Philippe Jolivet for their help with S2R+ cells as well as Xiaofeng Wang and Dominic Filion for their technical assistance.

Finally, I would like to acknowledge my friends and family for their unconditional support.

Foreword

Vincent Lapointe-Roberge, an undergraduate student under my supervision, carried out the Western blot experiments and analysis and helped in the making of figure 16 (p.122).

1. Chapter 1 – Introduction

1.1. Epigenetic Inheritance

During the development of a multi-cellular organism, a single stem cell gives rise to a variety of cell types or cell identities through a combination of proliferation and differentiation. These different cell types share common genetic information. This is because cellular identity relies on gene expression profile rather than genetic information (Barrero et al., 2010). Epigenetics provides a mechanism for development, cellular differentiation and by extension cellular identity (Francis, 2009). While Waddington first defined "epigenetics" as "the mechanism by which the genes of the genotype bring about phenotypic effects", the meaning of this word has since been the subject of many reconsiderations (Henikoff & Greally, 2016; Jablonka & Lamb, 2002; Probst et al., 2009; Waddington, 2012). In the present work, any heritable change that is stable in the absence of the event that initiated it and without alteration of the deoxyribonucleic acid (DNA) sequence will qualify as epigenetic (Francis, 2009; Probst et al., 2009; Ptashne, 2007).

Both the establishment of cellular identity, and the maintenance of cellular identity through cell divisions are essential to avoid dire consequences such as developmental defects or cancer (Bracken & Helin, 2009; Francis & Kingston, 2001; Sparmann & van Lohuizen, 2006; Thiagalingam, 2020). This implies that during mitosis, information beyond the genetic information must be transmitted from parent cell to progeny cells to ensure the maintenance of cellular identity. This phenomenon is referred to as epigenetic inheritance, with epigenetic memory referring to the transmitted information (Probst et al., 2009; Steffen & Ringrose, 2014). Heritable chromatin features have been proposed as candidates for epigenetic memory (Margueron & Reinberg, 2010).

1.2. Chromatin Organization in *Drosophila*

Chromatin is the combination of DNA and proteins forming the chromosomes within the nuclei of eukaryotic cells. The basic unit of chromatin is the nucleosome: an octamer of two copies of each four core histone proteins (H3, H4, H2A and H2B) wrapped by about 146 base pairs of DNA

(Clapier et al., 2008). Histone tails protruding out of the nucleosome can be post-translationally modified, mainly by phosphorylation, methylation, acetylation or ubiquitylation (Kouzarides, 2007; F. Wang & Higgins, 2013; Y. Zhao & Garcia, 2015). These modifications can influence nucleosomes' biophysical properties and can recruit proteins to specific sites on chromatin. Histone modifying enzymes and proteins that recognize specific modifications (also termed "marks") are often referred to as "writers" and "readers", reflecting the idea that histone modifications are believed to carry information (F. Wang & Higgins, 2013). Chromatin is organized at large scales into gene expression and chromosome behaviour regulatory units. In the *Drosophila* genome, this organization includes small loops in the 1-10 kilobase range, and larger domains at the level of 10s-100s of kilobases (Hou et al., 2012; Wei et al., 2005).

1.2.1. Chromatin Domain Classes

Chromatin domains can be identified structurally as genomic regions with increased physical interactions in three dimensions (referred to as "topologically associating domains", or "TADs"). They can also be identified as genomic regions with similar biochemical chromatin features (i.e. histone modifications and chromatin binding proteins). Remarkably, domains defined by the two methods show considerable overlap, so that structural domains can be subdivided into different functional classes. An initial domain classification based solely on biochemical features in *Drosophila* Kc cells described 5 classes of domains: red, yellow, black, green and blue chromatin (Filion et al., 2010). Subsequently, physical domains were mapped in *Drosophila* embryos, and assigned to one of four classes based on biochemical features (Sexton et al., 2012). These classes are: "Active"--enriched with active marks; "Null"-- no specific enrichment; "Heterochromatin"--enriched with HP1 and Su(var)3-9; "Polycomb"-- enriched with PcG proteins (Sexton et al., 2012).

"Active" domains, and red and yellow chromatin in the classification of Filion et al. (2010), are associated with high levels of histone acetylation, and histone H3 with trimethylation at lysine 4 and 36 (H3K4me3 and H3K36me3 respectively) (Filion et al., 2010; Sexton et al., 2012). Red and yellow chromatin are also both associated with high levels of RNA polymerase and low levels of histone H3 with dimethylation at lysine 9 (H3K9me2) and histone H3 with trimethylation at lysine 27 (H3K27me3). They are associated with proteins such as histone deacetylases, DF31, ASH2 and

MAX. However, red and yellow chromatin differ by the other proteins associated with them, the Gene Ontology (GO) terms associated with the genes in them, and their DNA replication timing (earlier for red than yellow chromatin) (Filion et al., 2010).

"Null" domains and black chromatin both displayed no specific enrichment of histone modifications or chromatin associated proteins, are larger than domains of other classes, and have a low transcriptional output. However, "Null" domains had similar gene density when compared to other domain classes of the same study whereas black chromatin was overall relatively gene poor in the other study (Filion et al., 2010; Sexton et al., 2012).

HP1 and Su(var)3-9 bound domains and green chromatin were associated with classical heterochromatin. These classes are enriched in H3K9me2 marks deposited by Su(var)3-9 (Filion et al., 2010; Sexton et al., 2012).

Both studies identified "Polycomb" domains as a distinct chromatin class. PcG protein bound chromatin domains in Sexton et al. (2012), largely correspond to blue chromatin in Filion et al (2010), as both are enriched in H3K27me3 marks (Filion et al., 2010; Sexton et al., 2012).

1.2.2. Chromatin Domain Boundaries

Chromatin domain boundaries are characterized by the binding of insulator proteins such as CP190, CTCF and Beaf-32. In some cases, they are flanked by transcriptionally active sites. Because chromatin domain boundaries overlap with only a fraction of insulator binding sites, it has been hypothesized that other insulator binding sites act as scaffold for border formation in different conditions (Sexton et al., 2012). In general, the number of insulator proteins bound at a site correlates with whether it is a functional chromatin border (Van Bortle et al., 2014).

1.3. Discovery of the PcG

PcG genes were discovered decades ago, when in 1940, a *Drosophila melanogaster* (fruit fly) with extra sex combs on each of its six legs was found. This phenotype was due to a recessive mutation of the *esc* gene (Slifer, 1942). Flies with a similar phenotype but carrying mutations in other genes were described in subsequent decades (Gehring, 1970; Kassis et al., 2017; P. H. Lewis, 1947; Renato Paro, 1990; Shearn et al., 1978).

One of these was *Polycomb* (*Pc*), discovered by Lewis (E. B. Lewis, 1978). At the embryonic, larval and adult stages, the *Drosophila* body is divided into segments along its anterior-posterior axis. The identities of such segments are specified by the combination of activation or repression of a special class genes that control the development of body structures: homeotic (Hox) genes. In *Drosophila*, Hox genes are subdivided in two gene complexes: the bithorax complex (BX-C) and the Antennapedia complex (ANT-C) (Kassis et al., 2017). In homozygous *Pc* mutant larvae, the thoracic and first seven abdominal segments were partially transformed toward a more posterior segment identity. This led Lewis to suggest a revolutionary theory for the function of the product of the *Pc* gene: that it represses all BX-C genes (E. B. Lewis, 1978).

Over the next years, as additional genes with similar phenotype were discovered, Jürgens proposed that genes for which zygotic mutations leads to a phenotype that resembled that of weak *Pc* mutants would be referred to as the "*Pc* group" (I. M. Duncan, 1982; Dura et al., 1985; Ingham, 1984; Jürgens, 1985).

1.4. Functional Characterization of PcG Proteins

PcG proteins act in the form of complexes (Kassis et al., 2017). Although PcG proteins are conserved across evolution, they are less diversified in *Drosophila* than in vertebrate species where most PcG proteins have multiple paralogs (Beh et al., 2012; Whitcomb et al., 2007). In *Drosophila*, PcG proteins are divided into two main complexes: Polycomb repressive complex 1 (PRC1) and Polycomb repressive complex 2 (PRC2) (Whitcomb et al., 2007). Other PcG complexes include Polycomb repressive deubiquitinase (PR-DUB), Pho Repressive Complex (PhoRC), and dRing-associated factors (dRAF) (Kassis et al., 2017; Klymenko et al., 2006; Lagarou et al., 2008; Scheuermann et al., 2010). There are also additional PcG proteins that are not part of core PcG complexes, or that associate with these complexes at substoichiometric ratios (Kassis et al., 2017) (Table 1, p.31; Figure 1, p.35).

Table 1. – *Drosophila* PcG Proteins.

(Interacting) Protein complex	Gene Symbol	Name
Core PRC1	*Pc*	Polycomb
Core PRC1	*ph-p*	polyhomeotic proximal
Core PRC1	*ph-d*	polyhomeotic distal
Core PRC1, dRAF	*Psc*	Posterior sex combs
Core PRC1, dRAF	*Sce/dRing*	Sex combs extra
Core PRC2	*E(z)*	Enhancer of zeste
Core PRC2	*Su(z)12*	Su(z)12
Core PRC2	*p55*	p55 subunit
Core PRC2	*esc*	extra sex combs
PR-DUB	*calypso*	calypso
PR-DUB	*Asx*	Additional sex combs
PhoRC	*pho*	pleiohomeotic
PhoRC	*phol*	pleiohomeotic like
PhoRC	*Sfmbt*	Scm-related gene containing four mbt domains
dRAF	*Kdm2*	Lysine (K)-specific demethylase 2
PRC2	*Jarid2*	Jumonji, AT rich interactive domain 2
PRC2	*jing*	jing
PRC2	*escl*	escl
PRC2	*Pcl*	Polycomblike
-	*crm*	cramped
-	*mxc*	multi sex combs
-	*Ogt*	super sex combs
PRC1, PRC2, PhoRC	*Scm*	Sex comb on midleg

1.4.1. PRC1

Drosophila PRC1 is composed of four core proteins, namely Polycomb (Pc); polyhomeotic distal or proximal (Ph-d, Ph-p); Posterior sex combs (Psc) and Sex combs extra (Sce) (Shao et al., 1999). PRC1 inhibits transcription and chromatin remodeling, compacts the chromatin and ubiquitylates chromatin. One of its components, Pc, contains a 37 amino acid long chromo domain responsible for its binding, and thereby PRC1 binding, to H3K27me3 (Cao et al., 2002; R. Paro & Hogness, 1991). This domain is also sufficient to target Pc to PcG-regulated genes (Kassis et al., 2017). Ph-p and Ph-d are nearly identical proteins encoded by adjacent genes and containing a sterile α-motif (SAM) protein-protein interaction domain (Kassis et al., 2017). Ph-p and Ph-d SAM can self-associate as a helical polymer *in vitro* and is required for clustering PRC1 complexes (Kim et al., 2002; Wani et al., 2016). Ph SAM can also polymerize with the SAM of another PcG protein called Sex comb on midleg (Scm) (Kim et al., 2005). Psc, on the other hand, is responsible for the chromatin compaction and the inhibition of chromatin remodeling and transcription functions of PRC1 via its C-terminal region. Its homology region, which includes a ring finger and a helix-turn-helix motif, is involved in Psc incorporation into PRC1 (Kassis et al., 2017). The last component of PRC1, Sce, contains a ring finger domain involved in the ubiquitylation of histone H2A at lysine 118 (H2AK118ub) (Gutiérrez et al., 2012; Kassis et al., 2017; Schuettengruber et al., 2017) (Table 1, p.31; Figure 1, p.35). In mammalian cells, PRC1 is considered to come in two main classes: canonical and non-canonical. Canonical PRC1s contain homologues of the four core PRC1 proteins mentioned above. Non-canonical PRC1s lacks Pc (Cbx) and Ph (PHC) homologues (Schuettengruber et al., 2017). Within these classes, there are multiple isoforms defined by which of several Cbx and/or Pcgf subunits is present, and other accessory proteins (Schuettengruber et al., 2017).

1.4.2. dRAF

dRAF is analogous to non-canonical PRC1 in mammalian cells (Schuettengruber et al., 2017). It contains Lysine (K)-specific demethylase 2 (Kdm2) as well as Psc and Sce, but lacks Pc or Ph (Lagarou et al., 2008). Kdm2 demethylates H3K36me2 (Kassis et al., 2017) (Table 1, p.31; Figure 1, p.35).

1.4.3. PRC2

Drosophila PRC2 core is made up of Enhancer of zeste (E(z)), Su(z)12, p55 and extra sex combs (Esc) (Müller et al., 2002; Ng et al., 2000; Tie et al., 2001). The SET domain of E(z) is responsible for the main activity of PRC2, which is the methylation of H3K27. The VEFS domain of Su(z)12 is known to reinforce E(z) histone methyltransferase activity. p55 is a WD-repeat protein, whose role in PRC2 is currently unclear (Kassis et al., 2017). Finally, Esc is also a WD-repeat protein, which can bind E(Z), H3K27me3 and the histone core (Kassis et al., 2017) (Table 1, p.31; Figure 1, p.35).

1.4.4. PR-DUB

PR-DUB consists of Calypso and Additional sex combs (Asx). Calypso is the catalytic subunit containing a ubiquitin C-terminal hydrolases domain which deubiquitinates H2AK118ub. Asx reinforces calypso's activity (Kassis et al., 2017) (Table 1, p.31; Figure 1, p.35).

1.4.5. PhoRC

PhoRC contains pleiohomeotic (Pho) or pleiohomeotic like (Phol) and Scm-related gene containing four mbt domains (Sfmbt) (Klymenko et al., 2006; Scheuermann et al., 2010) (Table 1, p.31). Both Pho and Phol contain four zinc fingers allowing a specific DNA-binding activity and a "spacer" domain which binds to the malignant brain tumor (MBT) repeats of Sfmbt (Brown et al., 2003; Kassis et al., 2017). Sfmbt contains four MBT domains and a SAM. The MBT domains of Sfmbt can bind mono- or di-methylated H3K9 or H3K20 (lysine 20 of histone H3) (Klymenko et al., 2006). Like Ph SAM, Sfmbt SAM can bind the Scm-SAM (Figure 1, p.35). Unlike the other PcG complexes, PhoRC has not been clearly identified outside of *Drosophila* (Frey et al., 2016).

1.4.6. Other PcG Proteins

Other members of the PcG have been identified either genetically, or biochemically in other species. These include Jumonji, AT rich interactive domain 2 (Jarid2); Jing; Escl; Polycomblike (Pcl); cramped (Crm); multi sex combs (Mxc); O-glycosyltransferase (Ogt) and Scm (Kassis et al., 2017). Jarid2 and jing are homologs of PcG proteins in mammalian PRC2, however, their role in *Drosophila* is unclear (Kassis et al., 2017). Escl is a functional homolog of Esc and can replace it in PRC2 (L. Wang et al., 2006). Pcl contains two plant homeodomain (PHD) domains mediating its

association with PRC2 via binding to E(z) (O'Connell et al., 2001). Pcl also contains a tudor domain, however, unlike other tudor domain, it does not recognize methylated lysine or arginine (Friberg et al., 2010). Although some studies suggest a developmental stage specific role for Pcl, its role is currently not fully understood (Kassis et al., 2017; Nekrasov et al., 2007; Savla et al., 2008). Mxc and Crm both have unknown functions. Ogt is the O-linked glycosyltransferase in *Drosophila*. It glycosylates Ph at a serine/threonine region, which seems to explain its PcG phenotype, although it also has other substrates (Kassis et al., 2017). Finally Scm contains two MBT repeats, a SAM and two zinc fingers (Bornemann et al., 1996). Scm is a substoichiometric component of PRC1 (Saurin et al., 2001; Shao et al., 1999). It also interacts weakly with PRC2 (H. Kang et al., 2015) (Table 1, p.31; Figure 1, p.35).

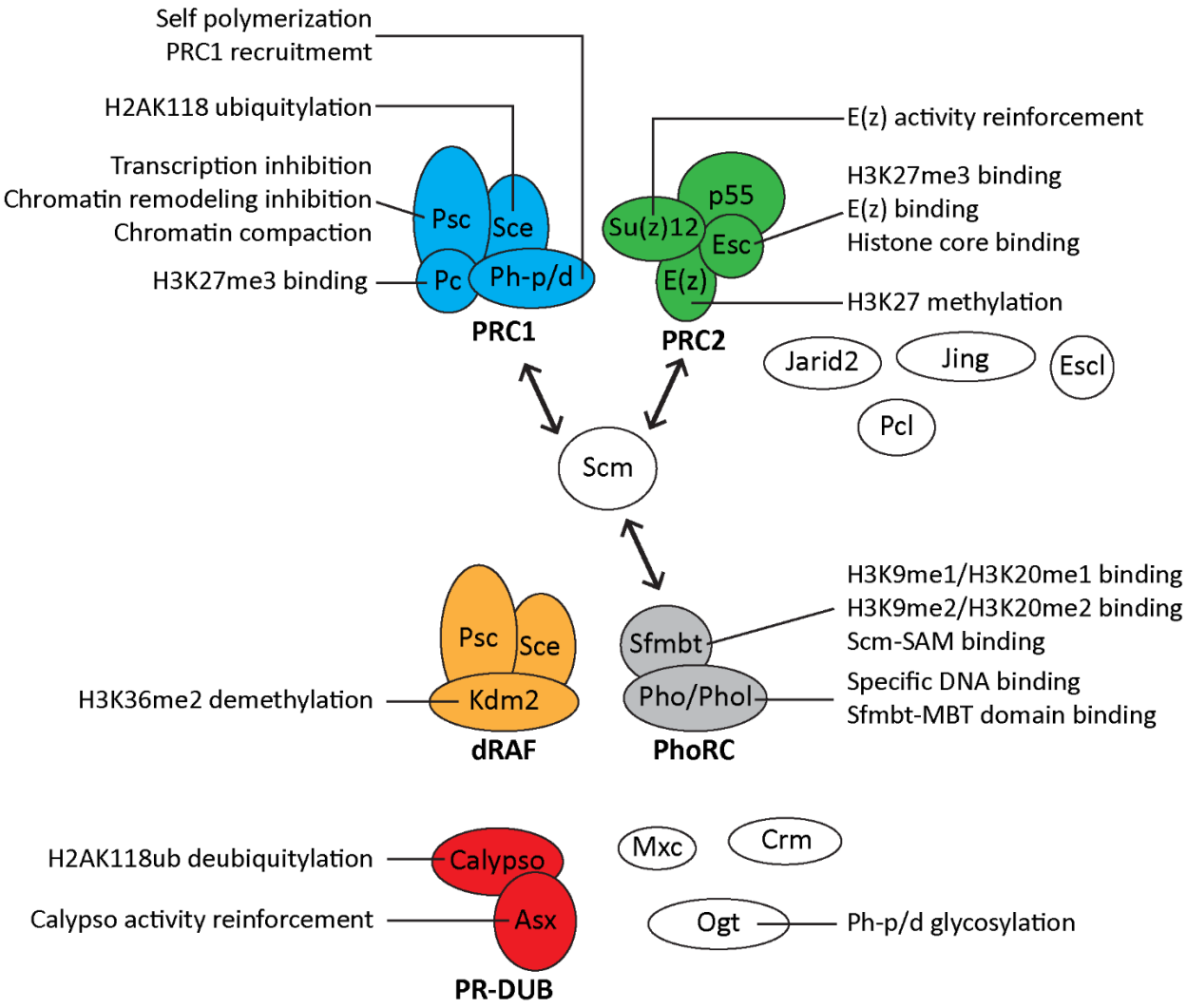

Figure 1. – ***Drosophila*** **PcG Complexes and Proteins.**

1.4.7. PcG Proteins Convey Epigenetic Memory of Gene Silencing

PcG proteins have various functions. Over the course of *Drosophila* embryogenesis, products of the maternal *gap* and *pair-rule* genes are responsible for the establishment of Hox gene expression pattern. Although these genes are only transiently expressed, the Hox gene expression pattern is fixed for the life of the fly. PcG proteins were discovered to provide the long term memory of Hox gene repressive state (Maeda & Karch, 2006). PcG protein action is mediated by epigenetic changes to chromatin including modification of histones (Kassis et al., 2017; Ringrose & Paro, 2004). Although PcG protein were initially discovered as regulators of Hox genes, studies revealed that PcG proteins are implicated in other cellular processes such as cell cycle control (Martinez & Cavalli, 2006). In addition to their role in the regulation of Hox genes, PcG proteins also target non-Hox genes, as illustrated by chromatin immunoprecipitation (ChIP) experiments which indicate that there are hundreds to thousands of PcG protein binding sites in *Drosophila* (Kassis et al., 2017; Steffen & Ringrose, 2014).

1.5. PcG Protein Recruitment

How PcG proteins are recruited to specific genes is currently poorly understood. The only PcG protein with defined sequence-specific DNA binding activity is Pho/Phol (Kassis et al., 2017). An initial model for PcG protein targeting was that Pho binds to specific sites (using the DNA sequence recognition activity of Pho) and recruits PRC2 to the chromatin by interacting with E(z) and esc. PRC2 then deposits H3K27me3 marks, which finally recruits PRC1 (L. Wang et al., 2004). This model did not withstand global tests: Pho binding sites alone are not sufficient for PcG protein recruitment and it was suggested that other DNA-binding proteins might facilitate Pho binding to DNA (Kassis et al., 2017; Kassis & Brown, 2013). It is currently thought that there are multiple recruitment mechanisms for both PRC1 and PRC2. These include interactions with transcription factors, interactions among PcG complexes, recognition of histone modifications, and likely additional mechanisms including those involving RNA (Alecki et al., 2020; Kassis et al., 2017).

1.5.1. Polycomb Response Elements

In *Drosophila*, at Hox gene complexes and other genes outside of Hox gene loci, PcG proteins bind to cis-regulatory DNA elements called Polycomb Response Elements (PREs) (Steffen & Ringrose, 2014). PREs are defined as DNA sequences which can recruit PcG proteins and mediate the repression of linked genes in transgenic studies (Delest et al., 2012). Each gene can be repressed by one or more PREs and their activity relies on the genomic context. Tens of kilobases can separate PREs and the promoter they regulate (Kassis & Brown, 2013). The mechanisms of PcG protein recruitment is currently not fully understood. However, since PREs contain binding site for a large number of DNA-binding proteins, it is believed that these proteins help recruit PcG proteins through physical interactions (Kassis et al., 2017). DNA binding proteins that bind at PREs include pho, GAGA factor (GAF), pipsqueak (psq), Sp1-like factor for pairing-sensitive silencing (Spps), combgap (cg), Dorsal switch protein 1 (Dsp1), grainy head (grh), Adh transcription factor 1 (Adf1), zeste (z) and female sterile (1) homeotic (fs(1)h) (Kassis et al., 2017).

PREs work with enhancers to maintain gene expression pattern in that the transcriptional status initially determined by transcription factors' action at enhancers can be maintained by PREs for several cell divisions and in the absence of the initial transcription factors. Thus, PREs mediate epigenetic memory of transcriptional states (Bauer et al., 2016).

1.5.2. SAM Scaffold

One pathway that may contribute to PcG recruitment can be termed a "SAM scaffold". Three PcG proteins, Sfmbt (part of PhoRC), Scm (can associate with PRC1), and Ph (part of PRC1) contain SAMs. The SAM of Sfmbt can bind to the Scm-SAM, which can interact with the Ph-SAM. This may form a recruitment pathway from PhoRC to PRC1 through Scm (Frey et al., 2016). This pathway may act together with the DNA binding activity of Pho, as well as with other PRE DNA-binding proteins that bind PRC1 (Kassis et al., 2017; Kassis & Brown, 2013).

1.5.3. PcG Recruitment by R-loops

Another mechanism of PcG protein recruitment may involve R-loops. A recent paper showed that a fraction of PREs form R-loops in *Drosophila* embryos and tissue culture cells. R-loops are three-

stranded nucleic acid structures that form when an RNA displaces a DNA strand by hybridizing with the complementary DNA. The authors also showed that PRC2 can induce the formation of RNA-DNA hybrids and that both PRC1 and PRC2 can recognize R-loops (or open DNA bubbles) *in vitro* (Alecki et al., 2020). A study in mammalian cells also identified R-loops at some PcG protein binding sites and implicated them in the targeting of PRC1 (Skourti-Stathaki et al., 2019).

1.5.4. Histone Modifications Further Stabilize PcG Protein Recruitment

Because H3K27me3 placed by PRC2 can be specifically recognized by PRC1, H3K27me3 was though to be essential for the recruitment of PRC1. However, explicit tests of this model indicate that PRC1 is still recruited to PREs in the absence of H3K27me3. Nevertheless, the level of PRC1 binding is lower in the absence of H3K27me3, suggesting this modification, which surrounds PREs, stabilizes PcG protein binding (Kahn et al., 2016).

1.6. Trithorax Group Proteins Counteract PcG Proteins

Trithorax Group genes were initially identified as genes that suppress the PcG phenotype. Mutation of TrxG genes causes embryonic segments to transform into more anterior ones by antagonizing PcG genes (Kassis et al., 2017; Schuettengruber et al., 2017). TrxG proteins include ATP-dependent chromatin remodeling factors, members of the Mediator complex, members of the cohesin complex, chromatin binding proteins, and histone modifying enzymes. TrxG proteins constitute another group of epigenetic interactors that can counteract PcG proteins action, in part through modification of chromatin (Steffen & Ringrose, 2014).

Histone modifications catalyzed by TrxG proteins can antagonize those catalyzed by PcG proteins. For example, H3K4 and H3K36 methylation catalyzed by TrxG proteins inhibit H3K27 trimethylation by PRC2. Further, acetylation of H3K27 by a TrxG protein, and its trimethylation by PRC2 are mutually exclusive (Steffen & Ringrose, 2014). Antagonism between PcG and TrxG protein is also illustrated by their opposing action on chromatin: PRC1 promotes chromatin compaction while H3K27ac, facilitated by TrxG proteins, promotes open chromatin (Steffen & Ringrose, 2014).

TrxG proteins are also recruited to PREs and thus share common binding sites with PcG proteins in polytene chromosome staining and ChIP studies. Even less is understood about how TrxG proteins are recruited to PREs than how PcG proteins are (Kassis et al., 2017). Nevertheless, several PREs have been shown to be switchable elements capable of maintaining both silenced and activated states, through the respective actions of PcG or TrxG proteins. The activities of TrxG and PcG proteins are balanced to maintain gene expression states (Ringrose & Paro, 2004). It is important to note that regulation of transcription of PcG and TrxG targets goes beyond a binary, "on" and "off", state: transcriptional output might range from a decreased or increased to complete silencing or activation (Delest et al., 2012; Ringrose & Paro, 2004).

1.7. PcG Protein Removal from Chromatin

PcG proteins are removed from chromatin in 2 cases: during development when genes switch from "off" to "on" and each time cells go through mitosis.

1.7.1. PcG Proteins Can be Removed from Chromatin During Development

In the context of spermatocyte differentiation, transcription factors can displace PcG Proteins. Indeed, testis-specific homologs of TATA-binding protein-associated factors allow the transcription of terminal differentiation genes partly by displacing PcG proteins from their promoters (X. Chen et al., 2005, 2011).

An excessive dose of an activator can also overcome PcG Silencing. A study was carried on a transgenic *Drosophila* line carrying a heat-shock inducible GAL4 driver regulating a lacZ reporter flanked by a PRE. Massive doses of GAL4 induced in embryos could disrupt PcG silencing of the reporter, and this effect persisted. However, disruption of PcG-mediated silencing was less effective after embryogenesis. This suggests that PcG-repressed chromatin is more plastic in embryos and progressively becomes more committed over the course of development, although the molecular basis of this effect is not known (Cavalli & Paro, 1998, 1999; Schwartz & Pirrotta, 2007).

Finally, cell signalling can also lead to PcG protein removal. Cluster of cells contained in imaginal discs of *Drosophila* are precursors of adult cuticular structures (Lee et al., 2005). When imaginal

disc cells are cultivated over a long period, and then implanted in larvae, corresponding structures are differentiated from the implanted cells: for example, leg disc cells lead to the formation of leg structures. In a phenomenon called "transdetermination", some disc cells can change their determined state (Klebes et al., 2005). In studies analyzing the transdetermination of cells upon ectopic overexpression of *wingless*, PcG gene expression was reduced in cells switching identity. This could alter the balance between TrxG and PcG protein mechanisms thereby favouring the resetting of epigenetic state (Klebes et al., 2005; Lee et al., 2005; Schwartz & Pirrotta, 2007).

1.7.2. PcG Proteins Can Be Removed During Mitosis

Mitosis is defined as the process by which duplicated chromosomes are equally segregated to daughter cells (Boettcher & Barral, 2013). Several events of mitosis alter the binding of chromatin proteins, including PcG proteins.

1.7.2.1. Nuclear Envelope During Mitosis

In eukaryotic organisms like *Drosophila*, chromosomes are surrounded by a double membrane: the nuclear envelope. It can adopt three types of morphology during mitosis: it can remain intact (closed mitosis), completely disassembled (opened mitosis) or fenestrated (semi-opened mitosis). Semi-opened mitosis occurs in *Drosophila* early embryonic and neuroblast divisions, in Kc cells and in S2R+ cells. This means that during early stages of mitosis, remnants of the nuclear envelope are still visible (Boettcher & Barral, 2013; Debec & Marcaillou, 1997; Maiato et al., 2006, 2006). Because the nuclear envelope breaks down during mitosis, nuclear proteins may access the whole cell volume, and thereby be diluted (Fonseca et al., 2012; Steffen & Ringrose, 2014). This dilution may shift binding equilibria to the unbound state, and thereby contribute to decreased chromatin binding in mitosis. Dilution might be limited in semi-opened mitosis.

1.7.2.2. Chromatin During Mitosis

Some attributes of the chromatin can also alter the binding of chromatin proteins. During mitosis, transcription is silenced. This was demonstrated by experiments showing that mitotic cells failed to incorporate radioactive NTPs (Johnson & Holland, 1965; Prescott & Bender, 1962). Large-scale changes also occur at the higher order chromatin structure, as chromatin compaction represents one of the main events in mitosis (Festuccia et al., 2017). Although chromatin

compaction was initially proposed as a cause of transcriptional silencing by decreased accessibility of mitotic chromosomes to the transcriptional machinery, this hypothesis was later refuted (Gottesfeld & Forbes, 1997; Johnson & Holland, 1965). Indeed, a subsequent study showed that mitotic chromatin remained accessible to both structural proteins and transcription factors (D. Chen et al., 2005).

Post translational modification (PTM) of proteins, however, is key to transcriptional silencing in mitosis and is another way to alter chromatin protein binding. Indeed, in a mechanism referred to as "phospho-methyl switching", phosphorylation of histone residues next to ones that can be methylated and read by chromatin proteins can lead to their displacement. Thus, phosphorylation of histone H3 at threonine 3 has been shown to cause the displacement of TFIID, a protein complex capable of reading H3K4me3 mark (Festuccia et al., 2017; Varier et al., 2010). Another example of phospho-methyl switching involved HP1. This protein recognizes H3K9me3 marks and has a greatly reduced binding activity upon phosphorylation of histone H3 at serine 10 (H3S10p) and binds poorly to histone tails containing both modifications (Fischle et al., 2005, p. 1; Hirota et al., 2005). Finally, H3S28 is phosphorylated in mitosis, and this can reduce binding of Pc to H3K27me3, and likely contributes to the release of PRC1 from chromatin in mitosis (Fonseca et al., 2012). Modification of non-histone chromatin proteins themselves can also alter their chromatin binding in mitosis and is implicated in silencing transcription in mitosis. One example is the inactivation of the ATP-dependent chromatin remodeling complex SWI/SNF by phosphorylation in mitosis (Sif et al., 1998). Phosphorylation of the transcription factors Ikaros and Sp1, disrupts their DNA binding activity in mitosis (Dovat et al., 2002).

After mitosis, transcription must restart, and the gene expression profile must be resumed for the sake of cellular identity maintenance. This implies that previously silenced genes in the parent cells must remain silenced in the daughter cell while previously expressed genes must be re-expressed upon mitotic exit. Transcriptional silencing and the alteration of both chromatin composition and structure described above thus reveal a potential problem: how can gene expression profiles be restored after mitosis?

1.7.2.3. Mitotic Bookmarking

Despite transcriptional repression, the release of many chromatin proteins occurring during mitosis, and the drastic reorganization of the nuclear content in general, not all traces of gene transcription or repression are erased from chromatin during mitosis (Kadauke & Blobel, 2013). Certain DNA binding proteins and transcription co-factors were found to persist on mitotic chromatin (Kadauke & Blobel, 2013). In fact, it has been suggested that the number of persistent transcription factors on mitotic chromosome may be underestimated. This is due in part to technical limitations such as a recently described formaldehyde-induced exclusion of some proteins from mitotic chromosomes (Teves et al., 2016). Other persistent traces of gene activity might stem from stable histone modifications and nucleosome architecture (Kadauke & Blobel, 2013). Together, these observations prompted a model referred to as the "mitotic bookmarking model", where it is believed that so called "bookmarking factors" help convey regulatory information to daughter cells by binding to specific regulatory elements during mitosis (Festuccia et al., 2017).

1.7.2.4. PcG Proteins in Mitosis

The behaviour of PcG proteins during mitosis remains poorly understood. Some studies have reported that PcG proteins such as Pc, Ph and Psc are detached from chromatin during mitosis (Beck et al., 2010; Buchenau et al., 1998). However, as previously mentioned, results from these experiments may be impacted by the use of formaldehyde to fix samples (Fanti et al., 2008; Teves et al., 2016).

Experiments on live samples or using different fixation conditions, which overcome this problem, have reported that PcG proteins can be retained on mitotic chromosomes (Fanti et al., 2008; Fonseca et al., 2012). The study on live samples showed that only a small fraction of GFP-PC and GFP-PH bound metaphase chromosomes (0.4-2%) compared to interphase chromosome (30-70% for GFP-PC and 10-20% for GFP-PH). Residence time of some PcG proteins was up to 300-fold longer compared to interphase cells, which led to the suggestion that PcG protein chromatin binding properties in metaphase are different from those of interphase (Fonseca et al., 2012).

Another study used immunofluorescence and subcellular fractionation to show that Psc and Ph remain on the chromatin during mitosis. ChIP experiments showed that the persistent binding sites of these proteins were specific and corresponded to a subset of interphase binding sites. Persistent sites often overlap borders between chromatin domains. The same study also showed that the histone mark H3K27me3 level were unchanged in mitosis. From there, persistent binding sites have been proposed to act as nucleation sites recruiting PcG proteins after mitosis while the H3K27me3 histone mark and possibly other persistent chromatin features at non specific binding sites may help the spreading and recruitment of PcG proteins into chromatin domain regions (Follmer et al., 2012) (Figure 2, p.44).

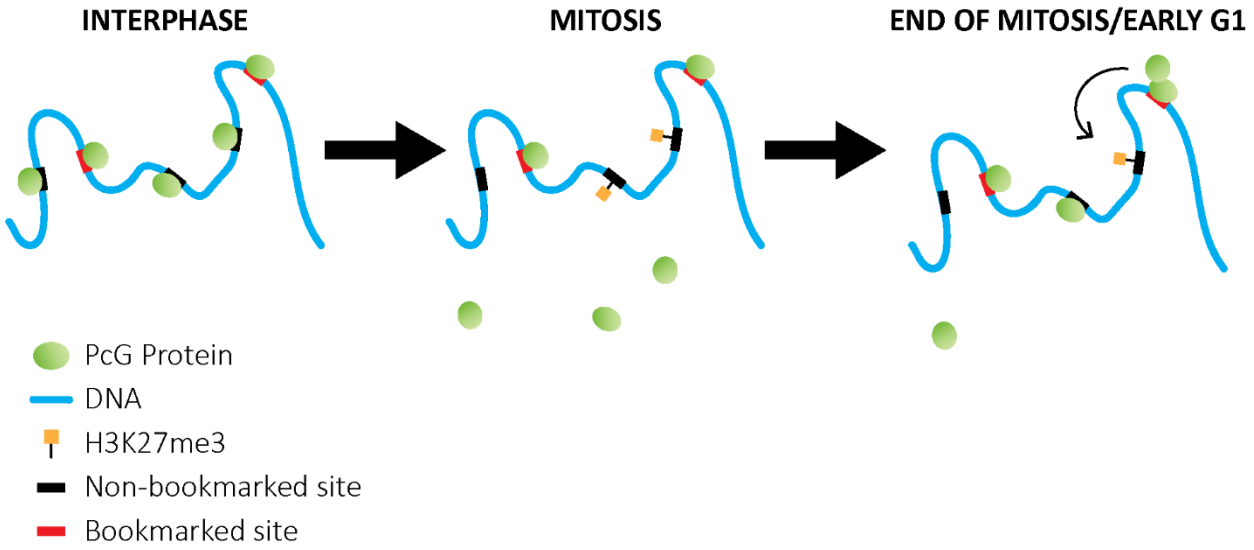

Figure 2. – Mitotic Bookmarking by PcG Proteins. PcG proteins bind their target sites during interphase, including those at chromatin domain borders. During mitosis, PcG proteins remain at some chromatin border but not at PREs and other well-known targets. H3K27m3 marks remain unchanged which prompts the hypothesis that persistent binding sites are nucleation sites that help recruit PcG proteins back onto the chromatin while H3K27me3 helps spread and recruit the proteins to the vacated interphase binding sites. Adapted from Follmer et al., 2012.

1.8. Summary

Mitosis is a short step of the cell cycle during which the chromatin structure is greatly altered by events like chromatin compaction, transcriptional repression and the release of many transcription factors. Despite these events, a cell can still maintain its gene expression profile and transmit it to daughter cells (Festuccia et al., 2017; Kadauke & Blobel, 2013). To understand how gene expression profiles may be maintained through mitosis, the present work focuses on the well conserved PcG proteins. PcG proteins act on chromatin to maintain gene repression through multiple cell divisions during development (Steffen & Ringrose, 2014). In the cell cycle context, these proteins are known to mainly bind their chromatin target during interphase, while during mitosis, only a small fraction of targets remain occupied. Because H3K27me3 marks also persist during mitosis, it has been hypothesized that these persistent PcG proteins binding sites act as nucleation sites while the H3K27me3 marks (and potentially other chromatin features) help in the spreading of PcG proteins to sites vacated in mitosis (Follmer et al., 2012). However, little is known about how the behaviour of PcG proteins is controlled in mitosis. Hence the purpose of this project: the identification of factors influencing the chromatin binding of PcG proteins across the cell cycle. To this end, a high throughput imaging-based RNA interference (RNAi) screen in *Drosophila* S2R+ cells was performed.

1.9. Proof of Concept

1.9.1. RNAi Screen

RNAi is the process by which small ribonucleic acids (RNAs), from either external or internal sources, reduce gene expression, usually by causing the degradation of complementary cellular messenger RNAs. In *Drosophila*, this pathway can be triggered by the recognition of an internally or externally supplied double-stranded RNA (dsRNA) by a ribonuclease III called Dicer-2 (Dcr-2). Dcr-2 cleaves the dsRNA into small fragments called small interfering RNAs (siRNAs). The siRNAs are then bound by proteins of the RNA-induced silencing complex (RISC) including Argonaute 2 (Ago2) which is required for siRNA unwinding. Guided by the small RNA, RISC can then cut target RNAs through the use of Ago2's piwi domain (Tomari & Zamore, 2005). In an RNAi screen, the

RNAi pathway is harnessed to decrease target gene expression by providing long dsRNAs, synthetic siRNAs, short hairpin RNAs (shRNAs) or endoribonuclease-prepared siRNAs (esiRNAs) (S. Mohr et al., 2010) (Figure 3, p.47). In the case of the present work, the impact of RNAi-induced gene repression on binding of the PcG protein Ph to chromatin was assessed by immunofluorescence.

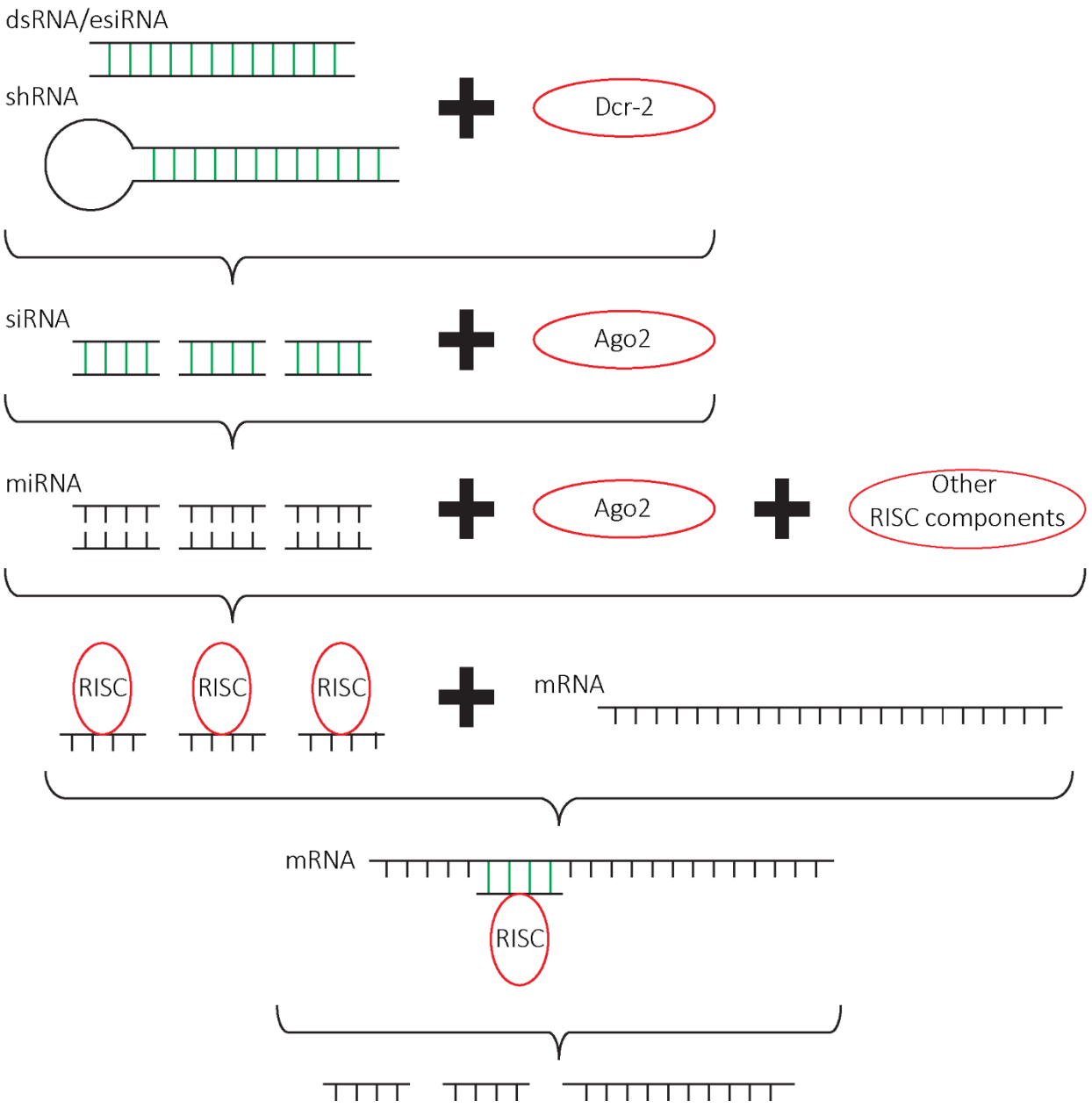

Figure 3. – **RNAi in *Drosophila*.** Externally supplied dsRNAs or esiRNAs are recognized by Dcr-2. Dcr-2 cleaves dsRNAs or esiRNAs into siRNAs which are then bound and unwound by Ago2. Other proteins bind Ago2 and the siRNA to form the RISC complex, which, guided by the siRNA, binds to complementary mRNA and induce their degradation.

RNAi screens in *Drosophila* cells have been used previously to identify genes that control events in mitosis, the binding of chromatin-associated proteins, and the formation of PcG bodies (Gonzalez et al., 2014; Somma et al., 2008; Swenson et al., 2016). As previously mentioned, PcG proteins are well conserved across species and the system is simpler in *Drosophila* than in mammals, thus justifying the use of this model for this study (Whitcomb et al., 2007). *Drosophila* cells are also good for RNAi screens as they can grow under ambient CO_2 levels and at room temperature (Echeverri & Perrimon, 2006). The S2R+ cell line, used for our experiments and many RNAi screens, takes up dsRNA without requiring transfection, and is adherent, which facilitates imaging based screens (Clemens et al., 2000; Echeverri & Perrimon, 2006; Ramadan et al., 2007; Rogers & Rogers, 2008; Yanagawa et al., 1998). Unlike S2 cells, PcG proteins are not commonly studied in S2R+ cells. Nevertheless, S2 and S2R+ cells are both derived from embryos near hatching (I. Schneider, 1972; Yanagawa et al., 1998). Besides, S2 cells were previously used to study PcG protein binding on chromatin and PcG proteins were shown to bind PREs in S2R+ cells (Follmer et al., 2012; Orsi et al., 2014).

1.9.2. RNAi Screen Analysis

Data analysis is an important aspect of RNAi screen. It can be subdivided into four steps: data triage, data normalization, quality control and hit identification. The increasing popularity of RNAi screens over the years has lead to the development of various analysis methods for each of the last three steps (Birmingham et al., 2009).

1.9.2.1. Data Triage

Data triage is the process of removing any unusable data based on specific criteria. It is initiated while the screen is in progress to ensure the proper progression of the screen (in other words: to ensure that usable data are being generated). Several potential issues should be evaluated. For instance, the experimenter should check for any position effects and unusual plate hit rates. An efficient way to do this is to use plate visualization methods, including heat maps, plate-well scatter plots (also known as plate-well series plots) and replicate correlation plots. Another way to ensure the production of usable data is the calculation of quality metrics (discussed below) (Birmingham et al., 2009; Douglas Zhang et al., 2006). In the case of an imaging screen such as

the present work, checking that the images acquired can be automatically processed, and confirming the validity of image processing should also be done at this stage.

1.9.2.2. Data Normalization

Following data triage, is data normalization: the process by which systematic errors are removed and comparison and combination of data from different plates is made possible. Two categories of normalization methods can be applied: per plate or per experiment. Unless there is a known per-plate bias, per plate normalization is usually performed. Another attribute to address at the normalization stage is the choice of sample to use as negative controls. Some methods use all samples as *de facto* negative controls, while others only use control samples as negative controls. When experimental samples are more numerous than controls (as is typically the case) or when no efficient negative control is available, using samples as *de facto* negative controls should provide more accurate measurements. However, this is only true when most samples are expected not to display any biological effect. Displaying samples randomly in the screening plates and using robust analyses should allow the use of samples as *de facto* negative controls, and was done in the present work (Birmingham et al., 2009; Malo et al., 2006).

Sample normalization methods include fraction or percent of control, fraction or percent of samples, z score, robust z score and B score. Similar to z score and robust z score, B score is the ratio of an adjusted value over a measure of variability while fraction or percent of control and fraction or percent of samples methods do not correct for sample variation. z score and percent of control methods can be sensitive to outliers since these are calculated based on sample mean and standard deviation, and control mean respectively. z score and B score can also be skewed if real hits are unevenly distributed on plates, a drawback that can be avoided by randomization of sample distribution across plates. Finally, B score is the only normalization method that adjusts for positional effects within plates. From the previous points, the use of either robust z-score or B score normalization methods were recommended (Birmingham et al., 2009; Brideau et al., 2003; Malo et al., 2006).

One study aimed at comparing different normalization methods: background subtraction, scaling, cellHTS2, interquartile range measurement, quantile normalization, background subtraction

followed by quantile normalization and scaling followed by quantile normalization. Out of the seven established normalization methods tested, only one has previously been used in RNAi screen (cellHTS2) and results suggest that no single method excelled (Wiles et al., 2008). In most cases, acceptable results are obtainable when reasonable choices are made and screeners should pick a normalization method that is suitable to their data and analysis capacities (Birmingham et al., 2009).

1.9.2.3. Quality Control

Quality control is based on the degree to which known negatives are negative and known positives are positive. When appropriate controls are selected, quality control defines the likely range of biological effects and helps to insure that biological effects will be detectable and interpretable (Birmingham et al., 2009). Various metrics for quality control have been developed. One set of popular quality metrics is the Z-factor and the Z'-factor, which are used in small-molecule screens, and can also be used for RNAi screens. Z-factor measures the separation between samples and negative controls while Z'-factor measures the separation between positive and negative controls. Thus, good Z'-factor values can be generated with strong positive controls but might not be representative of positive screen hits. Because small effects can be relevant in RNAi screens, and because signal-to-background ratio can be lower in RNAi screens than in small molecule screens, less stringent quality thresholds (for either Z-factor and Z'-factor) may be used (Birmingham et al., 2009). Another quality control metric was developed for RNAi screens to address moderate control limitations: strictly standardized mean difference (SSMD). SSMD also measures the magnitude of difference between two populations. However, with this metric, set threshold values depend on positive control strength. SSMD is more statistically rigorous, less conservative and has a clear probability interpretation (Birmingham et al., 2009; Zhang, 2007). SSMD was used for the present RNAi screen.

1.9.2.4. Hit Identification

Hit identification is the ultimate goal of RNAi screen. It is defined as "the process of deciding which sample values differ meaningfully from those of the negative controls". In some cases, an arbitrary number of top-scoring samples can be selected as hits. However, this does not permit

the limitation of false positive identification (Birmingham et al., 2009). In order to limit the likelihood of false positive identification, the screener can use various reagents to test the same candidate and select hits based on results from all reagents. Selecting hits based on various screening outputs also limit the identification of false positives (Birmingham et al., 2009). Another way to proceed would be to use one of the methods described below.

Some small molecule-derived techniques can be used for hit identification in RNAi screen. These include mean ± k standard deviation, median ± k median absolute deviation (MAD) and multiple t-tests methods (Birmingham et al., 2009; Chung et al., 2008). Other hit identification methods that can be used for RNAi screen include: SSMD for hit identification, quartile-based, redundant siRNA activity, rank product and Bayesian models methods (Birmingham et al., 2009; Douglas Zhang et al., 2006). The simplest methods in terms of calculations are small molecule-derived techniques and the quartile-based method. Among these, the mean ± k standard deviation can miss weak positives and is sensitive to outliers, since it uses mean and standard deviation values. The multiple t-tests method is also sensitive to outliers, in addition to requiring at least triplicates that are normally distributed. Meanwhile, the median ± k MAD and quartile-based methods can both identify weaker hits and are not sensitive to outliers since these are based on median or quartile values. The quartile-based method also offers the advantage of being robust to non-symmetrical data distributions (Birmingham et al., 2009; Chung et al., 2008; Douglas Zhang et al., 2006). For these reasons, median ± k MAD and quartile-based methods were used for the present RNAi screen.

Both methods are similar in principle: in any given sample value data distribution, any sample whose value locates at the extreme ends of the data distribution would qualify as a hit. The difference between both methods rely on the calculation of threshold values used to determine the extreme ends on the data distribution. With the median ± k MAD or MAD-based method, any sample whose value is superior to or equal to sample median + k MAD, or whose value is inferior to or equal to sample median - k MAD, with k being a constant, would qualify as a hit. The higher the k value is, the more stringent the analysis is. With the quartile-based method, the upper threshold corresponds to the value of the biggest sample value that is strictly inferior to Q3+2c(Q3-Q2) while the lower threshold is the smallest sample value that is strictly superior to

Q1-2c(Q2-Q1). Q stands for quartile and c is a constant. Similar to k in the MAD-based method: the higher the c value is, the more stringent the analysis is. A value of 0.9826 for c would correspond to a k value of 2, and a value of 1.7239 for c would correspond to a k value of 3 (Chung et al., 2008; Douglas Zhang et al., 2006).

2. Chapter 2 – Experimental Procedures

2.1. Overall Strategy

To identify genes that control levels of PcG proteins on chromatin, we performed an imaging-based RNAi screen in *Drosophila* cells. The overall strategy is depicted in figure 4 (p.54): 541 candidate genes were selected and dsRNAs were produced by *in vitro* transcription from polymerase chain reaction (PCR)-generated DNA templates made from RNAi template libraries (Open Biosystems), or from S2 cell genomic DNA. S2R+ cells were plated on 96 well imaging plates and treated with dsRNA targeting one gene. Negative (irrelevant dsRNA) and positive (dsRNA targeting Ph) controls were included on each plate. Prior to fixation, cells were treated with colchicine, which blocks cells in metaphase, to increase the number of mitotic cells (Follmer et al., 2012; Leung et al., 2015). Cells were fixed and processed for immunofluorescence with antibodies against the PcG protein Ph and α-tubulin (to label the cytoplasm). Hoechst was used to label the DNA. 24 pictures per well were acquired in each of the three channels (Ph, α-tubulin, Hoechst) using a high content screening (HCS) microscope (Molecular Devices). Images were processed with CellProfiler™ (Version 3.0.0) (Carpenter et al., 2006). The intensity of Ph staining in the nucleus (or on chromatin for mitotic cells) and cytoplasm was measured in each well. Screen hits (increased or decreased Ph binding to chromosomes) were identified from the processed data using MAD-based and quartile-based analysis methods (Birmingham et al., 2009; Chung et al., 2008; Douglas Zhang et al., 2006). For primary screen hits, quantitative Western blot analysis of dsRNA treated cells was used to determine if changes in Ph levels on chromatin reflect changes in total protein level.

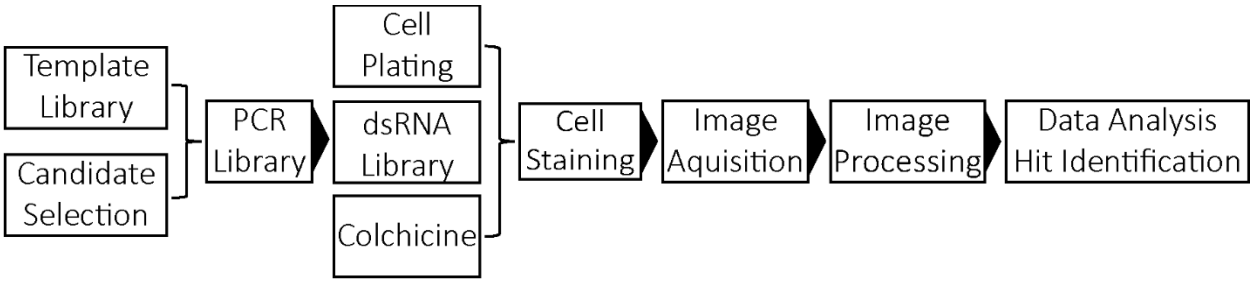

Figure 4. – Schematic Representation of Screening Workflow.

2.2. Candidate Gene Selection

An initial set of 1000 candidate genes that met at least one of the following criteria was generated from the literature and public databases:

- genes involved in chromosome morphology in mitosis (only newly identified genes that are implicated in chromosome integrity and mitosis) (Somma et al., 2008);
- kinases and phosphatases involved in cell cycle progression (Bettencourt-Dias et al., 2004; F. Chen et al., 2007);
- genes associated with GO terms (identified using QueryBuilder in Flybase) "mitotic cell cycle" (GO:0000278) and "chromatin binding" (GO:0003682), "histone modification" (GO:0016570), "DNA binding" (GO:0003677) or "chromatin remodeling" (GO:0006338) but not with "cytokinesis" (GO:0000910), "spindle assembly" (GO:0051225) or "spindle organization" (GO:0007051) (Ashburner et al., 2000; The Gene Ontology Consortium, 2019; Thurmond et al., 2019);
- PcG genes (FBgg0000309) (Thurmond et al., 2019);
- TrxG genes (FBgg0000303) (Thurmond et al., 2019);
- PcG and TrxG genetic and physical interactors (Thurmond et al., 2019);
- genes encoding proteins that co-purified with Ph in affinity purification-mass spectrometry experiments (AP-MS) performed in the lab (unpublished) (Jonathan Boulais, Ajaz Wani, Christine Munger);
- cherry-picked candidates

Cherry picked candidates included cyclin-dependent kinases, helicases, heat shock proteins, structural maintenance of chromosomes (SMC) genes, topoisomerases, ribonucleases (ribonuclease H1 and CG13690), genes related to SUMOylation or ubiquitylation, and genes coding for members of TFIID. Cyclin-dependent kinases were selected for their role in cell cycle regulation which might affect PcG protein binding to chromatin across the cell cycle (Roskoski, 2019). Helicases were selected because it has been suggested that they could switch the repressed state of R-loop containing PREs to the active state by resolving R-loop (Alecki et al., 2020). Heat shock proteins were selected for their role as chaperone, which might impact PcG

binding to chromatin either directly or indirectly (Wu et al., 2017). SMC genes and topoisomerases were selected for their effect on chromatin structure (Carter & Sjögren, 2012). Cherry-picked ribonucleases were selected for their DNA-RNA hybrid nuclease activity which could resolve R-loops at PRE and switch their state (Alecki et al., 2020; H. Zhao et al., 2018). PcG protein have previously been related to SUMOylation and some PcG proteins are known to have a role in ubiquitylation hence the inclusion of genes related to these processes (Gonzalez et al., 2014; X. Kang et al., 2010; Kassis et al., 2017). Finally, TFIID, a component of the preinitiation complex, is necessary for transcription and might impact PcG binding to chromatin, hence the addition of its members to the list of candidate genes (Antonova et al., 2019).

Since the screen was semi-automated, this primary list was refined through several rounds of filtering to obtain a manageable number of candidates. First, candidates that were not expressed in S2R+ cells were removed using a tool available at: https://www.flyrnai.org/cellexpress (Cherbas et al., 2011; Flockhart et al., 2012; S. E. Mohr et al., 2014). For the remaining of the refining process, genes present in the primary list based on a single criterion were removed. Genes related to cytokinesis, spindle assembly and spindle organization based on their associated GO term and/or results of an RNAi screen aimed at identifying genes required for spindle assembly were removed (Ashburner et al., 2000; Goshima et al., 2007; The Gene Ontology Consortium, 2019). Weakly expressed genes were also removed (Cherbas et al., 2011; Flockhart et al., 2012; S. E. Mohr et al., 2014). Genes that were selected only because of their association with the "histone modification" (GO:0016570) GO term were removed: as a biological process, those genes can be only remotely related to the term itself (Ashburner et al., 2000; The Gene Ontology Consortium, 2019). Genes involved in chromosome morphology in mitosis but also required for spindle assembly were removed (Somma et al., 2008). Kinases involved in cell cycle progression but for which knockdown leads to an abnormal cytokinetic index, centrosome defects and/or spindle defect with a phenotypic score outside the 95% confidence interval were removed (Bettencourt-Dias et al., 2004). Phosphatases with cell-cycle progression roles for which knockdown lead to either centrosome or spindle defects with a z-score of 3 or higher in a previous screen for genes that regulate mitosis were also removed (F.

Chen et al., 2007). Finally, genes that were not involved in either "gene expression" (GO:0010467) or "regulation of gene expression" (GO:0010468) were removed (Ashburner et al., 2000; The Gene Ontology Consortium, 2019). Weakly expressed or unexpressed candidates were removed since knocking them down should not have significant impact on PcG protein binding to chromatin. Genes related to cytokinesis, spindle organisation or assembly were removed as those are less likely to affect PcG protein binding to chromatin compared to other candidates. In total, 541 genes were selected as candidates for the RNAi screen (Table 2, p.58).

Table 2. – RNAi Screen Candidates. "Somma 2008"= newly identified genes involved in chromosome integrity and mitosis, "Bettencourt-Dias 2004"= kinases involved in cell cycle progression, "Chen 2007"= phosphatases involved in cell cycle progression, "PPI"=protein-protein interaction, "GI"=genetic interaction, "Mass Spec"= proteins which co-purified with Ph in an AP-MS experiment.

FlyBase ID	Annotation symbol	Gene symbol	Somma 2008	Bettencourt-Dias 2004	Chen 2007	Mitotic cell cycle and				PcG Protein	PcG PPI	PcG GI	TrxG Protein	TrxG PPI	TrxG GI	Cherry picks	Mass Spec
						Chromatin Binding	Histone modification	DNA binding	Chromatin remodeling								
FBgn0250848	CG8947	*26-29-p*															X
FBgn0052016	CG32016	*4E-T*															X
FBgn0027620	CG1966	*Acf*												X	X		
FBgn0000043	CG12051	*Act42A*											X	X	X		
FBgn0000042	CG4027	*Act5C*									X		X	X	X		
FBgn0263738	CG43663	*Ada2a*												X			
FBgn0037555	CG9638	*Ada2b*									X			X			
FBgn0030891	CG7098	*Ada3*												X			
FBgn0284249	CG15845	*Adf1*									X	X				X	
FBgn0087035	CG7439	*AGO2*															X
FBgn0082598	CG8580	*akirin*												X			
FBgn0012036	CG3752	*Aldh*															X
FBgn0029512	CG12276	*Aos1*														X	
FBgn0034231	CG11419	*APC10*	X													X	
FBgn0010348	CG8385	*Arf79F*															X
FBgn0000117	CG11579	*arm*													X		
FBgn0038576	CG7940	*Arp5*									X					X	
FBgn0030877	CG7846	*Arp8*									X					X	
FBgn0032329	CG16840	*Art8*												X			
FBgn0029094	CG9383	*asf1*												X	X		
FBgn0005386	CG8887	*ash1*										X		X	X		
FBgn0000139	CG6677	*ash2*											X	X	X		X
FBgn0261823	CG8787	*Asx*				X	X	X		X	X	X		X	X		X
FBgn0000147	CG3068	*aurA*		X								X					
FBgn0030093	CG7055	*Bap111*											X	X	X		
FBgn0042085	CG3274	*Bap170*											X	X	X		
FBgn0025716	CG6546	*Bap55*											X	X			
FBgn0025463	CG4303	*Bap60*											X	X	X		

FlyBase ID	Annotation symbol	Gene symbol	Somma 2008	Bettencourt-Dias 2004	Chen 2007	Mitotic cell cycle and				PcG Protein	PcG PPI	PcG GI	TrxG Protein	TrxG PPI	TrxG GI	Cherry picks	Mass Spec
						Chromatin Binding	Histone modification	DNA binding	Chromatin remodeling								
FBgn0014127	CG10726	*barr*				X					X						
FBgn0015602	CG10159	*BEAF-32*	X														
FBgn0263231	CG9748	*bel*														X	
FBgn0284243	CG9277	*betaTub56D*															X
FBgn0004581	CG30170	*bgcn*														X	
FBgn0026262	CG2009	*bip2*														X	X
FBgn0035608	CG10630	*blanks*															X
FBgn0011211	CG3612	*blw*															X
FBgn0283451	CG11491	*br*									X						
FBgn0033155	CG1845	*Br140*									X						X
FBgn0010300	CG10719	*brat*									X				X		
FBgn0000212	CG5942	*brm*					X		X			X	X	X	X		
FBgn0004101	CG3411	*bs*												X	X		
FBgn0263108	CG43365	*BtbVII*														X	X
FBgn0025457	CG7581	*Bub3*															X
FBgn0033526	CG12892	*Caf1-105*									X			X			X
FBgn0030054	CG12109	*Caf1-180*									X	X		X			X
FBgn0263979	CG4236	*Caf1-55*	X							X	X	X	X	X			X
FBgn0262166	CG8445	*calypso*								X	X						X
FBgn0042134	CG18811	*Capr*															X
FBgn0029093	CG1548	*cathD*															X
FBgn0285954	CG3606	*caz*														X	
FBgn0026143	CG3658	*CDC45L*				X		X								X	
FBgn0028360	CG32742	*Cdc7*		X			X										
FBgn0004106	CG5363	*Cdk1*	X	X			X				X					X	
FBgn0037093	CG7597	*Cdk12*		X												X	
FBgn0004107	CG10498	*Cdk2*		X			X								X	X	
FBgn0030269	CG18292	*CDK2AP1*									X		X	X			
FBgn0016131	CG5072	*Cdk4*		X												X	
FBgn0015618	CG10572	*Cdk8*		X										X		X	
FBgn0019949	CG5179	*Cdk9*		X												X	
FBgn0030121	CG17446	*Cfp1*	X										X	X			
FBgn0000289	CG8367	*cg*									X					X	X

FlyBase ID	Annotation symbol	Gene symbol	Somma 2008	Bettencourt-Dias 2004	Chen 2007	Mitotic cell cycle and				PcG Protein	PcG PPI	PcG GI	TrxG Protein	TrxG PPI	TrxG GI	Cherry picks	Mass Spec
						Chromatin Binding	Histone modification	DNA binding	Chromatin remodeling								
FBgn0035720	CG10077	*CG10077*												X		X	X
FBgn0036277	CG10418	*CG10418*	X														
FBgn0029822	CG12236	*CG12236*															X
FBgn0031252	CG13690	*CG13690*														X	
FBgn0031037	CG14207	*CG14207*												X		X	
FBgn0031052	CG14215	*CG14215*															X
FBgn0031036	CG14220	*CG14220*															X
FBgn0037924	CG14712	*CG14712*															X
FBgn0036958	CG17233	*CG17233*															X
FBgn0042111	CG18766	*CG18766*															X
FBgn0035213	CG2199	*CG2199*															X
FBgn0050122	CG30122	*CG30122*															X
FBgn0052441	CG32441	*CG32441*															X
FBgn0029861	CG3815	*CG3815*												X			
FBgn0262617	CG43143	*CG43143*															X
FBgn0038787	CG4360	*CG4360*															X
FBgn0263993	CG43736	*CG43736*															X
FBgn0043456	CG4747	*CG4747*															X
FBgn0032354	CG4788	*CG4788*															X
FBgn0039182	CG5728	*CG5728*															X
FBgn0030631	CG6227	*CG6227*														X	
FBgn0035872	CG7185	*CG7185*												X			
FBgn0037573	CG7483	*CG7483*														X	
FBgn0026577	CG8677	*CG8677*												X			
FBgn0027504	CG8878	*CG8878*	X														
FBgn0031317	CG5118	*Charon*												X			
FBgn0023395	CG9594	*Chd3*														X	
FBgn0029504	CG12690	*CHES-1-like*						X									
FBgn0013764	CG3924	*Chi*												X	X		
FBgn0028387	CG5229	*chm*										X		X	X		
FBgn0040477	CG13329	*cid*									X			X			
FBgn0027598	CG31012	*cindr*															X
FBgn0264492	CG17520	*CkIIalpha*		X												X	

FlyBase ID	Annotation symbol	Gene symbol	Somma 2008	Bettencourt-Dias 2004	Chen 2007	Mitotic cell cycle and				PcG Protein	PcG PPI	PcG GI	TrxG Protein	TrxG PPI	TrxG GI	Cherry picks	Mass Spec
						Chromatin Binding	Histone modification	DNA binding	Chromatin remodeling								
FBgn0261573	CG42687	*CoRest*												X			
FBgn0013770	CG6692	*Cp1*															X
FBgn0000283	CG6384	*Cp190*									X			X			
FBgn0004396	CG7450	*CrebA*													X		
FBgn0265784	CG6103	*CrebB*													X		
FBgn0020309	CG14938	*crol*															X
FBgn0001994	CG7664	*crp*															X
FBgn0000382	CG3954	*csw*			X												
FBgn0004198	CG11387	*ct*						X				X		X	X		
FBgn0020496	CG7583	*CtBP*												X			
FBgn0035769	CG8591	*CTCF*									X			X			
FBgn0033260	CG8711	*Cul4*	X													X	
FBgn0000395	CG15671	*cv-2*													X		
FBgn0010382	CG3938	*CycE*										X		X	X	X	
FBgn0039858	CG11525	*CycG*									X						
FBgn0027490	CG13400	*D12*												X			
FBgn0267821	CG5102	*da*												X			
FBgn0010220	CG12759	*Dbp45A*														X	
FBgn0034921	CG11183	*DCP1*															X
FBgn0034246	CG6493	*Dcr-2*													X	X	
FBgn0015075	CG9054	*Ddx1*														X	
FBgn0260632	CG6667	*dl*												X			
FBgn0001624	CG1725	*dlg1*										X			X		
FBgn0034537	CG11132	*DMAP1*												X			
FBgn0263106	CG10578	*DnaJ-1*															X
FBgn0259676	CG5553	*DNApol-alpha60*	X					X									
FBgn0265998	CG42320	*Doa*		X													
FBgn0267390	CG6498	*dop*		X													
FBgn0011763	CG4654	*Dp*	X					X									
FBgn0015929	CG1616	*dpa*										X				X	
FBgn0032293	CG6444	*Dpy-30L1*											X	X			
FBgn0002183	CG1828	*dre4*															X
FBgn0015664	CG5838	*Dref*									X			X	X		

FlyBase ID	Annotation symbol	Gene symbol	Somma 2008	Bettencourt-Dias 2004	Chen 2007	Mitotic cell cycle and				PcG Protein	PcG PPI	PcG GI	TrxG Protein	TrxG PPI	TrxG GI	Cherry picks	Mass Spec
						Chromatin Binding	Histone modification	DNA binding	Chromatin remodeling								
FBgn0038145	CG8863	*Droj2*															X
FBgn0278608	CG12223	*Dsp1*										X			X	X	X
FBgn0000541	CG32346	*E(bx)*							X		X		X	X	X		X
FBgn0000581	CG7776	*E(Pc)*										X					
FBgn0002609	CG8346	*E(spl)m3-HLH*												X			
FBgn0000617	CG6474	*e(y)1*									X					X	X
FBgn0000618	CG15191	*e(y)2*												X			
FBgn0087008	CG12238	*e(y)3*											X		X		
FBgn0000629	CG6502	*E(z)*					X	X		X	X	X		X	X		X
FBgn0011766	CG6376	*E2f1*						X				X			X		
FBgn0024371	CG1071	*E2f2*						X									
FBgn0035624	CG12756	*Eaf6*									X						X
FBgn0026441	CG4913	*ear*														X	
FBgn0263933	CG4063	*ebi*									X	X		X			
FBgn0069242	CG33104	*eca*															X
FBgn0000546	CG1765	*EcR*												X	X		
FBgn0036735	CG6311	*Edc3*															X
FBgn0284245	CG8280	*eEF1alpha1*															X
FBgn0011217	CG7425	*eff*										X			X	X	
FBgn0024996	CG2677	*eIF2Bbeta*															X
FBgn0022023	CG9124	*eIF3h*															X
FBgn0001942	CG9075	*eIF4A*														X	X
FBgn0005640	CG10579	*Eip63E*		X												X	
FBgn0039066	CG6755	*EloA*													X		
FBgn0266711	CG9291	*EloC*													X		
FBgn0004875	CG10847	*enc*												X	X		X
FBgn0034975	CG11290	*enok*									X						X
FBgn0035060	CG16932	*Eps-15*															X
FBgn0035909	CG6822	*ergic53*															X
FBgn0033663	CG8983	*ERp60*															X
FBgn0000588	CG14941	*esc*								X	X	X		X	X		X
FBgn0004583	CG4114	*ex*													X		
FBgn0033859	CG6197	*fand*	X														

FlyBase ID	Annotation symbol	Gene symbol	Somma 2008	Bettencourt-Dias 2004	Chen 2007	Mitotic cell cycle and				PcG Protein	PcG PPI	PcG GI	TrxG Protein	TrxG PPI	TrxG GI	Cherry picks	Mass Spec
						Chromatin Binding	Histone modification	DNA binding	Chromatin remodeling								
FBgn0015222	CG2216	*Fer1HCH*															X
FBgn0003062	CG9888	*Fib*															X
FBgn0013269	CG6226	*FK506-bp1*															X
FBgn0000711	CG2096	*flw*			X									X			
FBgn0028734	CG6203	*Fmr1*							X								
FBgn0036964	CG6480	*FRG1*	X														
FBgn0004652	CG14307	*fru*												X			
FBgn0004656	CG2252	*fs(1)h*		X							X				X	X	
FBgn0031873	CG9207	*Gas41*														X	X
FBgn0032223	CG5034	*GATAd*															X
FBgn0019990	CG1609	*Gcn2*		X													
FBgn0020388	CG4107	*Gcn5*												X			
FBgn0032643	CG6453	*GCS2beta*															X
FBgn0011802	CG6539	*Gem3*														X	
FBgn0033081	CG3183	*geminin*												X	X		
FBgn0250732	CG33546	*gfzf*															X
FBgn0005198	CG6975	*gig*									X			X			
FBgn0283724	CG12734	*Girdin*												X			
FBgn0015391	CG11397	*glu*				X		X								X	
FBgn0266580	CG7897	*Gp210*															X
FBgn0039562	CG5520	*Gp93*														X	X
FBgn0264495	CG42803	*gpp*										X			X		
FBgn0001139	CG8384	*gro*												X	X		
FBgn0010825	CG6964	*Gug*												X	X		
FBgn0037376	CG2051	*Hat1*									X			X			
FBgn0001179	CG8019	*hay*														X	
FBgn0039904	CG1710	*Hcf*										X	X	X			X
FBgn0015805	CG7471	*HDAC1*									X	X	X	X	X		
FBgn0025825	CG2128	*HDAC3*												X	X		
FBgn0022787	CG4261	*Hel89B*														X	
FBgn0010303	CG4353	*hep*													X		
FBgn0001197	CG5499	*His2Av*									X					X	
FBgn0001565	CG1666	*Hlc*														X	X

FlyBase ID	Annotation symbol	Gene symbol	Somma 2008	Bettencourt-Dias 2004	Chen 2007	Mitotic cell cycle and				PcG Protein	PcG PPI	PcG GI	TrxG Protein	TrxG PPI	TrxG GI	Cherry picks	Mass Spec
						Chromatin Binding	Histone modification	DNA binding	Chromatin remodeling								
FBgn0015737	CG3373	*Hmu*															X
FBgn0267791	CG13425	*HnRNP-K*												X			
FBgn0025777	CG11324	*homer*															X
FBgn0004864	CG1594	*hop*		X											X		
FBgn0264491	CG10293	*how*															X
FBgn0030082	CG7041	*HP1b*									X						
FBgn0261456	CG11228	*hpo*		X								X			X	X	
FBgn0004838	CG10377	*Hrb27C*															X
FBgn0004237	CG12749	*Hrb87F*						X						X			
FBgn0001218	CG4147	*Hsc70-3*														X	X
FBgn0266599	CG4264	*Hsc70-4*									X	X		X	X	X	X
FBgn0001225	CG4183	*Hsp26*														X	X
FBgn0001226	CG4466	*Hsp27*									X					X	X
FBgn0001233	CG1242	*Hsp83*										X		X		X	X
FBgn0027655	CG9995	*htt*							X			X			X		
FBgn0032516	CG9293	*Ing5*															X
FBgn0086613	CG31212	*Ino80*									X					X	
FBgn0283499	CG18402	*InR*		X													
FBgn0011604	CG8625	*Iswi*									X		X	X	X	X	
FBgn0001276	CG13201	*ix*												X			
FBgn0040309	CG1633	*Jafrac1*															X
FBgn0036004	CG3654	*Jarid2*									X			X	X		
FBgn0020412	CG6297	*JIL-1*		X													X
FBgn0086655	CG9397	*jing*									X	X					
FBgn0035166	CG13902	*JMJD5*				X									X		
FBgn0001291	CG2275	*Jra*												X	X		X
FBgn0001297	CG33956	*kay*						X						X	X	X	X
FBgn0037659	CG11033	*Kdm2*								X	X	X			X		
FBgn0262127	CG33967	*kibra*													X		
FBgn0266557	CG3696	*kis*										X			X	X	
FBgn0001324	CG8491	*kto*										X					
FBgn0026713	CG32604	*l(1)G0007*														X	
FBgn0027330	CG1994	*l(1)G0020*												X			

FlyBase ID	Annotation symbol	Gene symbol	Somma 2008	Bettencourt-Dias 2004	Chen 2007	Mitotic cell cycle and				PcG Protein	PcG PPI	PcG GI	TrxG Protein	TrxG PPI	TrxG GI	Cherry picks	Mass Spec
						Chromatin Binding	Histone modification	DNA binding	Chromatin remodeling								
FBgn0284251	CG12050	*l(2)05287*	X														
FBgn0002031	CG10691	*l(2)37Cc*															X
FBgn0263599	CG5931	*l(3)72Ab*	X													X	
FBgn0002441	CG5954	*l(3)mbt*				X		X						X			
FBgn0002525	CG6944	*Lam*															X
FBgn0011640	CG8597	*lark*															X
FBgn0262976	CG32711	*lawc*										X			X		
FBgn0034657	CG17952	*LBR*															X
FBgn0031759	CG9088	*lid*										X		X	X		
FBgn0041111	CG8817	*lilli*													X		
FBgn0029800	CG15929	*lin-52*									X			X			
FBgn0038167	CG9374	*Lkb1*		X										X			
FBgn0250903	CG34440	*lmgA*									X					X	
FBgn0019686	CG10895	*lok*													X		
FBgn0283521	CG12052	*lola*															X
FBgn0022238	CG5738	*lolal*										X					
FBgn0263667	CG5591	*Lpt*											X	X	X		X
FBgn0037621	CG9797	*M1BP*						X									
FBgn0011648	CG12399	*Mad*						X									
FBgn0035640	CG17498	*mad2*															X
FBgn0016034	CG11254	*mael*															X
FBgn0029979	CG10777	*mahe*														X	
FBgn0031655	CG3753	*Marcal1*														X	
FBgn0043884	CG33106	*mask*															X
FBgn0027950	CG8208	*MBD-like*									X		X	X			
FBgn0038016	CG10042	*MBD-R2*	X			X		X						X			
FBgn0262732	CG4143	*mbf1*													X		
FBgn0032929	CG9241	*Mcm10*						X								X	
FBgn0284442	CG4206	*Mcm3*	X					X								X	
FBgn0020633	CG4978	*Mcm7*	X					X								X	
FBgn0260959	CG42572	*MCPH1*															X
FBgn0004419	CG4916	*me31B*														X	
FBgn0036581	CG5057	*MED10*												X			

FlyBase ID	Annotation symbol	Gene symbol	Somma 2008	Bettencourt-Dias 2004	Chen 2007	Mitotic cell cycle and				PcG Protein	PcG PPI	PcG GI	TrxG Protein	TrxG PPI	TrxG GI	Cherry picks	Mass Spec
						Chromatin Binding	Histone modification	DNA binding	Chromatin remodeling								
FBgn0036811	CG6884	*MED11*												X			
FBgn0035145	CG12031	*MED14*												X			
FBgn0027592	CG4184	*MED15*												X			
FBgn0034707	CG5465	*MED16*												X			
FBgn0038578	CG7957	*MED17*												X			
FBgn0026873	CG14802	*MED18*												X			
FBgn0013531	CG18780	*MED20*												X			
FBgn0034795	CG3695	*MED23*												X			
FBgn0035851	CG7999	*MED24*												X			
FBgn0037359	CG1245	*MED27*												X			
FBgn0035149	CG17183	*MED30*												X			
FBgn0035754	CG8609	*MED4*												X			
FBgn0024330	CG9473	*MED6*												X			
FBgn0051390	CG31390	*MED7*												X			
FBgn0034503	CG13867	*MED8*												X			
FBgn0035357	CG1244	*MEP-1*									X		X	X			
FBgn0086384	CG14228	*Mer*													X		
FBgn0262519	CG8103	*Mi-2*									X	X	X	X		X	X
FBgn0031399	CG7074	*mio*															X
FBgn0033846	CG6061	*mip120*									X			X			
FBgn0023509	CG3480	*mip130*									X			X			
FBgn0034430	CG15119	*mip40*									X			X			
FBgn0002774	CG11680	*mle*												X	X	X	
FBgn0034051	CG8295	*Mlf*															X
FBgn0031885	CG13778	*Mnn1*				X	X	X					X	X			
FBgn0014340	CG3025	*mof*												X	X		
FBgn0002783	CG18740	*mor*						X	X			X	X	X	X		
FBgn0027378	CG6363	*MRG15*												X			
FBgn0261109	CG7764	*mrn*														X	
FBgn0002775	CG8631	*msl-3*												X			
FBgn0027951	CG2244	*MTA1-like*									X		X	X			
FBgn0040305	CG3743	*MTF-1*													X		
FBgn0025742	CG9115	*mtm*			X									X	X		

FlyBase ID	Annotation symbol	Gene symbol	Somma 2008	Bettencourt-Dias 2004	Chen 2007	Mitotic cell cycle and				PcG Protein	PcG PPI	PcG GI	TrxG Protein	TrxG PPI	TrxG GI	Cherry picks	Mass Spec
						Chromatin Binding	Histone modification	DNA binding	Chromatin remodeling								
FBgn0013756	CG8274	*Mtor*	X								X						
FBgn0002899	CG7972	*mus301*														X	
FBgn0260789	CG12124	*mxc*										X			X		
FBgn0002914	CG9045	*Myb*									X			X	X		
FBgn0262656	CG10798	*Myc*										X		X	X		
FBgn0004647	CG3936	*N*				X					X			X	X		
FBgn0015268	CG5330	*Nap1*									X						
FBgn0261530	CG6754	*nbs*						X								X	
FBgn0028926	CG4185	*NC2beta*												X			
FBgn0031698	CG14023	*Ncoa6*											X	X			X
FBgn0261617	CG15319	*nej*					X				X	X	X	X			
FBgn0038872	CG5874	*Nelf-A*															X
FBgn0053554	CG33554	*Nipped-A*															X
FBgn0026401	CG17704	*Nipped-B*				X						X			X		X
FBgn0266570	CG2982	*NO66*													X		
FBgn0026196	CG10206	*nop5*															X
FBgn0038964	CG13849	*Nop56*															X
FBgn0033029	CG8426	*Not3*	X														
FBgn0266464	CG33101	*Nsf2*										X			X		
FBgn0262527	CG4699	*nsl1*						X						X			
FBgn0027868	CG6743	*Nup107*															X
FBgn0021761	CG4579	*Nup154*															X
FBgn0030943	CG6540	*Nup35*															X
FBgn0039302	CG11856	*Nup358*															X
FBgn0038609	CG7671	*Nup43*															X
FBgn0033247	CG8722	*Nup44A*															X
FBgn0033264	CG2158	*Nup50*															X
FBgn0033737	CG8831	*Nup54*															X
FBgn0034118	CG6251	*Nup62*															X
FBgn0027537	CG11092	*Nup93-1*															X
FBgn0039120	CG10198	*Nup98-96*												X			X
FBgn0016687	CG4634	*Nurf-38*									X		X	X			X
FBgn0038344	CG5205	*obe*														X	

FlyBase ID	Annotation symbol	Gene symbol	Somma 2008	Bettencourt-Dias 2004	Chen 2007	Mitotic cell cycle and				PcG Protein	PcG PPI	PcG GI	TrxG Protein	TrxG PPI	TrxG GI	Cherry picks	Mass Spec
						Chromatin Binding	Histone modification	DNA binding	Chromatin remodeling								
FBgn0266083	CG3363	*ocm*									X						X
FBgn0002989	CG3736	*okr*	X														
FBgn0264307	CG43782	*orb2*												X			
FBgn0261885	CG7467	*osa*										X	X	X	X		
FBgn0014868	CG9022	*Ost48*															X
FBgn0266420	CG5581	*Ote*	X														X
FBgn0039044	CG33336	*p53*				X		X						X			
FBgn0030294	CG11750	*Pa1*											X	X			
FBgn0265297	CG5119	*pAbp*															X
FBgn0010247	CG40411	*Parp*														X	
FBgn0266053	CG5208	*Patr-1*															X
FBgn0003042	CG32443	*Pc*				X		X		X	X	X		X	X		X
FBgn0036184	CG7351	*PCID2*															X
FBgn0003044	CG5109	*Pcl*									X	X		X	X		X
FBgn0014002	CG6988	*Pdi*															X
FBgn0016694	CG17888	*Pdp1*						X									
FBgn0086895	CG8241	*pea*	X													X	
FBgn0023517	CG14816	*Pgam5*															X
FBgn0039776	CG31022	*PH4alphaEFB*															X
FBgn0004860	CG3895	*ph-d*				X		X		X	X	X					X
FBgn0283509	CG3832	*Phm*													X		
FBgn0002521	CG17743	*pho*								X	X	X		X			X
FBgn0035997	CG3445	*phol*								X	X						
FBgn0004861	CG18412	*ph-p*				X		X		X	X	X		X	X		X
FBgn0015278	CG11621	*Pi3K68D*												X	X		
FBgn0015279	CG4141	*Pi3K92E*												X			
FBgn0260962	CG7769	*pic*	X					X								X	
FBgn0003117	CG3978	*pnr*													X		X
FBgn0003118	CG17077	*pnt*													X		
FBgn0039227	CG11375	*polybromo*											X	X	X		
FBgn0040078	CG4003	*pont*									X			X	X	X	X
FBgn0004363	CG6647	*porin*															X
FBgn0004103	CG5650	*Pp1-87B*			X						X	X		X	X		

FlyBase ID	Annotation symbol	Gene symbol	Somma 2008	Bettencourt-Dias 2004	Chen 2007	Mitotic cell cycle and				PcG Protein	PcG PPI	PcG GI	TrxG Protein	TrxG PPI	TrxG GI	Cherry picks	Mass Spec
						Chromatin Binding	Histone modification	DNA binding	Chromatin remodeling								
FBgn0261119	CG5519	*Prp19*															X
FBgn0036915	CG7757	*Prp3*	X														
FBgn0011474	CG3307	*PR-Set7*									X						
FBgn0261552	CG42670	*ps*															X
FBgn0005624	CG3886	*Psc*						X	X	X	X	X		X	X		X
FBgn0261976	CG18013	*Psf2*														X	
FBgn0014870	CG8912	*Psi*												X			
FBgn0263102	CG2368	*psq*									X	X				X	X
FBgn0038948	CG5383	*PSR*													X		
FBgn0052133	CG32133	*Ptip*											X	X			X
FBgn0243512	CG7850	*puc*			X										X		
FBgn0032006	CG8222	*Pvr*		X													X
FBgn0259785	CG7752	*pzg*				X					X			X			X
FBgn0022986	CG3613	*qkr58E-1*															X
FBgn0022985	CG5821	*qkr58E-2*															X
FBgn0039966	CG17515	*Rab21*												X	X		
FBgn0014010	CG3664	*Rab5*															X
FBgn0025808	CG7825	*Rad17*				X		X									
FBgn0034646	CG9862	*Rae1*												X			X
FBgn0003079	CG2845	*Raf*												X	X		
FBgn0020255	CG1404	*Ran*															X
FBgn0003346	CG9999	*RanGAP*															X
FBgn0003205	CG9375	*Ras85D*													X		
FBgn0031868	CG10354	*Rat1*	X														
FBgn0036973	CG5585	*Rbbp5*											X	X			X
FBgn0015799	CG7413	*Rbf*						X			X			X	X		
FBgn0038390	CG5083	*Rbf2*						X			X			X			
FBgn0002638	CG10480	*Rcc1*				X									X		
FBgn0033897	CG8233	*Rcd1*	X											X			
FBgn0264493	CG12537	*rdx*									X	X					
FBgn0040290	CG7487	*RecQ4*						X								X	
FBgn0027375	CG4879	*RecQ5*						X								X	
FBgn0014018	CG11992	*Rel*												X			X

FlyBase ID	Annotation symbol	Gene symbol	Somma 2008	Bettencourt-Dias 2004	Chen 2007	Mitotic cell cycle and				PcG Protein	PcG PPI	PcG GI	TrxG Protein	TrxG PPI	TrxG GI	Cherry picks	Mass Spec
						Chromatin Binding	Histone modification	DNA binding	Chromatin remodeling								
FBgn0040075	CG9750	*rept*					X		X		X	X			X	X	X
FBgn0039209	CG13624	*REPTOR*															X
FBgn0032244	CG5313	*RfC3*															X
FBgn0028700	CG6258	*RfC38*															X
FBgn0004635	CG1004	*rho*										X			X		
FBgn0031006	CG8002	*rictor*									X			X			
FBgn0003256	CG12559	*rl*													X		
FBgn0003261	CG10279	*Rm62*										X				X	X
FBgn0023171	CG8729	*rnh1*														X	
FBgn0003277	CG1554	*RpII215*						X			X			X	X		
FBgn0024733	CG17521	*RpL10*															X
FBgn0015288	CG7434	*RpL22*															X
FBgn0010078	CG3661	*RpL23*															X
FBgn0035422	CG12740	*RpL28*															X
FBgn0086710	CG10652	*RpL30*															X
FBgn0064225	CG17489	*RpL5*															X
FBgn0000100	CG7490	*RpLP0*															X
FBgn0028691	CG10230	*Rpn9*															X
FBgn0004403	CG1524	*RpS14a*															X
FBgn0034743	CG4046	*RpS16*															X
FBgn0005533	CG3922	*RpS17*															X
FBgn0015521	CG2986	*RpS21*												X			
FBgn0039300	CG10423	*RpS27*															X
FBgn0002622	CG6779	*RpS3*						X									X
FBgn0017545	CG2168	*RpS3A*															X
FBgn0038269	CG7292	*Rrp6*												X			
FBgn0011305	CG5655	*Rsf1*												X			
FBgn0267790	CG9373	*rump*															X
FBgn0034763	CG12190	*RYBP*									X	X			X		
FBgn0283472	CG10539	*S6k*		X										X			
FBgn0262866	CG17596	*S6kII*		X							X			X			
FBgn0024188	CG12352	*san*					X							X			
FBgn0262714	CG11006	*Sap130*															X

FlyBase ID	Annotation symbol	Gene symbol	Somma 2008	Bettencourt-Dias 2004	Chen 2007	Mitotic cell cycle and				PcG Protein	PcG PPI	PcG GI	TrxG Protein	TrxG PPI	TrxG GI	Cherry picks	Mass Spec
						Chromatin Binding	Histone modification	DNA binding	Chromatin remodeling								
FBgn0003317	CG1891	*sax*													X		
FBgn0285917	CG5580	*sbb*													X		
FBgn0025802	CG6939	*Sbf*			X	X	X				X		X	X			
FBgn0003330	CG5595	*Sce*								X	X	X					X
FBgn0025682	CG9148	*scf*										X			X		
FBgn0003334	CG9495	*Scm*									X	X					X
FBgn0003345	CG8544	*sd*										X		X	X		
FBgn0263260	CG12918	*sel*															X
FBgn0263006	CG3725	*SERCA*															X
FBgn0003360	CG16944	*sesB*															X
FBgn0040022	CG40351	*Set1*											X	X			
FBgn0283477	CG6987	*SF2*						X									
FBgn0032475	CG16975	*Sfmbt*								X	X			X			X
FBgn0036804	CG13379	*Sgf11*									X						
FBgn0266411	CG45051	*sima*									X			X			
FBgn0010762	CG32067	*simj*									X		X	X			
FBgn0022764	CG8815	*Sin3A*				X	X				X	X		X	X		X
FBgn0024191	CG7238	*sip1*														X	
FBgn0024291	CG5216	*Sirt1*										X			X		
FBgn0003415	CG9936	*skd*										X		X	X		
FBgn0040283	CG6057	*SMC1*	X								X					X	
FBgn0027783	CG10212	*SMC2*				X										X	
FBgn0015615	CG9802	*SMC3*	X								X					X	
FBgn0052438	CG32438	*SMC5*									X					X	
FBgn0016070	CG5263	*smg*									X			X			
FBgn0025800	CG2262	*Smox*				X		X									
FBgn0265523	CG4013	*Smr*				X		X									
FBgn0264922	CG4494	*smt3*												X	X		
FBgn0011715	CG1064	*Snr1*										X	X	X	X		
FBgn0001965	CG7793	*Sos*						X									
FBgn0016977	CG18497	*spen*												X			
FBgn0005672	CG10334	*spi*										X			X		
FBgn0003483	CG3158	*spn-E*														X	

FlyBase ID	Annotation symbol	Gene symbol	Somma 2008	Bettencourt-Dias 2004	Chen 2007	Mitotic cell cycle and				PcG Protein	PcG PPI	PcG GI	TrxG Protein	TrxG PPI	TrxG GI	Cherry picks	Mass Spec
						Chromatin Binding	Histone modification	DNA binding	Chromatin remodeling								
FBgn0039169	CG5669	*Spps*										X				X	
FBgn0037981	CG3169	*Spt3*														X	
FBgn0040273	CG7626	*Spt5*				X		X			X						
FBgn0263396	CG16901	*sqd*															X
FBgn0010768	CG5557	*sqz*															X
FBgn0003507	CG3992	*srp*													X		X
FBgn0011509	CG33162	*SrpRbeta*															X
FBgn0011481	CG7187	*Ssdp*												X			
FBgn0011016	CG5474	*SsRbeta*															X
FBgn0016917	CG4257	*Stat92E*												X	X		
FBgn0003520	CG5753	*stau*									X						
FBgn0002466	CG10522	*sti*		X										X			
FBgn0033051	CG7863	*Strica*															X
FBgn0003459	CG3836	*stwl*															X
FBgn0052676	CG32676	*stx*									X	X			X		
FBgn0014388	CG1921	*sty*													X		
FBgn0003567	CG8573	*su(Hw)*												X			
FBgn0003575	CG6222	*su(sable)*												X			
FBgn0014037	CG32217	*Su(Tpl)*													X		
FBgn0003607	CG8409	*Su(var)205*				X	X	X	X		X						X
FBgn0026427	CG12864	*Su(var)2-HP2*						X	X								
FBgn0260397	CG17149	*Su(var)3-3*												X	X		
FBgn0020887	CG8013	*Su(z)12*								X	X			X			X
FBgn0265623	CG3905	*Su(z)2*									X	X					X
FBgn0034709	CG3074	*Swim*															X
FBgn0261403	CG10392	*sxc*										X					X
FBgn0038826	CG17838	*Syp*															X
FBgn0010355	CG17603	*Taf1*		X							X					X	X
FBgn0028398	CG2859	*Taf10*														X	
FBgn0026324	CG3069	*Taf10b*														X	
FBgn0011291	CG4079	*Taf11*														X	X
FBgn0011290	CG17358	*Taf12*														X	
FBgn0032847	CG10756	*Taf13*														X	

FlyBase ID	Annotation symbol	Gene symbol	Somma 2008	Bettencourt-Dias 2004	Chen 2007	Mitotic cell cycle and				PcG Protein	PcG PPI	PcG GI	TrxG Protein	TrxG PPI	TrxG GI	Cherry picks	Mass Spec
						Chromatin Binding	Histone modification	DNA binding	Chromatin remodeling								
FBgn0037792	CG6241	*TAF1B*													X		
FBgn0011836	CG6711	*Taf2*														X	
FBgn0010280	CG5444	*Taf4*									X					X	X
FBgn0010356	CG7704	*Taf5*									X					X	X
FBgn0010417	CG32211	*Taf6*	X								X					X	X
FBgn0024909	CG2670	*Taf7*														X	
FBgn0022724	CG7128	*Taf8*														X	X
FBgn0021795	CG9035	*Tapdelta*															X
FBgn0040071	CG6889	*tara*										X			X		
FBgn0003687	CG9874	*Tbp*									X					X	X
FBgn0283681	CG4933	*Tcs3*												X			
FBgn0037874	CG4800	*Tctp*					X							X			
FBgn0045035	CG6535	*tefu*					X								X		
FBgn0261014	CG2331	*TER94*															X
FBgn0263392	CG43444	*Tet*												X			
FBgn0004915	CG5193	*TfIIB*									X						
FBgn0003716	CG14026	*tkv*		X											X		
FBgn0283657	CG34412	*Tlk*		X			X										
FBgn0026160	CG7958	*tna*										X		X	X		
FBgn0004924	CG6146	*Top1*														X	
FBgn0284220	CG10223	*Top2*				X		X			X			X		X	X
FBgn0267351	CG15104	*Topors*						X								X	
FBgn0033636	CG10897	*tou*										X		X	X		
FBgn0028978	CG5408	*trbl*		X												X	
FBgn0261793	CG18009	*Trf2*									X	X		X			
FBgn0023518	CG3848	*trr*											X	X	X		X
FBgn0003862	CG8651	*trx*									X	X	X	X	X		X
FBgn0026317	CG6147	*Tsc1*									X			X			
FBgn0039117	CG10210	*tst*														X	
FBgn0086356	CG13345	*tum*															X
FBgn0040091	CG4414	*Ugt58Fa*															X
FBgn0004395	CG4620	*unk*															X
FBgn0030354	CG1559	*Upf1*														X	X

FlyBase ID	Annotation symbol	Gene symbol	Somma 2008	Bettencourt-Dias 2004	Chen 2007	Mitotic cell cycle and				PcG Protein	PcG PPI	PcG GI	TrxG Protein	TrxG PPI	TrxG GI	Cherry picks	Mass Spec
						Chromatin Binding	Histone modification	DNA binding	Chromatin remodeling								
FBgn0036398	CG9007	*upSET*										X		X			X
FBgn0003963	CG2762	*ush*												X			
FBgn0003964	CG4380	*usp*												X	X		
FBgn0052479	CG32479	*Usp10*												X			X
FBgn0030366	CG1490	*Usp7*										X					
FBgn0260749	CG5640	*Utx*										X	X	X	X		X
FBgn0035713	CG10107	*velo*															X
FBgn0016075	CG16858	*vkg*															X
FBgn0260987	CG17436	*vtd*				X					X	X					X
FBgn0266848	CG14614	*wap*															X
FBgn0027492	CG5643	*wdb*															
FBgn0032030	CG17293	*Wdr82*	X										X	X			
FBgn0040066	CG17437	*wds*					X		X				X	X	X		X
FBgn0010328	CG5965	*woc*	X														
FBgn0011739	CG12072	*wts*		X							X	X			X		
FBgn0261850	CG9433	*Xpd*						X								X	
FBgn0034970	CG4005	*yki*												X	X		
FBgn0004050	CG7803	*z*									X	X		X	X	X	

2.3. Primer Design for Additional dsRNAs

For follow up analysis of screen hits, additional dsRNAs were designed, where possible. Using SnapDragon, primers were designed to target regions different from the ones targeted in the Open Biosystems RNAi template libraries and found with GenomeRNAi, except for *ph-p*, which primers were used for both the RNAi screen and the Western blot quantitative analysis (Flockhart et al., 2012; Horn et al., 2007; S. E. Mohr et al., 2014; Schmidt et al., 2013). Forward primers contained a 5' T3 RNA polymerase promoter sequence (AATTAACCCTCACTAAAG) or a 5' T7 RNA polymerase promoter sequence (GAATTAATACGACTCACTATAGGGAGACCACCCCAAAGCTTTCAGA for *ph-p* or TAATACGACTCACTATAG) and reverse primers contained a 5' T7 RNA polymerase promoter sequence to allow either T3 or T7 RNA polymerase binding for dsRNA synthesis. Off-target regions were minimized as much as possible and product size were at least 150 base pair long (Flockhart et al., 2012; Kulkarni et al., 2006; S. E. Mohr et al., 2014) (Table 3, p.76).

Table 3. – Gene Specific Primers Used. Forward primers contained a 5' T3 RNA polymerase binding site (5'-AATTAACCCTCACTAAAG-3'), while reverse primers contained a 5' T7 RNA polymerase binding site (5'-TAATACGACTCACTATAG-3') except for *ph-p*, which primers both contained a 5' T7 RNA polymerase biding site (5'-GAATTAATACGACTCACTATAGGGAGA-3').

Gene Symbol	Forward primer	Reverse primer	Annealing temperature (°C)
asf1	T3 + GCAGTTATCCATCCCGAAGA	T7 + ACGAGGACCAGGAGTGCTAA	59.9
Cp1	T3 + GGAGCACCGCAAGAACTATC	T7 + GCAGTTGCTTGTGCAGAGTG	59.9
CtBP	T3 + GTTCGGCTTCAACGTCATCT	T7 + ATGATGGTTGTGCTCGTTGA	58.2
Dpy-30L1	T3 + AGACCGACGCACCCATCT	T7 + GATTTGTGGACTGGCCAAC	59.1
MED30	T3 + GTGCGCATCATCTACGAGAA	T7 + TTGCTGTTTGGCAATGTTTC	56.6
nej	T3 + CCAGCACCACTCTCTGTCAA	T7 + GTCCTGCATGGTCGTAGGAT	59.9
Nurf-38	T3 + TCGTACAGAGCCATCTCGTG	T7 + TGAAGAAAATGTTGGCGAAA	56
okr	T3 + TAACGTGCTAGGGGTGAAGG	T7 + AATCCGGACGTTGCTATACG	58.2
Rab5	T3 + CAGGGGACGAATTTCATTTG	T7 + AAAACCCTGCGCTTTCTTCT	62.1
Rel	T3 + CTTAATGGAGTGCCAACCGT	T7 + CTCCCTTCTCCGGATACACA	59.9
Sbf	T3 + CGAGACCAGCCTTCAAAAAG	T7 + TCGAGGAACTGCAGAAAGGT	59.1
SF2	T3 + GACGGCTACGACTACGATGG	T7 + TTGCGTACTTCATGTCCTCG	62.1
ph-p	T7 + AACTGACAATGGCGATCCTA	T7 + CCACCCCAAAGCTTTCAGA	63
ph-d	T3 + TGTGACTTCTCCAGTTTGCG	T7 + CACCGAAAGTGAATCAGCAA	58.3

2.4. RNAi Template (DNA) Preparation

DNA templates were collected from two RNAi template libraries (Open Biosystems). Both libraries consisted of ribonuclease free dsDNA fragments corresponding to exonic sequences and containing dual T7 promoters. One of these (*Drosophila* RNAi Library – Release 1.0) covered 50% of the *Drosophila* genome with 300-600 base pair long templates amplified by gene specific primers. For certain genes, several constructs were available but in separate locations in the library. The other library (*Drosophila* RNAi Library – Release 2.0) covered over 50% of the *Drosophila* genome with 200-800 base pair long templates amplified by a two-step nested PCR to ensure specificity.

DNA templates (1:10 dilution from the RNAi template libraries), were amplified by hot start PCR in 100 microliter (µl) reactions assembled on ice and containing 4 units of Taq enzyme, 0.25 micromolar (µM) T7 primer, 5% of DNA template, 3% dimethyl sulfoxide (DMSO), 0.1 millimolar (mM) deoxyribonucleotide triphosphate (dNTP) (each), 1.5 mM magnesium chloride ($MgCl_2$), 1X PCR buffer and double-distilled water (ddH_2O). PCR programs were identical for all genes with a 63 degrees Celsius (^oC) annealing temperature and 40 cycles. The quality and size of PCR products were verified on 1% agarose gels in 1X TAE buffer (4.84g/L (gram per liter) Tris Base, 2mM EDTA, 0.1142 % Acetic acid, ddH_2O), which were stained with ethidium bromide. To quantify the PCR products (which were not purified), a known amount of a single purified PCR product was loaded on each gel as a standard. DNA concentrations were measured from band intensities using ImageJ (C. A. Schneider et al., 2012). The quantification standard was purified with a DNA purification kit (Macherey-Nagel) to remove primers and free dNTPs, and its concentration determined by measuring the absorbance at 260 nanometers (nm) using a Nanodrop spectrophotometer. PCR products were stored at -80^oC or -20^oC. DNA templates for follow up RNAi experiments were made the same way but with different annealing temperature (Table 3, p.76).

2.5. dsRNA Synthesis

2.5.1. RNAi Screen

dsRNAs were synthesized by *in vitro* transcription in the following reaction conditions: 150 to 200 nanograms (ng) PCR product, 1X T7 RNA polymerase buffer, 1mM DTT, 1mM ribonucleotide triphosphate (rNTP) (each), 80 to 160 units of murine ribonuclease inhibitor and 300 units of T7 polymerase in an 80µl total volume. Reactions were assembled on ice, incubated 6 hours (hrs) at 37^{o}C for transcription, incubated 5 minutes (mins) at 99^{o}C for complete denaturation, and cooled to room temperature for annealing (-2^{o}C/min for 40mins). The concentration was determined using the Nanodrop as previously described: by measuring the absorbance at 260nm, and the quality and size confirmed on a 1% agarose gel in 1X TAE buffer stained with ethidium bromide. dsRNAs were stored at -80^{o}C or -20^{o}C.

2.5.2. Follow-up RNAi Experiments

For follow-up RNAi experiments, each strand for the dsRNAs was synthesized separately, then equally mixed and annealed to control for the production of both transcripts. dsRNAs were synthesized by *in vitro* transcription in the following reaction conditions: 150 to 200ng PCR product, 1X RNA polymerase buffer, 1mM DTT, 1mM each rNTP, 80 to 160 units of ribonuclease inhibitor and 300 units of T7 or T3 polymerase (depending on the primer used for generating the PCR products, see Table 3 (p.76)) in a 80µl total volume. Reactions were assembled on ice and then incubated 6hrs at 37^{o}C for transcription. Successful transcription reactions often yield a magnesium pyrophosphate precipitate as a result of nucleoside triphosphates hydrolysis which, in our hands, affected cells during dsRNA treatments (Brunelle & Green, 2013). Thus, reactions were centrifuged for 5mins at 17 900*g and supernatants were collected. Concentration of single-stranded RNAs was measured using the Nanodrop and equal amounts of the two strands (T3 and T7 RNA polymerase synthetized) were mixed and incubated 5mins at 99^{o}C for complete denaturation, and cooled to room temperature for annealing (-2^{o}C/30 seconds for 37 cycles). dsRNAs were centrifuged 5mins at 17 900*g to get rid of residual magnesium pyrophosphate precipitate. The supernatants were collected and stored at -80^{o}C or -20^{o}C. Final concentrations

were measured by Nanodrop, and the quality and size confirmed on a 1% agarose gel in 1X TAE buffer stained with ethidium bromide.

2.6. S2R+ Cells

S2R+ cells were kept in culture in M3+BPYE media with 10% FBS for no longer than 6 weeks. M3+BPYE media was prepared from Shields and Sang M3 Insect Medium powder, 0.5g/L potassium bicarbonate ($KHCO_3$), 1g/L Select Yeast Extract, 2.5g/L of Bacto™ Peptone and MilliQ H_20. Foetal bovine serum was added to a final concentration of 10%, and media was sterile filtered and stored at 4°C.

2.7. Plate Design

When cells are plated onto multi-well plates, systematic measurement errors related to well position can occur. Measurements can adopt either a linear or a bowl-shaped relationship to well position. Thus, to avoid position effects, screening candidate genes were arranged randomly on the plates and top and bottom rows were left empty. Control wells were strategically scattered across the plate with positive and negative controls sharing both columns and rows (Brideau et al., 2003; Zhang, 2008) (Figure 5, p.80).

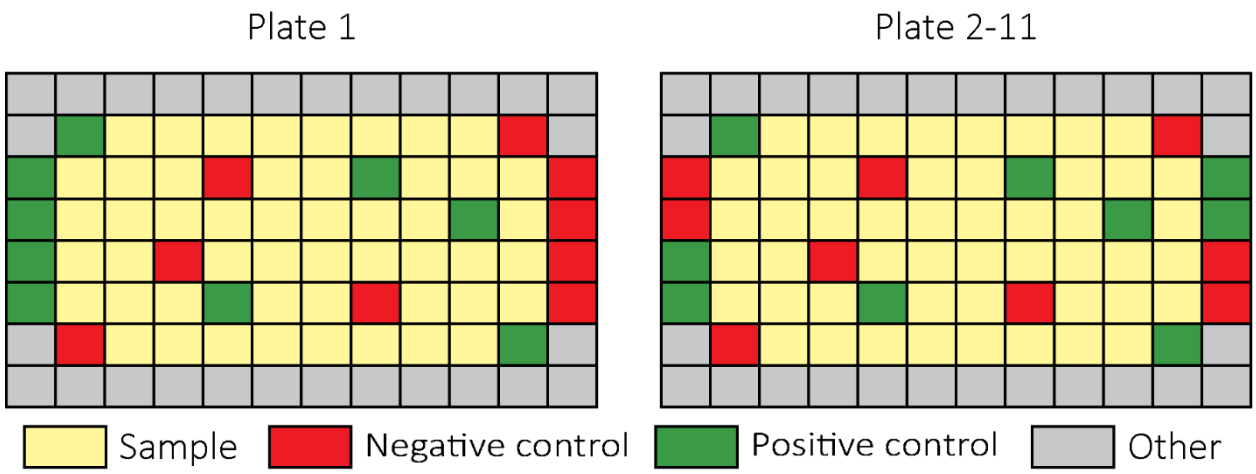

Figure 5. – Plate Design for the Screen. To avoid position effect, control wells were spread across the plate and shared common columns and lines. Edge wells were also avoided, and samples were displayed randomly. Since initial plate design (see plate 1) could affect B-score calculation, side columns contained controls of both type (negative and positive) for subsequent plates (plate 2-11).

2.8. S2R+ Cells Treatment for RNAi Screen

Once confluent, S2R+ cells were collected, centrifuged for 3mins at 207*g, washed in one volume of fresh media and re-centrifuged. 32 000 S2R+ cells/well were plated on CellBind® surface treated 96-well plates (Corning 3340) in up to 70µl media, and treated with 2 micrograms (µg) dsRNA. After 1hr, the well volume was completed to 100µl. 48hrs later, cells were treated with 2µg dsRNA for an additional 16hrs. The day the cells were fixed, they were first treated with colchicine at a final concentration of 125 nanograms per milliliter (ng/ml) for 4hrs.

Positive control wells were treated with dsRNA targeting both p*h-d* and *ph-p* (2µg each for each treatment) and negative control wells were treated with dsRNA targeting *Venus*, a gene absent from the *Drosophila* genome.

2.9. Immunocytochemistry

Immunocytochemistry was performed based on a modified protocol from Fanti *et al*. and Follmer *et al*. (Fanti et al., 2008; Follmer et al., 2012). 96-well plates were centrifuged for 4mins at 298*g. Cells were washed twice in 0.7% sodium chloride (NaCl)/ddH_2O, then swollen by incubation for 10mins in 0.5% sodium citrate/ddH_2O hypotonic solution, and fixed for 8mins in 5% acetic acid/95% ice cold (-20°C) methanol (MeOH). Fixation solution was replaced with 1X PBS (8g/L NaCl, 0.2g/L potassium chloride (KCl), 1.15g/L sodium phosphate dibasic heptahydrate (Na_2HPO_4-$7H_2O$) dibasic, 0.22g/L potassium phosphate (KH_2PO_4) monobasic, ddH_2O) and cells were washed twice for 5mins in 1X PBS before a 10mins permeabilization step in 1% triton-X 100/1X PBS. Cells were washed twice for 5mins in 1X PBS and blocked for 1hr at room temperature in 5% milk/0.03% TWEEN® 20/1X PBS. After a 5mins wash in 1X PBS, cells were incubated for 1hr at room temperature in 1:1 000 rabbit anti-Ph and mouse anti-α-tubulin/1% bovine serum albumin (BSA)/0.1% TWEEN® 20/1X PBS before an overnight incubation at 4°C. Cells were then washed three times for 5mins in 1X PBS and stained in 1:250 2 milligrams per milliliter (mg/ml) Alexa 488 anti-rabbit or Alexa 647+ anti-mouse/1% BSA/0.1% TWEEN® 20/1X PBS solution. Cells were washed in 1X PBS, in 0.02% TWEEN® 20/1X PBS and in 1X PBS again for 5mins each before a 10mins post-fixation in 4% formaldehyde/1X PBS, three 5mins 1X PBS washes and a 15mins incubation in 1µg/ml Hoechst/1X PBS. Finally, Hoechst solution was replaced with 1X PBS.

2.10. Image Acquisition

96-well imaging plates were placed in an automated high content screening inverted fluorescent microscope (IMAGE X PRESS MICRO, Molecular Devices) and images were acquired via MetaXpress® software (version 3.1.0.81) (Molecular Devices). Samples in each well were exposed to 3 different excitation wavelengths: FITC for Ph localization, Cy5 for tubulin localization and DAPI for chromatin localization (Hoechst staining).

A total of 24 sites per well were defined, which avoided well edges and were similarly localized for every well (Figure 6, p.83). One 12bit picture per site and staining was acquired using a 40X magnification objective. Focus was automatically adjusted for each site and staining.

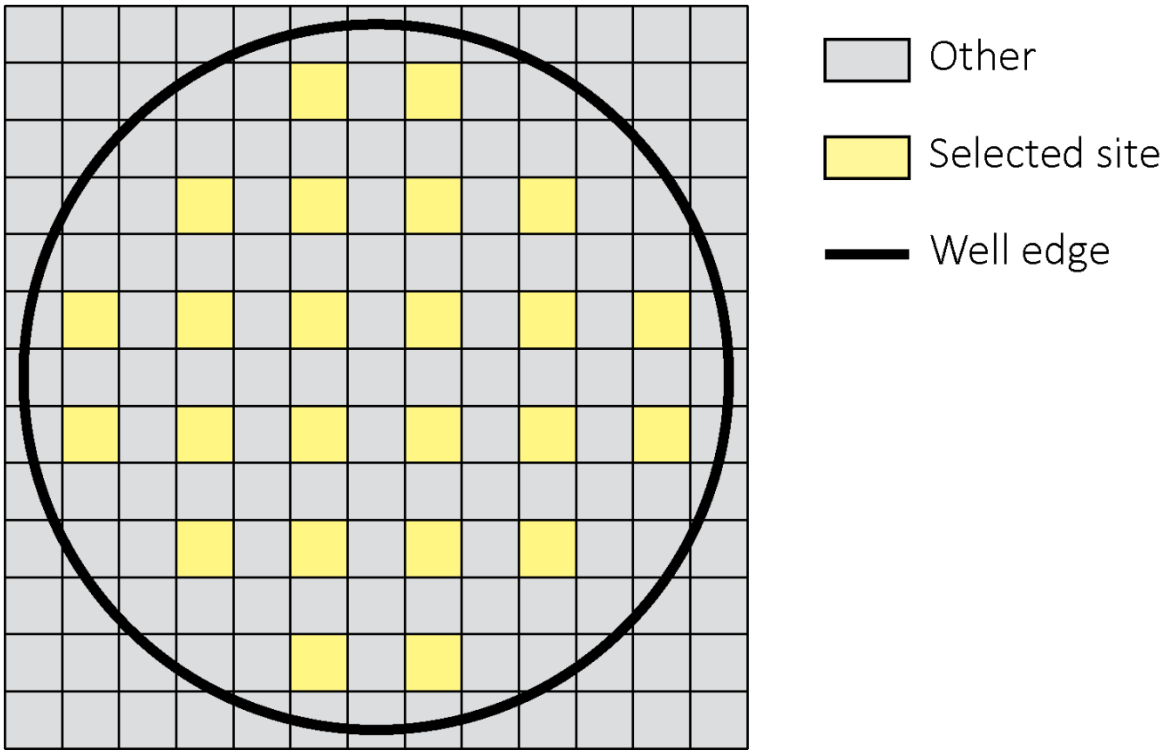

Figure 6. – Schematic Representation of Site Selection. For every captured well, 24 universal sites were defined. Sites did not overlap well borders.

2.11. Image Processing

Images were processed using CellProfiler™ (Version 3.0.0) (Carpenter et al., 2006). Different analysis pipelines were used for interphase and mitotic cells. Both pipelines shared general modules: cells were identified using the tubulin stain, nuclei/chromosomes with the Hoechst stain and cytoplasm by subtracting the nucleus/chromosome area from the corresponding cell (Figure 7, p.85). Cells touching image borders were not considered. The median value of the median Ph staining pixel intensity per nuclei of interphase cells or chromosome set of mitotic cells were used for the analysis described in the next section (RNAi screen Analysis). The ratio of the median Ph staining pixel intensity in the nucleus or chromosome set over the median Ph staining pixel intensity in the rest of the cells was also used for the analysis. These values will be referred to as median values and ratio values respectively. Commented CellProfiler™ pipelines are available in supplemental material (Annex 1 and 2).

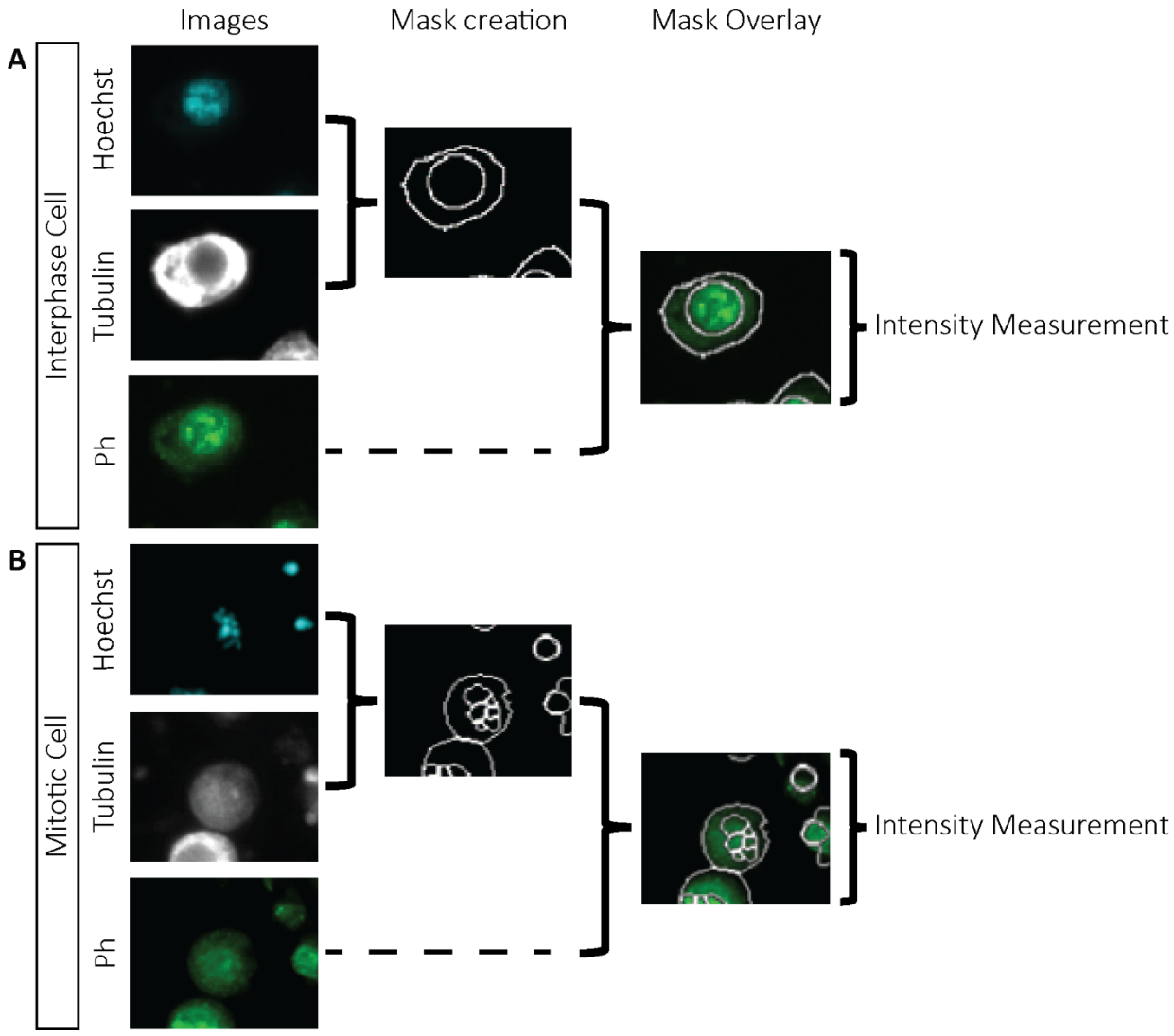

Figure 7. – Main Pipeline Steps. A) Pipeline Strategy for the Analysis of Interphase Cells. B) Pipeline Strategy for the Analysis of Mitotic Cells. Cell masks are created from tubulin and Hoechst staining pictures and overlaid onto Ph staining pictures to measure intensities in the different compartments defined by the masks.

2.11.1. Identification of Interphase and Mitotic Cells

Because we were not able to use a mitotic marker (the classical mitotic marker, H3S10p, cannot be used under our fixation conditions, which are important for detecting PcG proteins on chromosomes), mitotic cells were discriminated from interphase cells by image processing. Different values were used for two parameters to identify interphase or mitotic cells: the tubulin staining distribution across the cell (InnerOnOuter measurement in the pipelines) and the number of "chromosome" objects (named "MitoticIdentifier" in the pipelines) per cells. For mitotic cells, an additional parameter was used: the standard deviation of the pixel intensity for images of the tubulin staining in the whole cell.

2.11.1.1. Tubulin Staining Distribution

During mitosis, the nuclear envelope is disrupted, allowing tubulin staining across the whole cell (Güttinger et al., 2009). Thus, the tubulin staining distribution in the cells provides a means to differentiate mitotic cells (tubulin throughout the cell) from interphase cells (tubulin excluded from the nucleus). To this end, cells were divided into 3 ring-shaped areas radiating from the center of the cell and the ratio of the inner-most ring's mean tubulin intensity over the outer-most ring's mean intensity was calculated ("InnerOnOuter" in the pipelines). If the intensity of tubulin staining is uniform across the cell, this ratio would be equal to 1. In the case of interphase cells, where the tubulin staining would mostly be located in the outer and middle rings, this ratio should be less than 1 whereas in the case of mitotic cells, where the tubulin staining should be in all rings, this ratio should be close to 1.

2.11.1.2. "Chromosome" Object

Interphase and mitotic cells were also discriminated from each other based on the number of "chromosome" objects per cells. In the pipelines, such objects were defined as small bright areas that are positively stained by Hoechst and inside of cells. Therefore, the more "chromosome" objects a cell has the more likely the cell is mitotic.

2.11.1.3. Standard Deviation of Pixel Intensity for Tubulin Staining

Colchicine can form complexes with soluble tubulin in a poorly reversible manner. At low concentration, those complexes can inhibit microtubule assembly and elongation by binding their

ends. High colchicine concentration can also promote microtubule depolymerization (Leung et al., 2015). Thus, in mitotic cells, the standard deviation of tubulin staining pixel intensity in the whole cell was also used to help discriminate the cell cycle stage. A small standard deviation should be indicative of a mitotic cell.

2.11.2. Pipeline Validation

Pipelines were validated by manual inspection of identified cells for random image sets. To limit false positives, module parameters were set so that at least 80% of identified "mitotic cells" were actual mitotic cells in manual validation and at least 80% of identified "interphase cells" were actual interphase cells. False negatives were not limited.

2.12. RNAi Screen Analysis

Raw median and ratio values of Ph intensities were calculated with the pipelines for each identified cell of each well. The median of these values per well was used for the analysis and normalized using the B score method (Brideau et al., 2003). B scores were calculated using the BScore function of RNAither package (version 2.34.0) from R (version 3.6.2) (Rieber et al., 2009). Controls were excluded for the computation of the median polish. Two hit selection methods were used namely the MAD-based method and the quartile-based method (Birmingham et al., 2009; Chung et al., 2008; Douglas Zhang et al., 2006). Hits were selected based on both median and ratio values (described in the previous section) as well as the MAD-based method with k=3 and the quartile-based method with c=1.7239. Both duplicates had to score as hits with the same effect on Ph chromatin binding. All samples, except for positive controls, were used to calculate hit selection thresholds. We calculated SSMD and robust SSMD (SSMD*) to assess data quality, with samples and/or negative controls as negative reference (Zhang, 2007).

2.13. S2R+ Cells Treatment for Western Blot

The Western blot experiments and analysis were carried out by an undergraduate student under my supervision (Vincent Lapointe-Roberge). Once confluent, S2R+ cells were collected, centrifuged for 3mins at 207*g, washed in one volume of fresh media and re-centrifuged. Approximatively 35 000 S2R+ cells/well were plated on a 96 well plate (flat bottom) in up to 70µl

media, and treated with 2µg dsRNA. One hour later, the well volume was completed to 100µl. After 48hrs, cells were treated a second time with 2µg dsRNA. For samples treated with colchicine, 125ng/ml colchicine was added after 7.5hrs and cells were incubated for an additional 14hrs while samples without colchicine were incubated for 21.5hrs.

Positive control wells were treated with dsRNA targeting both *ph-d* and *ph-p* (2µg each for each treatment) and negative control wells were treated with dsRNA targeting *Venus*, a gene absent from the *Drosophila* genome. Other samples were treated with dsRNA targeting RNAi screen hits. Experiments were done in triplicates. dsRNA used targeted different sequences than those used in the RNAi screen, except for *ph-p* and *Venus*.

2.14. Western Blot

dsRNA-treated cells were harvested after centrifuging plates for 5mins at 1 193*g and 4°C. Pellets were re-suspended in 2X SDS-PAGE buffer (232µl/ml Tris pH 6.8, 100µl/ml glycerol, 34mg/ml sodium dodecyl sulfate (SDS), 120mg/ml bromophenol blue, ddH_2O) and boiled for 5mins. Samples were run on 8% SDS-PAGE gels for 80mins at 120 Volts in running buffer (14.4g/L glycine, 5.2g/L tris base, 1g/L SDS, ddH_2O), then transferred to a nitrocellulose membrane at 0.3 Ampere for 100mins in transfer buffer (14.4g/L glycine, 5.2g/L tris base, 1g/L SDS, 20% MeOH, ddH_2O). Membranes were blocked for 20mins in 5% milk/PBST (1XPBS, 3% TWEEN® 20, ddH_2O), then incubated overnight at 4°C on a shaker in primary antibody diluted in 5% milk/PBST. Primary antibodies used are as follows: anti-α-tubulin (mouse, 1:1 000), anti-Ph (rabbit, 1:1 000). Membranes were washed 3 times for 8-10mins each in PBST, incubated for 1hr20mins to 2 hrs in secondary antibody diluted in 5% milk/PBST and washed 3 times again for 8-10mins in PBST. Secondary antibodies were conjugated to Alexa Fluor 680 (anti-rabbit and anti-mouse), and used at 1:25 000 in 5% milk/PBST. Blots were scanned on an Odyssey CLx imager.

2.15. Western Blot Quantification and Analysis

Image Studio™ Lite (version 5.2) was used to quantify blots. Briefly, the median pixel intensity in the 2 pixel-wide frames around each band shape was subtracted from the shape to obtain a background value. The product of the background value and the area of the bands was then

subtracted from the total shape intensity to obtain a band's signal value. The sum of the Ph bands signal was then normalized over the corresponding tubulin band signal. The ratio Ph bands over the tubulin band for each sample was compared to the corresponding ratio in the negative control samples treated with dsRNA targeting Venus that were loaded on the same gel. Average values of triplicates were calculated.

To confirm that Western blot signals were in the linear range, three different volumes of the Venus control sample (1, 3 and 9ul) and two volumes of each other sample (3 and 9ul) were loaded. In most cases, the ratio of Ph to tubulin was higher for the 9ul volume than for 3ul, as would occur if the tubulin signal was saturated. Therefore, the 3ul volume was used for the final quantification. A one-way ANOVA test was performed (α=0.05) and multiple comparisons were corrected with a Dunnett's test.

3. Chapter 3 – Results

3.1. High Throughput Imaging Based RNAi Screen

3.1.1. Library Preparations from RNAi Template Library

DNA templates for dsRNA synthesis prepared by PCR were validated by agarose gel electrophoresis, which showed single or (more rarely) double bands with no degradation. Double bands sample contained a band at expected size and another at a size equal to double the expected size because of the presence of a T7 sequence at both ends of double band PCR products. dsRNAs for the RNAi screen were produced by *in vitro* transcription at a concentration of at least 1 200ng/µl; agarose gel electrophoresis was used to confirm that they were the expected size.

3.1.2. Knockdown Efficiency

RNAi treatments were tested in both S2 and S2R+ cells and in the presence or absence of colchicine. Ph levels after RNAi treatments were reduced by ~50% knockdown. The same treatment was also tested for Su(z)12 and Pc and showed varying efficiency ranging from 50% to 70% reduction (Figure 8, p.92).

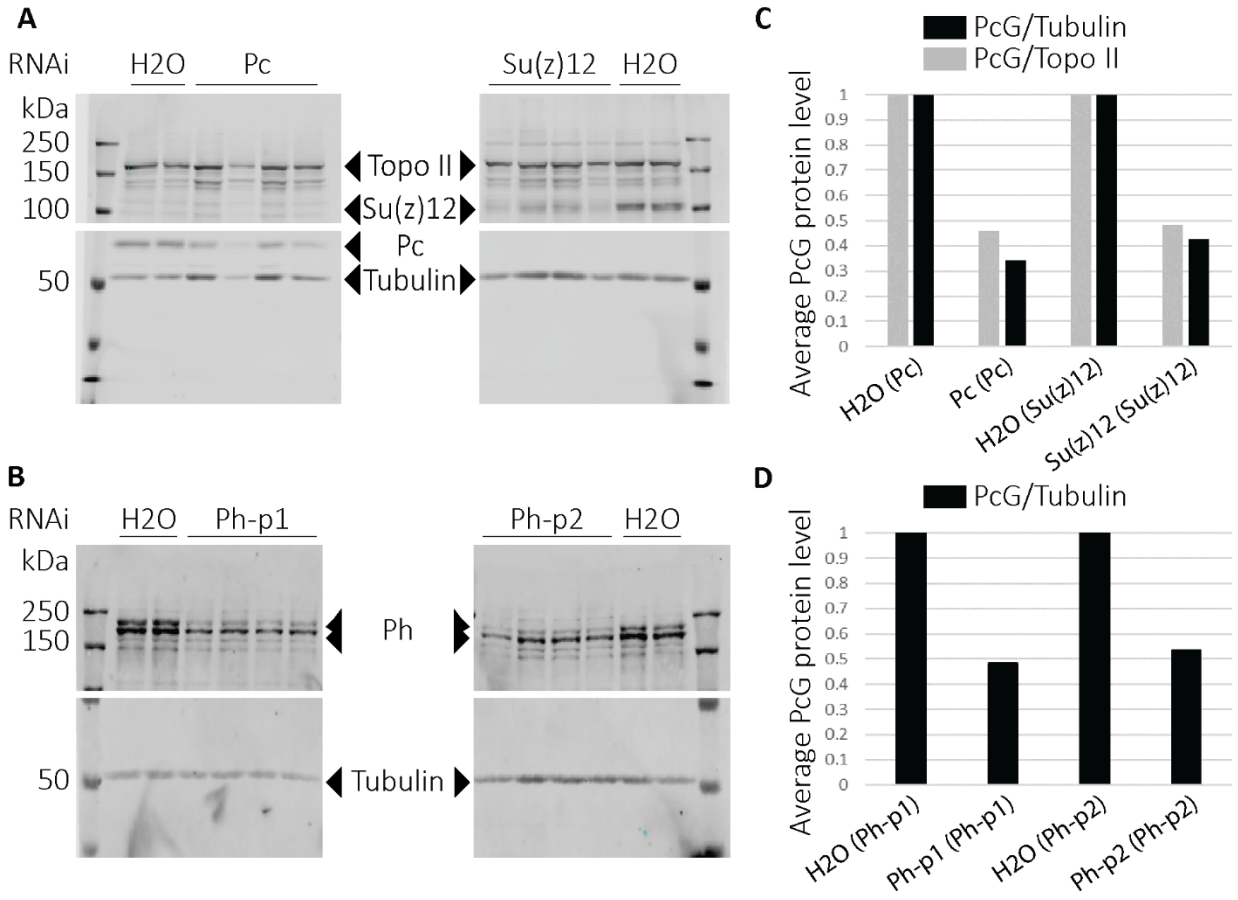

Figure 8. – RNAi Treatment Efficiency in S2 Cells. A) RNAi Treatment Against Pc and Su(z)12. B) RNAi Treatment Against Ph-p. C) Quantification of Pc and Su(z)12 Knockdown. Both Pc and Su(z)12 knockdown worked with an average efficiency of 60%. D) Quantification of Ph-p Knockdown. Ph-p1 and Ph-p2 both target *ph-p* but at different regions. Both dsRNA reagents led to an average knockdown of 50%. "RNAi"=RNA interference, "kDa"=Kilodalton, "Topo II"=Topoisomerase II.

3.1.3. Image Acquisition and Processing

Overall, 106 704 images were analyzed. Most wells contained less than 100 processed mitotic cells and more than 100 processed interphase cells. On average, 20 mitotic cells per well and 163 interphase cell per well were processed. Because mitotic cells had a lower number of processed cell/well compared to interphase cells, cells from which hits were identified were visually inspected and any cells which did not corresponded to actual mitotic cells were removed and a second round of hit identification analysis was performed. Finally, only hits for which duplicates are from wells with at least 10 cells processed were considered.

3.1.4. Normalization

The B score normalization method was used to correct the position effect observed in raw data where cell-plated top rows tended to have higher values than bottom rows. Position effect observed with raw data could not be experimentally explained nor corrected. Indeed, position bias seemed to happen from top to bottom row, which does not correspond to image acquisition order (bottom to top and left to right). Although the bias seemed to match the order of immunocytochemistry processing of the samples, delay between the processing of each row never exceeded 30secs. Thus, B score normalization was essential to data analysis for this screen.

Control wells had expected values after normalization: wells treated with dsRNA against Ph had lower values compared to the rest of the plate while wells treated with dsRNA against Venus had average values. Plate-well series plots of the screen results clearly illustrate the efficiency of the normalization method. The x-axis of these plots corresponds to well position and the y-axis to well value (Figure 9, p.94). Finally, the efficiency of the B score normalization method is also reflected by quality control (QC) metrics, where normalized values had better QC metrics than raw values (discussed below) (Table 6, p.98).

A

Plate 3b	1	2	3	4	5	6	7	8	9	10	11	12
A	1249	1250	1251	1252	1253	1254	1255	1256	1257	1258	1259	1260
B	1261	1262	1263	1264	1265	1266	1267	1268	1269	1270	1271	1272
C	1273	1274	1275	1276	1277	1278	1279	1280	1281	1282	1283	1284
D	1285	1286	1287	1288	1289	1290	1291	1292	1293	1294	1295	1296
E	1297	1298	1299	1300	1301	1302	1303	1304	1305	1306	1307	1308
F	1309	1310	1311	1312	1313	1314	1315	1316	1317	1318	1319	1320
G	1321	1322	1323	1324	1325	1326	1327	1328	1329	1330	1331	1332
H	1333	1334	1335	1336	1337	1338	1339	1340	1341	1342	1343	1344

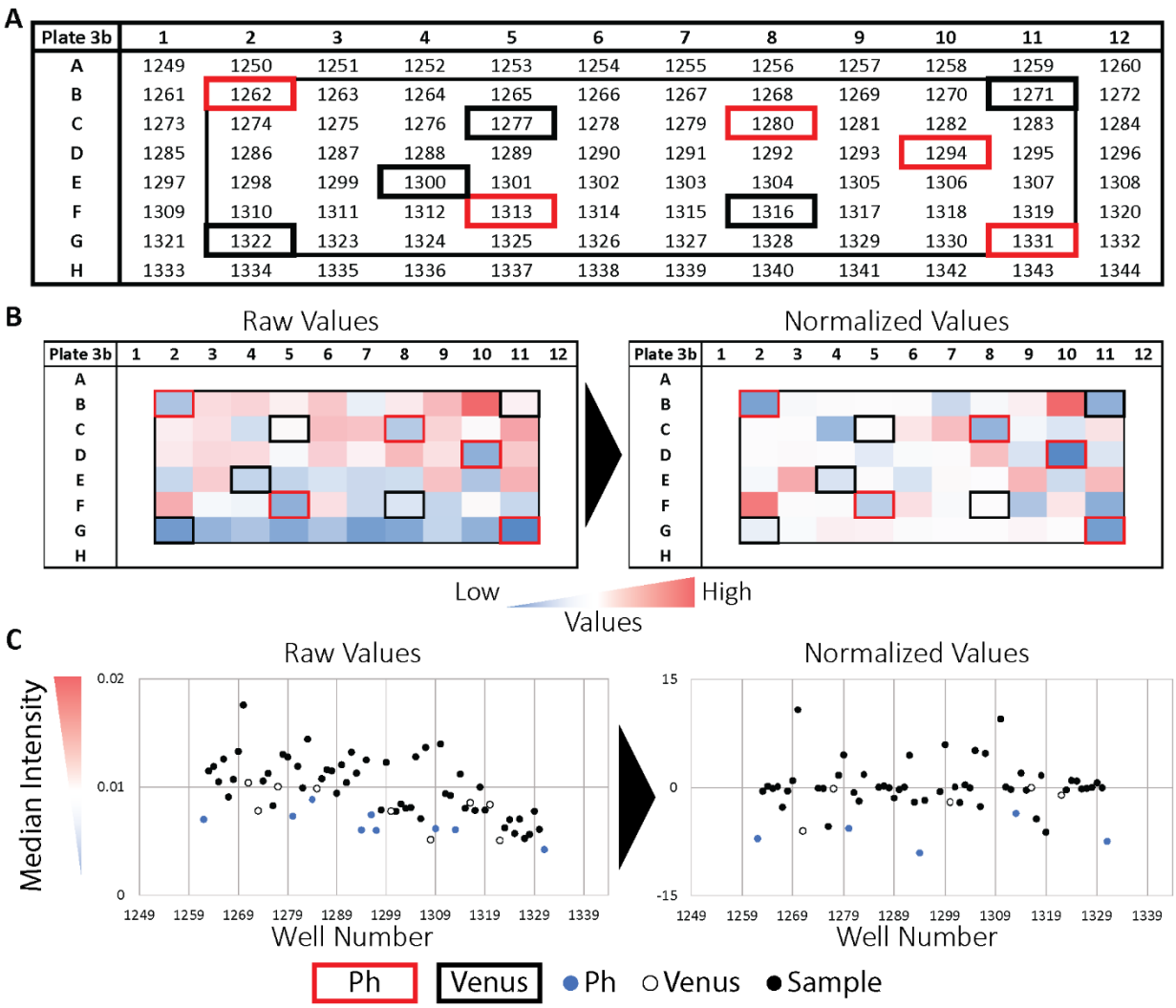

Figure 9. – Effect of B-score Normalization of Median Values from Interphase Cells. A) Well Numbers for Plate 3b. These number are used for the x-axes of panel C. B) Heatmap Of Median Values from Interphase Cells from Plate 3b Before and After B-Score Normalization. C) Plate-Well Series Plot of Median Values from Interphase Cells from Plate 3b Before and After B-Score Normalization. Position effect with a top to bottom bias is corrected with B-score normalization.

3.1.5. Quality Control

Several QC measurements were taken for both interphase and mitotic cells, from both median and ratio values as well as raw and normalized data: SSMD and SSMD* (Zhang, 2007). Different combinations of negative control well were used: Venus samples alone, or both true samples combined with Venus samples. Overall, values from interphase cells had better QC metric values than those from mitotic cells, similarly, normalized values had better metrics than raw values (Table 4-6, p.96-98). QC metrics also seemed to be influenced by the number of cells. Indeed, interphase cells were more numerous than mitotic cells and had better QC metric values. Only hits for which replicates were from plates with SSMD or SSMD* values of -0.5 or lower were considered to have passed QC (Zhang, 2011). Based on this threshold, most plates passed QC after normalization.

Table 4. – Quality Control Metrics for Interphase Cells. "Norm"= Normalized; "Int"= Interphase; Negative control: Venus (V), Samples (S); Positive control: Ph (P); "SSMD"= Strictly Standardized Mean Difference, "SSMD*"= Robust Strictly Standardized Mean Difference.

	Norm, Ratio, Int						Norm, Median, Int						Raw, Ratio, Int						Raw, Median, Int					
Plate	SSMD* (V, P)	SSMD* (S, V, P)	SSMD* (S, P)	SSMD (V, P)	SSMD (S, V, P)	SSMD (S, P)	SSMD* (V, P)	SSMD* (S, V, P)	SSMD* (S, P)	SSMD (V, P)	SSMD (S, V, P)	SSMD (S, P)	SSMD* (V, P)	SSMD* (S, V, P)	SSMD* (S, P)	SSMD (V, P)	SSMD (S, V, P)	SSMD (S, P)	SSMD* (V, P)	SSMD* (S, V, P)	SSMD* (S, P)	SSMD (V, P)	SSMD (S, V, P)	SSMD (S, P)
1a	-6.4	-6.4	-7.4	-3.4	-3.0	-3.1	-1.5	-2.7	-2.8	-2.0	-2.4	-2.5	-6.9	-3.9	-4.4	-4.6	-2.7	-2.8	-2.9	-2.8	-4.0	-4.0	-2.5	-2.6
1b	-1.5	-2.4	-2.4	-1.4	-2.3	-2.4	-0.8	-1.6	-1.6	-1.2	-1.7	-1.8	-0.9	-1.3	-1.4	-1.1	-1.2	-1.2	-0.5	-0.8	-0.8	-1.0	-1.1	-1.1
2a	-1.3	-1.0	-1.1	-1.0	-1.0	-1.0	-1.2	-0.9	-0.9	-1.1	-0.8	-0.7	-0.9	-0.6	-0.6	-0.9	-0.6	-0.6	-0.7	-0.5	-0.5	-0.7	-0.5	-0.4
2b	-3.5	-2.0	-2.1	-2.1	-1.3	-1.3	-1.5	-1.7	-1.7	-1.5	-1.2	-1.2	-1.4	-1.1	-1.0	-1.8	-1.2	-1.1	-1.6	-1.1	-1.0	-1.5	-1.0	-0.9
3a	-1.9	-0.3	-0.3	-2.3	-0.7	-0.6	-1.1	-0.2	-0.2	-2.0	-0.7	-0.6	-2.4	-0.8	-0.8	-1.6	-0.8	-0.7	-2.5	-0.8	-0.8	-1.5	-0.8	-0.7
3b	-2.5	-3.3	-3.5	-2.2	-2.5	-2.6	-2.4	-3.0	-3.1	-1.5	-1.9	-1.9	-1.2	-1.6	-1.8	-1.0	-1.4	-1.5	-0.9	-1.1	-1.2	-0.7	-1.1	-1.2
4a	-0.8	-1.5	-1.6	-1.2	-1.4	-1.4	-0.5	-1.4	-1.6	-0.6	-1.2	-1.3	-0.6	-0.7	-0.7	-0.7	-0.8	-0.8	-0.6	-0.6	-0.6	-0.4	-0.5	-0.5
4b	-3.5	-2.9	-2.9	-1.4	-1.5	-1.5	-1.8	-1.6	-1.6	-1.1	-1.4	-1.4	-1.2	-1.3	-1.3	-1.2	-1.4	-1.4	-1.6	-1.0	-1.0	-1.2	-1.2	-1.2
5a	-0.5	-0.7	-0.7	-0.6	-0.7	-0.7	-0.4	-0.6	-0.6	-0.6	-0.6	-0.6	-0.2	-0.6	-0.9	-0.3	-0.6	-0.6	-0.3	-0.4	-0.4	-0.2	-0.3	-0.3
5b	-0.5	-1.5	-1.6	-0.3	-1.2	-1.4	-1.0	-1.6	-1.8	-0.5	-1.3	-1.4	-0.6	-0.7	-0.7	-0.5	-0.8	-0.8	-0.4	-0.7	-0.7	-0.5	-0.7	-0.8
6a	-0.1	-1.7	-1.9	-0.5	-0.8	-0.8	-0.3	-1.2	-1.2	-0.5	-0.9	-0.9	-0.2	-0.7	-0.7	-0.4	-0.8	-0.8	-0.3	-0.7	-0.8	-0.5	-0.8	-0.9
6b	-0.5	-1.0	-1.0	-0.3	-0.5	-0.5	-0.3	-1.1	-1.1	-0.1	-0.4	-0.4	-0.3	-0.4	-0.3	-0.1	-0.2	-0.3	-0.2	-0.1	0.0	0.0	-0.1	-0.2
7a	-0.6	-1.4	-1.6	-0.7	-1.1	-1.1	-0.9	-1.2	-1.2	-0.9	-1.2	-1.2	-2.0	-0.9	-1.0	-0.6	-0.7	-0.7	-0.9	-0.9	-0.9	-0.8	-0.9	-0.9
7b	-2.7	-1.0	-1.2	-0.6	-0.6	-0.6	-1.8	-0.5	-0.5	-0.6	-0.3	-0.3	-0.7	-0.4	-0.2	-0.7	-0.4	-0.4	-1.0	-0.6	-0.5	-0.4	-0.3	-0.3
8a	-0.7	-0.2	-0.2	-1.0	-0.5	-0.5	-2.0	-0.8	-0.9	-1.2	-0.6	-0.5	-1.0	-0.4	-0.3	-1.4	-0.6	-0.5	-1.2	-0.4	-0.3	-1.4	-0.5	-0.4
8b	-0.6	-1.0	-1.0	-0.5	-0.7	-0.7	-0.6	-0.7	-0.7	-0.4	-0.5	-0.5	-0.5	-0.7	-0.7	-0.1	-0.5	-0.6	-0.1	-0.4	-0.5	0.0	-0.5	-0.6
9a	-2.5	-3.1	-3.2	-1.7	-1.1	-1.1	-3.9	-4.5	-4.5	-1.5	-1.2	-1.2	-1.4	-1.1	-1.1	-1.2	-0.9	-0.9	-1.2	-0.8	-0.7	-1.0	-0.7	-0.7
9b	-1.3	-1.0	-1.0	-0.5	-0.5	-0.5	0.1	-0.2	-0.2	-0.3	-0.5	-0.5	-0.1	-0.5	-0.6	-0.5	-0.6	-0.7	0.1	-0.3	-0.3	-0.2	-0.5	-0.6
10a	-0.6	-0.7	-0.7	-0.7	-0.4	-0.4	-0.7	-0.7	-0.8	-0.7	-0.3	-0.2	-0.2	0.1	0.1	-0.5	-0.3	-0.3	-0.1	0.3	0.4	-0.5	-0.2	-0.2
10b	0.9	-0.2	-0.2	0.5	0.0	-0.1	-0.3	-1.0	-1.0	0.3	-0.1	-0.1	-0.1	-0.6	-0.6	-0.3	-0.6	-0.6	0.0	-0.3	-0.4	-0.3	-0.4	-0.4
11a	0.0	-0.3	-0.3	-0.3	-0.5	-0.5	-0.2	-0.2	-0.2	-0.4	-0.5	-0.5	-0.5	-0.6	-0.6	-0.7	-0.7	-0.8	-0.6	-0.7	-0.7	-0.7	-0.7	-0.7
11b	-0.8	-0.5	-0.6	-0.5	-0.7	-0.7	-0.8	-0.8	-0.8	-0.5	-0.5	-0.5	-1.5	-1.1	-1.1	-0.8	-0.9	-0.9	-1.1	-0.9	-0.9	-0.7	-0.7	-0.7

Table 5. – Quality Control Metrics for Mitotic Cells. "Norm"= Normalized; "Mit"= Mitosis; Negative control: Venus (V), Samples (S); Positive control: Ph (P); "SSMD"= Strictly Standardized Mean Difference, "SSMD*"= Robust Strictly Standardized Mean Difference

	Norm, Ratio, Mit						Norm, Median, Mit						Raw, Ratio, Mit						Raw, Median, Mit					
Plate	SSMD* (V, P)	SSMD* (S, V, P)	SSMD* (S, P)	SSMD (V, P)	SSMD (S, V, P)	SSMD (S, P)	SSMD* (V, P)	SSMD* (S, V, P)	SSMD* (S, P)	SSMD (V, P)	SSMD (S, V, P)	SSMD (S, P)	SSMD* (V, P)	SSMD* (S, V, P)	SSMD* (S, P)	SSMD (V, P)	SSMD (S, V, P)	SSMD (S, P)	SSMD* (V, P)	SSMD* (S, V, P)	SSMD* (S, P)	SSMD (V, P)	SSMD (S, V, P)	SSMD (S, P)
1a	-1.2	-4.4	-4.5	-1.0	-2.6	-3.1	-2.4	-6.0	-6.5	-1.7	-2.3	-2.5	-1.0	-2.2	-2.3	-1.3	-2.3	-2.7	-2.5	-2.7	-2.7	-2.3	-2.0	-2.1
1b	-0.2	-1.0	-1.0	-0.6	-0.8	-0.9	-2.6	-2.3	-2.2	-1.3	-1.6	-1.6	-1.7	-1.6	-1.6	-0.9	-0.8	-0.8	-0.9	-1.0	-1.0	-1.0	-1.1	-1.1
2a	-0.6	-0.9	-0.9	-0.1	-0.5	-0.6	0.7	-0.4	-0.5	-0.1	-0.5	-0.6	-0.3	-0.4	-0.5	0.0	-0.4	-0.4	-0.1	-0.6	-0.9	-0.4	-0.6	-0.6
2b	-0.4	-0.9	-0.9	-0.3	-0.4	-0.4	0.5	1.0	1.0	-0.2	-0.1	-0.1	-0.3	-0.4	-0.4	-0.2	-0.2	-0.2	0.1	0.1	0.1	-0.2	-0.3	-0.3
3a	-0.2	0.1	0.1	-0.6	0.2	0.4	-2.3	-0.5	-0.5	-0.9	-0.3	-0.2	-0.5	0.0	0.0	-0.5	0.0	0.2	-3.1	-0.9	-1.0	-1.0	-0.4	-0.3
3b	-0.3	-0.3	-0.3	-0.1	-0.4	-0.4	-0.7	-2.0	-2.0	-0.6	-0.9	-0.9	-0.8	-0.8	-0.9	-0.4	-0.6	-0.6	-0.5	-0.8	-0.9	-0.6	-0.9	-1.0
4a	-2.8	-1.4	-1.6	-0.9	-0.9	-0.9	-0.4	-0.9	-0.9	-0.7	-1.1	-1.1	-0.8	-0.9	-1.0	-0.9	-0.7	-0.7	-1.0	-0.6	-0.5	-0.8	-0.8	-0.8
4b	-0.1	-1.7	-1.8	-0.1	-0.9	-1.0	-0.4	-1.4	-1.4	-0.3	-0.9	-1.0	-0.2	-0.6	-0.8	0.0	-0.6	-0.7	-0.4	-0.7	-0.7	-0.7	-0.9	-0.9
5a	-0.6	-1.2	-1.4	-0.9	-0.5	-0.5	-0.2	-1.1	-1.3	-0.6	-1.1	-1.2	-0.3	-0.8	-0.8	-0.8	-0.6	-0.6	-0.6	-0.6	-0.5	-0.4	-0.6	-0.6
5b	-0.3	-0.5	-0.5	-0.3	-0.6	-0.6	-0.4	-1.6	-2.0	-0.8	-1.3	-1.3	-0.7	-0.7	-0.5	0.0	-0.2	-0.2	-0.4	-0.5	-0.5	-0.2	-0.4	-0.5
6a	-3.2	-3.1	-3.3	0.1	-0.8	-1.0	0.0	-0.5	-0.5	0.2	-0.6	-0.7	-0.1	-0.6	-0.8	-0.3	-1.0	-1.1	0.1	-0.7	-0.8	-0.1	-0.8	-0.9
6b	-0.4	-0.6	-0.6	-0.6	-0.6	-0.6	0.2	0.0	0.0	0.1	-0.2	-0.2	0.0	-0.2	-0.3	-0.2	-0.3	-0.3	0.2	0.2	0.2	0.2	0.2	0.2
7a	0.1	-0.9	-0.9	0.0	-0.7	-0.8	0.6	-1.6	-1.9	0.3	-0.8	-0.9	-0.9	-0.8	-0.8	-0.1	-0.5	-0.6	-0.4	-0.9	-1.0	-0.5	-0.8	-0.9
7b	-0.6	-0.9	-0.9	0.1	-0.2	-0.3	-1.0	-1.2	-1.2	0.0	-0.2	-0.2	-1.2	-0.9	-0.8	-0.1	-0.3	-0.3	-0.4	-0.2	-0.2	-0.2	-0.2	-0.2
8a	-0.1	-0.3	-0.3	-0.2	-0.5	-0.5	-1.0	-0.7	-0.7	-0.5	-0.5	-0.5	-0.5	-0.5	-0.6	-0.5	-0.5	-0.6	-1.0	-0.4	-0.4	-0.8	-0.5	-0.5
8b	-0.7	-0.9	-0.9	-0.8	-0.8	-0.8	-1.6	-1.2	-1.1	-0.8	-0.8	-0.8	-0.6	-0.9	-0.9	-0.9	-1.0	-1.0	-0.4	-0.9	-1.0	-0.2	-0.7	-0.8
9a	-0.9	-0.7	-0.7	-0.5	-0.5	-0.5	-1.5	-1.7	-1.6	-1.3	-1.2	-1.1	-0.2	-0.3	-0.4	-0.4	-0.5	-0.6	-0.4	-0.5	-0.4	-0.4	-0.4	-0.4
9b	-1.1	-1.2	-1.2	-0.6	-0.6	-0.6	-0.9	-1.8	-2.1	-0.3	-0.7	-0.8	-0.2	-1.3	-1.5	-0.4	-0.7	-0.7	-0.6	-1.0	-1.1	-0.1	-0.6	-0.6
10a	-0.3	0.3	0.4	-0.3	-0.5	-0.5	-0.8	-0.3	-0.3	-0.9	-0.5	-0.4	-0.6	-0.7	-0.8	-0.9	-0.7	-0.7	-1.4	-0.6	-0.5	-0.8	-0.6	-0.5
10b	0.1	-0.8	-0.9	0.4	0.0	-0.1	-0.8	-0.8	-0.8	-0.1	-0.3	-0.3	-0.1	-0.2	-0.2	0.3	-0.1	-0.2	-0.2	-0.4	-0.4	-0.2	-0.2	-0.2
11a	0.9	-0.5	-0.6	-0.1	-0.6	-0.7	-0.1	-0.5	-0.5	-0.2	-0.5	-0.6	-0.1	-0.6	-0.7	-0.3	-0.7	-0.8	-0.4	-0.5	-0.5	-0.3	-0.5	-0.6
11b	0.0	-0.3	-0.3	0.2	-0.2	-0.2	0.0	0.2	0.2	-0.2	-0.2	-0.2	-0.5	-0.8	-0.8	0.2	-0.2	-0.3	-0.8	-0.6	-0.6	-0.2	-0.4	-0.5

Table 6. – Evaluation of Quality Control Metrics. A plate with any QC metric (SSMD or SSMD*) value lower than -0.5 is considered to pass quality control. "E"=Excellent (at least 1 QC≤-2), "G"= Good (at least 1 QC≤-1), "I"= Inferior (at least 1 QC≤-0.5), "P"= Poor (no QC >-0.5).

Plate	Norm, Ratio, Int	Norm, Median, Int	Raw, Ratio, Int	Raw, Median, Int	Norm, Ratio, Mit	Norm, Median, Mit	Raw, Ratio, Mit	Raw, Median, Mit
1a	E	E	E	E	E	E	E	E
1b	E	G	G	G	G	E	G	G
2a	G	G	I	I	I	I	P	I
2b	E	G	G	G	I	P	P	P
3a	E	E	E	E	I	E	I	E
3b	E	E	G	G	P	E	I	I
4a	G	G	I	I	E	G	I	I
4b	E	G	G	G	G	G	I	I
5a	I	I	I	P	G	G	I	I
5b	G	G	I	I	I	E	I	P
6a	G	G	I	I	E	I	G	I
6b	I	G	P	P	I	P	P	P
7a	G	G	E	I	I	G	I	I
7b	E	G	I	I	I	G	G	P
8a	G	E	G	G	I	G	I	G
8b	G	I	I	I	I	G	I	G
9a	E	E	G	G	I	G	I	P
9b	G	I	I	I	G	E	G	G
10a	I	I	P	P	I	I	I	G
10b	P	G	I	P	I	I	P	P
11a	I	I	I	I	I	I	I	I
11b	I	I	G	G	P	P	I	I

3.1.6. Hit Identification

Two types of hits or factors of interest were identified: genes which knockdown led to more Ph on chromatin (increased binding hits) and genes which knockdown led to less Ph on chromatin (decreased binding hits) compared to the negative control (any well except for Ph dsRNA wells). Some hits were identified exclusively from interphase cells (interphase specific hits), some exclusively from mitotic cells (mitotic specific hits) and some were identified from both interphase and mitotic cell (non cell cycle specific hits). In plate-well series plots, well position is indicated on the x-axis and intensity values are indicated on the y-axis. Threshold values for both MAD-based and quartile-based analyses are also present in the graph to facilitate hit visualization. Plots from Figure 10 (p.100) and 11 (p.101) indicate a good overlap between MAD-based and quartile-based analyses (see green dot amounts on plots) (Figure 10-12, p.100-102).

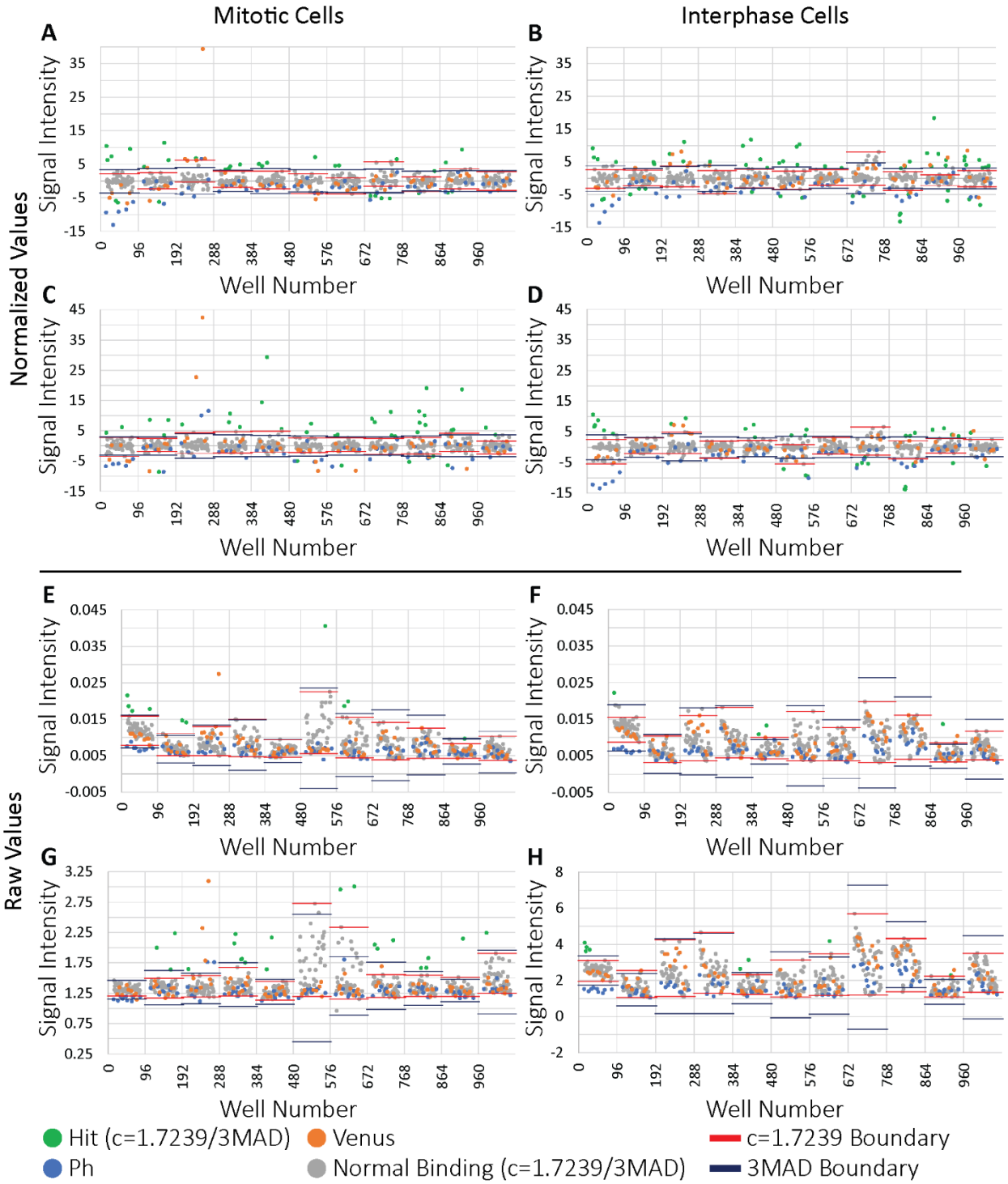

Figure 10. – Plate-Well Series Plot of Sample Replicate 1. A) Normalized Median Values from Mitotic Cells. B) Normalized Median Values from Interphase Cells. C) Normalized Ratio Values from Mitotic Cells. D) Normalized Ratio Values from Interphase Cells. E) Raw Median Values from Mitotic Cells. F) Raw Median Values from Interphase Cells. G) Raw Ratio Values from Mitotic Cells. H) Raw Ratio Values from Interphase Cells.

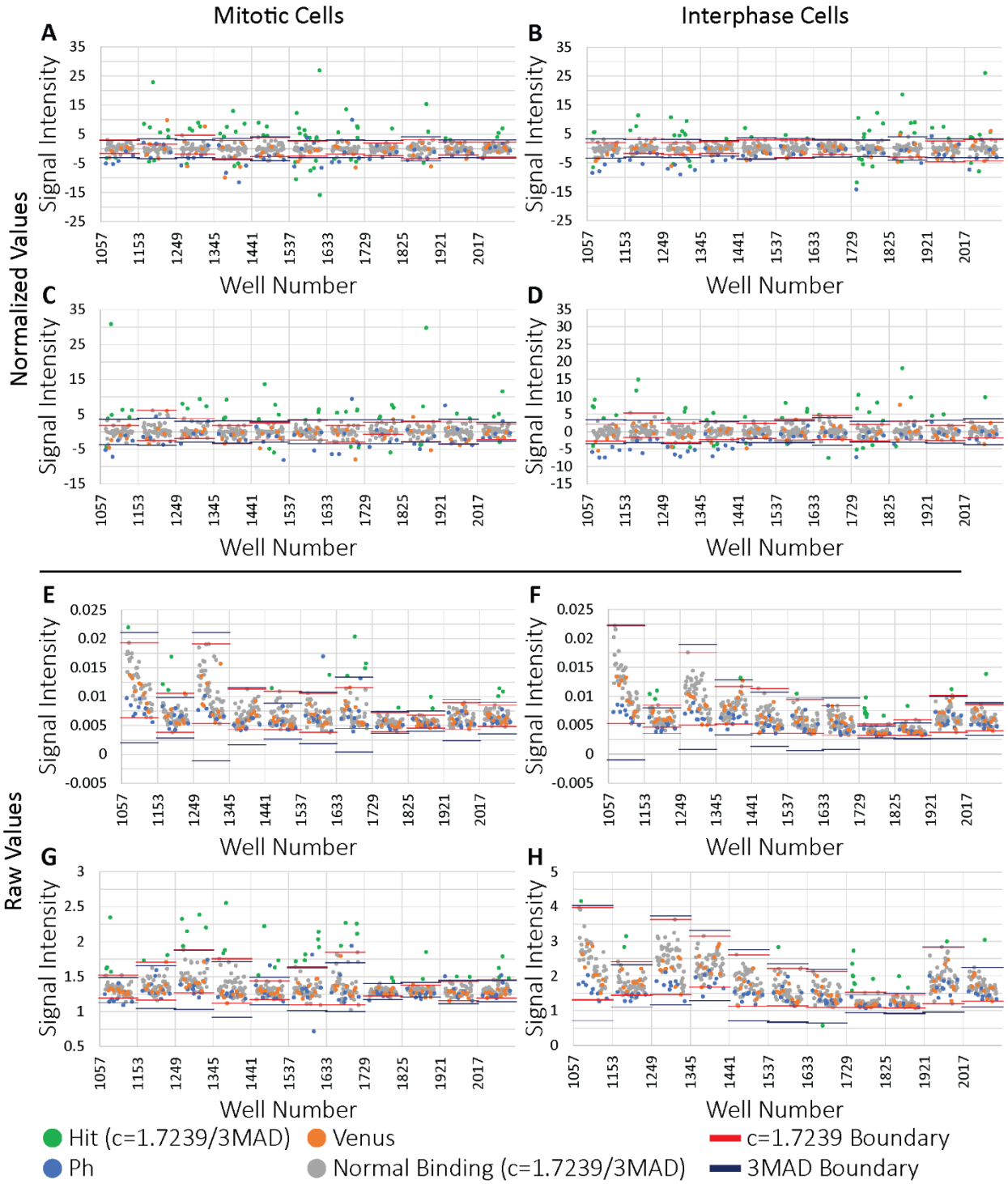

Figure 11. – Plate-Well Series Plot of Sample Replicate 2. A) Normalized Median Values from Mitotic Cells. B) Normalized Median Values from Interphase Cells. C) Normalized Ratio Values from Mitotic Cells. D) Normalized Ratio Values from Interphase Cells. E) Raw Median Values from Mitotic Cells. F) Raw Median Values from Interphase Cells. G) Raw Ratio Values from Mitotic Cells. H) Raw Ratio Values from Interphase Cells.

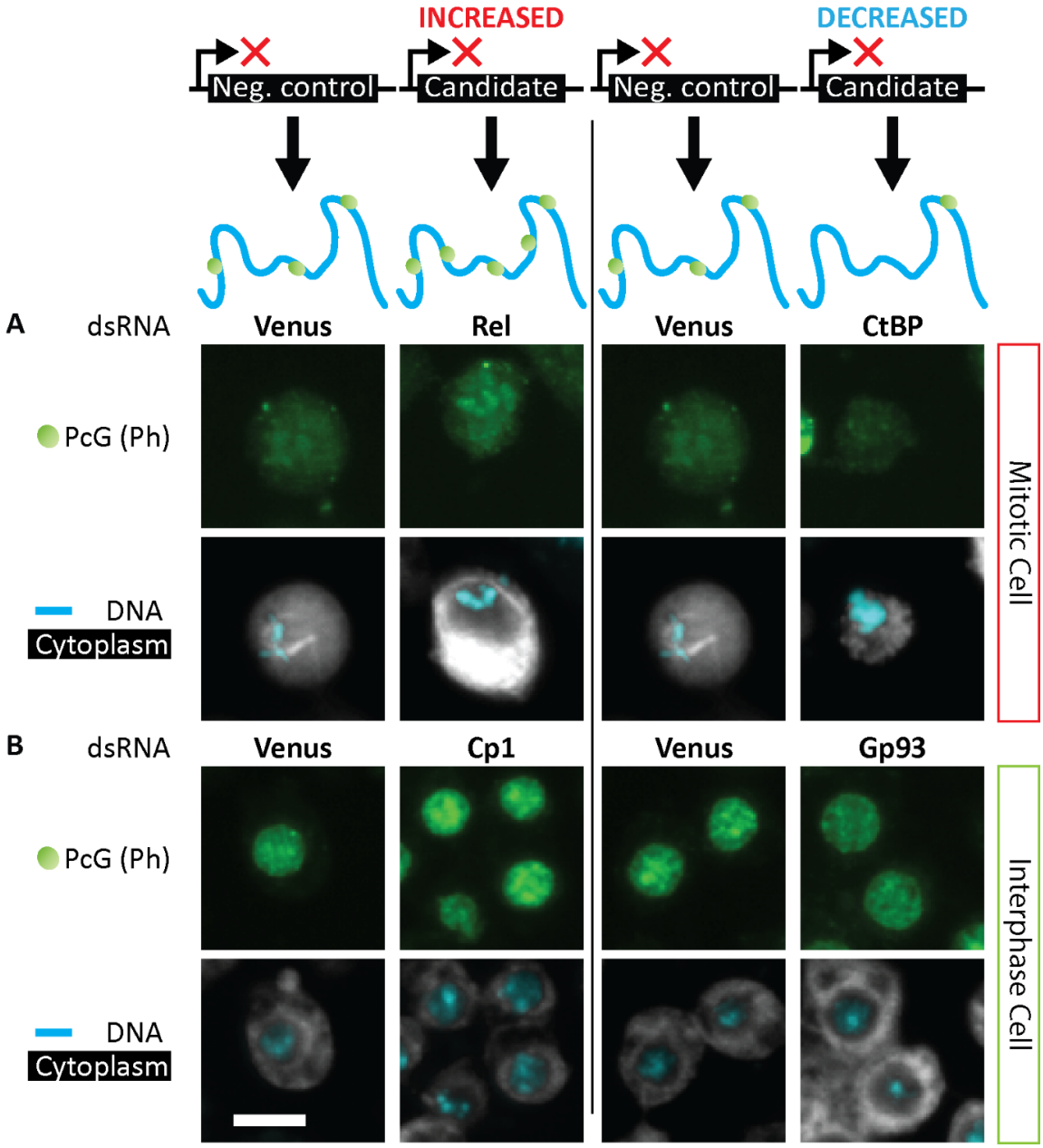

Figure 12. – Hit Examples. A) Examples of Mitosis Specific Hits. Rel knockdown led to more Ph on chromatin compared to Venus knockdown (negative control). CtBP knockdown led to less Ph on chromatin compared to Venus knockdown. B) Examples of Interphase Specific Hits. Cp1 knockdown led to more Ph on chromatin compared to Venus knockdown (negative control). Gp93 knockdown led to less Ph on chromatin compared to Venus knockdown. Nearby controls on the same plate were selected for these images to account for the plate position bias.

3.1.6.1. High Stringency Hits (3MAD or c=1.7239)

When k=3 and c=1.7239 in the MAD-based and the quartile-based method respectively, the knockdown of 27 candidate genes, or 19 after minimum number of cell processed and QC metric filtering (hereafter referred to as "quality filtering"), lead to significantly different chromatin binding levels of Ph across the cell cycle. Hits were mostly increased binding hits: genes whose knockdown led to more Ph on chromatin. Among the 19 quality filtered hits, 15 were interphase specific and only 2 were mitosis specific. Of the 15 interphase specific hits, the knockdown of 2 led to less Ph chromatin binding. Quality filtering left only decreased binding hits among mitosis specific hits. As opposed to mitosis specific hits, the knockdown of all non cell cycle specific hits (2) led to more Ph on chromatin (Table 7, p.104 and Figure 13, p.107).

Table 7. – Hit List for 3MAD and/or c=1.7239. P=plate; * = hits with at least one replicate with less than 10 processed cells or from a plate that did not pass QC (quality filtering), **= hits which were non cell cycle specific before quality filtering.

Flybase ID	Annotation symbol	Gene symbol	Specificity	Effect on binding	Value used (Mitosis)	Value used (Interphase)	Location (Replicate 1, Replicate 2)	Cell Count (Interphase) (Replicate 1, Replicate 2)	Cell Count (Mitosis) (Replicate 1, Replicate 2)
FBgn0014010	CG3664	*Rab5*	Both	Increased	Median	Both	P5aB07, P5bB07	32, 73	8, 11
FBgn0005533	CG3922	*RpS17*	Both	Increased	Median	Both	P1aB06, P1bB06	252, 224	35, 20
FBgn0284243	CG9277	*betaTub56D*	Interphase	Increased		Median	P9bF07, P11aG06	81, 69	
FBgn0023395	CG9594	*Chd3*	Interphase	Increased		Both	P8aG10, P8bG10	97, 107	
FBgn0013770	CG6692	*Cp1*	Interphase	Increased		Median	P11aE06, P11bE06	88, 87	
FBgn0260632	CG6667	*dl**	Interphase	Increased		Median	P3aB10, P3bB10	7, 6	
FBgn0002609	CG8346	*E(spl)m3-HLH**	Interphase	Increased		Both	P3aE11, P3bE11	22, 7	
FBgn0001942	CG9075	*eIF4A*	Interphase	Increased		Both	P10aD08, P10bD08	306, 124	
FBgn0283724	CG12734	*Girdin*	Interphase	Increased		Both	P1aD07, P1bD07	183, 182	
FBgn0039562	CG5520	*Gp93*	Interphase	Decreased		Both	P8aB03, P8bB03	111, 223	
FBgn0035149	CG17183	*MED30***	Interphase	Increased	Median	Ratio	P5aD04, P5bD04	13, 103	1, 4
FBgn0261617	CG15319	*nej**	Interphase	Increased		Median	P6aG09, P6bG09	2, 38	
FBgn0038872	CG5874	*Nelf-A*	Interphase	Increased		Ratio	P1aG03, P1bG03	50, 31	
FBgn0033264	CG2158	*Nup50*	Interphase	Decreased		Ratio	P1aB04, P1bB04	143, 147	
FBgn0002989	CG3736	*okr***	Interphase	Increased	Median	Both	P3aE09, P3bE09	50, 27	3, 1
FBgn0024733	CG17521	*RpL10*	Interphase	Increased		Ratio	P1aB08, P1bB08	234, 277	
FBgn0039300	CG10423	*RpS27*	Interphase	Increased		Ratio	P1aC04, P1bC04	260, 108	

FBgn0002622	CG6779	*RpS3*	Interphase	Increased		Both	P1aB03, P1bB03	282, 95	
FBgn0017545	CG2168	*RpS3A***	Interphase	Increased	Median	Both	P10aB03, P10bB03	140, 82	2, 2
FBgn0025802	CG6939	*Sbf*	Interphase	Increased		Median	P9aF06, P9bF06	111, 241	
FBgn0039117	CG10210	*tst**	Interphase	Increased		Both	P6aB05, P6bB05	4, 20	
FBgn0029094	CG9383	*asf1**	Mitosis	Increased	Ratio		P9aF02, P9bF02		4, 2
FBgn0020496	CG7583	*CtBP**	Mitosis	Decreased	Ratio		P2aE05, P2bE05		5, 8
FBgn0032293	CG6444	*Dpy-30L1*	Mitosis	Decreased	Median		P3aB05, P3bB05		30, 13
FBgn0016687	CG4634	*Nurf-38**	Mitosis	Increased	Median		P2aB03, P2bB03		13, 9
FBgn0014018	CG11992	*Rel**	Mitosis	Increased	Both		P2aG05, P2bG05		1, 5
FBgn0283477	CG6987	*SF2*	Mitosis	Decreased	Median		P1aD03, P1bD03		47, 21

44% (12/27) of non-filtered hits were part of the top 200 co-purifying proteins in an AP-MS experiment (performed by former lab members, data not shown) which aimed at identifying proteins interacting with Ph in the chromatin fraction of cells. This number goes up to 63% (12/19) after quality filtering. 40% (11/27) of the identified factors of interest were related to TrxG proteins and did not overlap with the list of Ph co-purifying hits. However, after quality filtering this number dropped to 21% (4/19), which still represents half of the non-Ph co-purifying hits (Figure 13, p.107). Mitosis specific hits were mostly related to TrxG proteins compared to interphase specific hits and non cell cycle specific hits (Figure 14, p.116). None of the mitosis specific hits with quality filtering are PcG related.

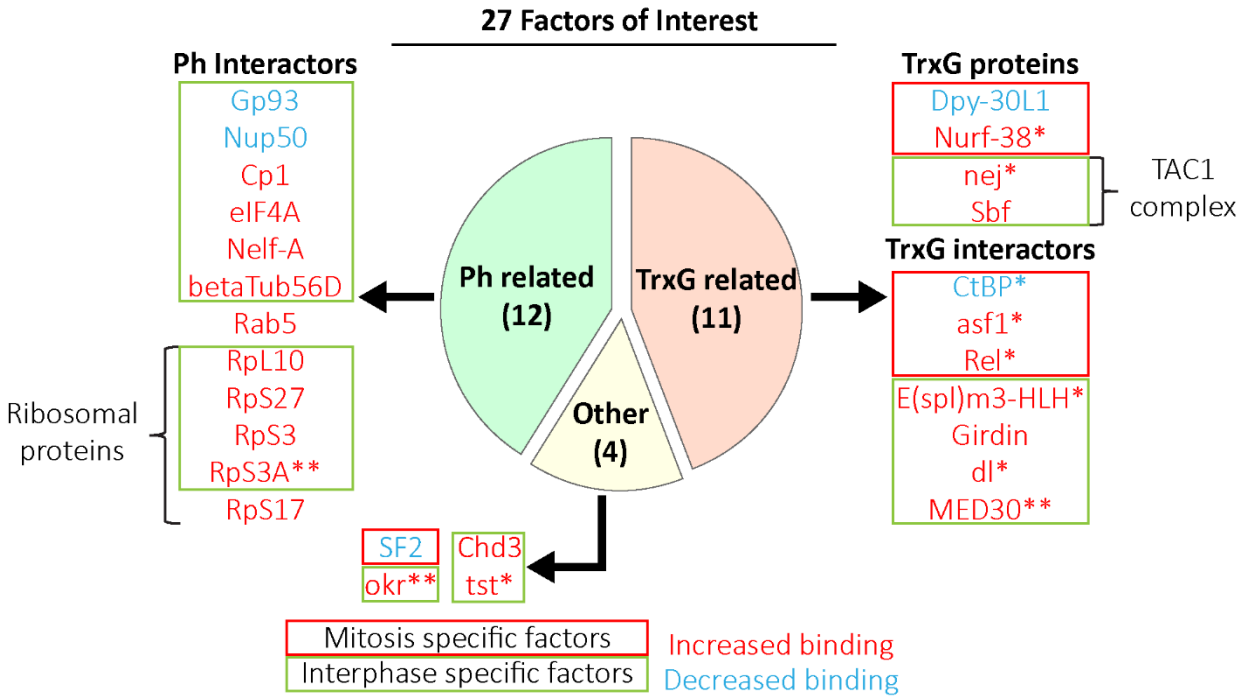

Figure 13. – Identified Factors of Interest (3MAD/c=1.7239). A substantial part of the hits co-purified with Ph in an AP-MS experiment where Ph-p was the bait for purification from the chromatin fraction. Mitosis specific hits are not Ph interactors. Several ribosomal proteins scored as hits as well as several members of the TAC1 complex (without quality filtering for the latter). * = hits with at least one replicate with less than 10 processed cells or from a plate that did not pass QC (quality filtering), **= hits which were non cell cycle specific before quality filtering.

Without quality filtering, Flybase gene group analysis of hits revealed similarities between hits. RpS17, Rps3A, RpL10, RpS27 and RpS3 are all increased binding hits identified from interphase cells and part of the ribosome. Interphase specific and increased binding hits nej and Sbf also share a common TrxG protein complex: Trithorax acetylation complex 1 (TAC1). CtBP and nej are involved in the regulation of Wnt-TCF Signaling Pathway, with CtBP being identified as a mitosis specific decreased binding hit however. Finally, Rel and dl are both increased binding hits and part of the NF-κB transcription factor family. However, Rel was exclusively identified from mitotic cells while dl was identified from interphase cells only. After quality filtering however, only ribosomal protein shared similarities (Table 8, p.109).

Table 8. – Flybase Gene Group Analysis (3MAD/c=1.7239). * = hits with at least one replicate with less than 10 processed cells or from a plate that did not pass QC.

Flybase Group Name	Hit Member Count	Members
Basic Helix-Loop-Helix Transcription Factors	1	E(spl)m3-HLH*
Beta Tubulins	1	betaTub56D
Chromodomain Helicases	1	Chd3
Compass Complex	1	Dpy-30L1
Cytoplasmic Large Ribosomal Proteins	1	RpL10
Cytoplasmic Translation Initiation Factors	1	eIF4A
DNA-(Apurinic Or Apyrimidinic Site) Lyases	1	RpS3
Dual Specificity Phosphatases	1	Sbf
Enhancer of Split Gene Complex	1	E(spl)m3-HLH*
Heat Shock Protein 90 Chaperones	1	Gp93
Lysine Acetyltransferases	1	nej*
Mediator Complex	1	MED30
Nuclear Pore Complex	1	Nup50
Nucleosome Remodeling Factor	1	Nurf-38*
Other CH-OH Oxidoreductases, NAD Or NADP As Acceptor	1	CtBP*
Positive Regulators of Hedgehog Signaling Pathway	1	nej*
Rab GTPases	1	Rab5
Rab Guanine Nucleotide Exchange Factors - Denn Domain	1	Sbf
TORC Complex	1	CtBP*
Trr Complex	1	Dpy-30L1
Trx Complex	1	Dpy-30L1
Negative Regulators of Wnt-TCF Signaling Pathway	2	nej*, CtBP*
Nuclear Factor - Kappa B	2	Rel*, dl*
Positive Regulators of Wnt-TCF Signaling Pathway	2	nej*, CtBP*
Trithorax Acetylation Complex 1	2	Sbf, nej*
Cytoplasmic Small Ribosomal Proteins	4	RpS27, RpS17, RpS3, RpS3A

3.1.6.2. Low Stringency Hits (2MAD or c=0.9826)

When k=2 and c=0.9826 in the MAD-based and the quartile-based method respectively, the knockdown of 63 candidate genes, or 46 after quality filtering, led to significantly different chromatin binding of Ph across the cell cycle. Most hits were increased binding hits. Of the 46 hits, 32 were interphase specific, 8 were mitosis specific and 6 were non cell cycle specific. In terms of decreased binding hits, 8 were interphase specific, 4 were mitosis specific and 3 were non cell cycle specific (Table 9, p.111).

Table 9. – Hit List for 2MAD and/or c=0.9826. P=plate; * = hits with at least one replicate with less than 10 processed cells or from a plate that did not pass QC (quality filtering), **= hits which were non cell cycle specific before quality filtering.

Flybase ID	Annotation symbol	Gene symbol	Specificity	Effect on binding	Value used (Mitosis)	Value used (Interphase)	Location (Replicate 1, Replicate 2)	Cell Count (Interphase) (Replicate 1, Replicate 2)	Cell Count (Mitosis) (Replicate 1, Replicate 2)
FBgn0013770	CG6692	*Cp1*	Both	Increased	Median	Median	P11aE06, P11bE06	88, 87	32, 23
FBgn0039562	CG5520	*Gp93*	Both	Decreased	Median	Both	P8aB03, P8bB03	111, 223	12, 47
FBgn0038872	CG5874	*Nelf-A*	Both	Increased	Median	Ratio	P1aG03, P1bG03	50, 31	36, 12
FBgn0033264	CG2158	*Nup50*	Both	Decreased	Ratio	Ratio	P1aB04, P1bB04	143, 147	47, 46
FBgn0005533	CG3922	*RpS17*	Both	Increased	Both	Both	P1aB06, P1bB06	252, 224	35, 20
FBgn0283477	CG6987	*SF2*	Both	Decreased	Median	Median	P1aD03, P1bD03	168, 163	47, 21
FBgn0000147	CG3068	*aurA*	Interphase	Increased		Ratio	P7aB04, P7bB04	20, 22	
FBgn0025463	CG4303	*Bap60*	Interphase	Decreased		Median	P7aE03, P7bE03	63, 13	
FBgn0263231	CG9748	*bel*	Interphase	Increased		Ratio	P7aB03, P7bB03	77, 46	
FBgn0284243	CG9277	*betaTub56D*	Interphase	Increased		Median	P9bF07, P11aG06	81, 69	
FBgn0026262	CG2009	*bip2*	Interphase	Increased		Median	P8aF09, P8bF09	103, 314	
FBgn0042134	CG18811	*Capr*	Interphase	Increased		Ratio	P6aD04, P6bD04	63, 46	
FBgn0015618	CG10572	*Cdk8*	Interphase	Decreased		Median	P11aB06, P11bB06	91, 58	
FBgn0023395	CG9594	*Chd3*	Interphase	Increased		Both	P8aG10, P8bG10	97, 107	
FBgn0004198	CG11387	*ct**	Interphase	Increased		Median	P6aC03, P6bC03	2, 25	
FBgn0015075	CG9054	*Ddx1*	Interphase	Decreased		Median	P9aC09, P9bC09	493, 459	

FBgn0260632	CG6667	*dl**	Interphase	Increased		Median	P3aB10, P3bB10	7, 6	
FBgn0002609	CG8346	*E(spl)m3-HLH**	Interphase	Increased		Both	P3aE11, P3bE11	22, 7	
FBgn0035624	CG12756	*Eaf6*	Interphase	Increased		Ratio	P1aF06, P1bF06	261, 275	
FBgn0284245	CG8280	*eEF1alpha1*	Interphase	Increased		Ratio	P6aC07, P6bC07	128, 56	
FBgn0001942	CG9075	*eIF4A*	Interphase	Increased		Both	P10aD08, P10bD08	306, 124	
FBgn0019990	CG1609	*Gcn2*	Interphase	Decreased		Both	P8aD07, P8bD07	172, 174	
FBgn0005198	CG6975	*gig*	Interphase	Decreased		Median	P11aC07, P11bC07	179, 164	
FBgn0283724	CG12734	*Girdin*	Interphase	Increased		Both	P1aD07, P1bD07	183, 182	
FBgn0036811	CG6884	*MED11*	Interphase	Increased		Ratio	P8aF07, P8bF07	17, 13	
FBgn0034795	CG3695	*MED23*	Interphase	Decreased		Median	P3aE06, P3bE06	182, 166	
FBgn0035149	CG17183	*MED30***	Interphase	Increased	Median	Ratio	P5aD04, P5bD04	13, 103	1, 4
FBgn0035357	CG1244	*MEP-1**	Interphase	Increased		Median	P6aF09, P6bF09	1, 5	
FBgn0261617	CG15319	*nej**	Interphase	Increased		Median	P6aG09, P6bG09	2, 38	
FBgn0002989	CG3736	*okr***	Interphase	Increased	Median	Both	P3aE09, P3bE09	50, 27	3, 1
FBgn0039776	CG31022	*PH4alphaEFB*	Interphase	Decreased		Median	P10aF09, P10bF09	497, 134	
FBgn0004861	CG18412	*ph-p*	Interphase	Decreased		Both	P8aC11, P8bC11	420, 320	
FBgn0014010	CG3664	*Rab5***	Interphase	Increased	Median	Both	P5aB07, P5bB07	32, 73	8, 11
FBgn0003261	CG10279	*Rm62*	Interphase	Increased		Ratio	P3aB04, P3bB04	250, 78	
FBgn0024733	CG17521	*RpL10*	Interphase	Increased		Both	P1aB08, P1bB08	234, 277	
FBgn0035422	CG12740	*RpL28*	Interphase	Increased		Ratio	P8aB04, P8bB04	236, 351	
FBgn0004403	CG1524	*RpS14a***	Interphase	Increased	Median	Ratio	P4aB05, P4bB05	10, 319	3, 10
FBgn0039300	CG10423	*RpS27***	Interphase	Increased	Both	Both	P1aC04, P1bC04	260, 108	29, 5
FBgn0002622	CG6779	*RpS3*	Interphase	Increased		Both	P1aB03, P1bB03	282, 95	

FBgn0017545	CG2168	*RpS3A***	Interphase	Increased	Median	Both	P10aB03, P10bB03	140, 82	2, 2
FBgn0025802	CG6939	*Sbf*	Interphase	Increased		Both	P9aF06, P9bF06	111, 241	
FBgn0039169	CG5669	*Spps*	Interphase	Increased		Median	P6aG10, P6bG10	22, 21	
FBgn0039117	CG10210	*tst**	Interphase	Increased		Both	P6aB05, P6bB05	4, 20	
FBgn0027492	CG5643	*wdb*	Interphase	Increased		Median	P11aF10, P11bF10	67, 207	
FBgn0029094	CG9383	*asf1**	Mitosis	Increased	Ratio		P9aF02, P9bF02		4, 2
FBgn0032354	CG4788	*CG4788**	Mitosis	Increased	Ratio		P4aD03, P4bD03		2, 16
FBgn0020496	CG7583	*CtBP**	Mitosis	Decreased	Ratio		P2aE05, P2bE05		5, 8
FBgn0000395	CG15671	*cv-2*	Mitosis	Decreased	Median		P9aD06, P9bD06		18, 49
FBgn0032293	CG6444	*Dpy-30L1*	Mitosis	Decreased	Both		P3aB05, P3bB05		30, 13
FBgn0036004	CG3654	*Jarid2*	Mitosis	Decreased	Ratio		P9aE03, P9bE03		33, 45
FBgn0036581	CG5057	*MED10**	Mitosis	Increased	Ratio		P7aE08, P7bE08		1, 3
FBgn0035145	CG12031	*MED14**	Mitosis	Increased	Ratio		P10aG05, P10bG05		1, 1
FBgn0035851	CG7999	*MED24**	Mitosis	Increased	Ratio		P11aG08, P11bG08		17, 12
FBgn0016687	CG4634	*Nurf-38**	Mitosis	Increased	Median		P2aB03, P2bB03		13, 9
FBgn0038344	CG5205	*obe*	Mitosis	Increased	Ratio		P9aD03, P9bD03		26, 38
FBgn0283509	CG3832	*Phm*	Mitosis	Increased	Ratio		P10aB10, P10bB10		10, 21
FBgn0011474	CG3307	*PR-Set7**	Mitosis	Increased	Ratio		P11aF03, P11bF03		19, 14
FBgn0014018	CG11992	*Rel**	Mitosis	Increased	Both		P2aG05, P2bG05		1, 5
FBgn0000100	CG7490	*RpLP0**	Mitosis	Increased	Median		P8aF11, P8bF11		2, 7
FBgn0266411	CG45051	*sima*	Mitosis	Decreased	Ratio		P1aB09, P1bB09		78, 37
FBgn0011715	CG1064	*Snr1**	Mitosis	Decreased	Ratio		P3aB03, P3bB03		30, 1
FBgn0263392	CG43444	*Tet*	Mitosis	Increased	Ratio		P8aD05, P8bD05		9, 19

FBgn0004395	CG4620	*unk*	Mitosis	Increased	Median		P10aF04, P10bF04		29, 5

31% (20/63) of total hits were part of the top 200 co-purifying proteins in the aforementioned AP-MS experiment. This number goes up to 41% (19/46) after quality filtering. 44% (28/63) were related to TrxG proteins and did not overlap with the list of Ph co-purifying hits. After quality filtering, this number dropped to 32% (15/46). Mitosis specific hits were mostly related to TrxG proteins compared to interphase specific hits and non cell cycle specific hits with or without quality filtering (Figure 14, p.116). The majority of hits were interphase specific, regardless of the stringency of the data analysis and the presence or absence of quality filtering (Figure 15, p.117).

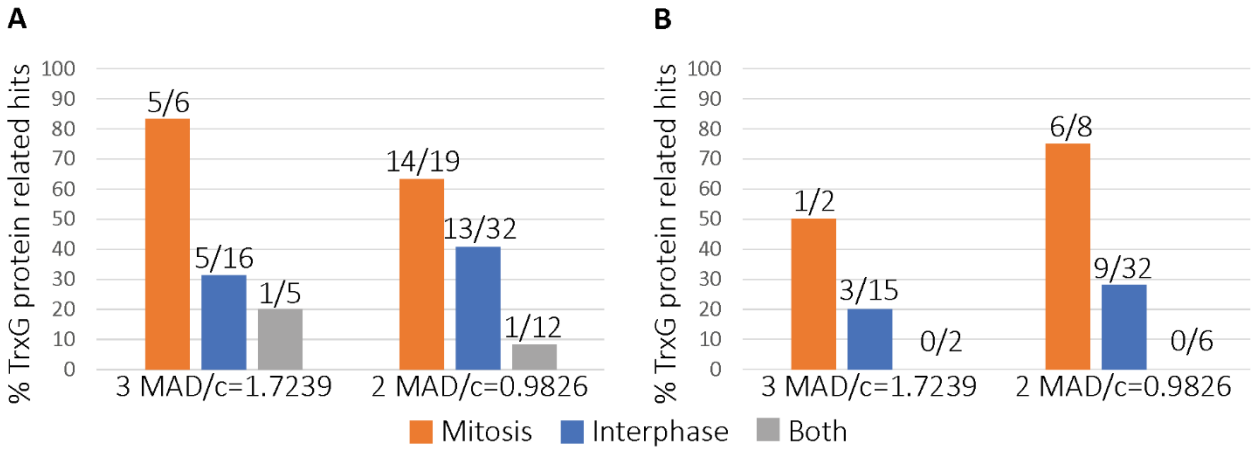

Figure 14. – Fraction of Cell Cycle Specific Genes Related to TrxG Proteins. A) Fraction of Cell Cycle Specific Genes Related to TrxG Proteins Before Quality Filtering. B) Fraction of Cell Cycle Specific Genes Related to TrxG Proteins After Quality Filtering. Quality filtering includes verification of quality control metrics and minimum processed cell number. Mitosis specific hits are enriched in TrxG related candidates compared to interphase specific hits and non cell cycle specific hits, regardless of the analysis stringency, quality control metric and cell number filtering.

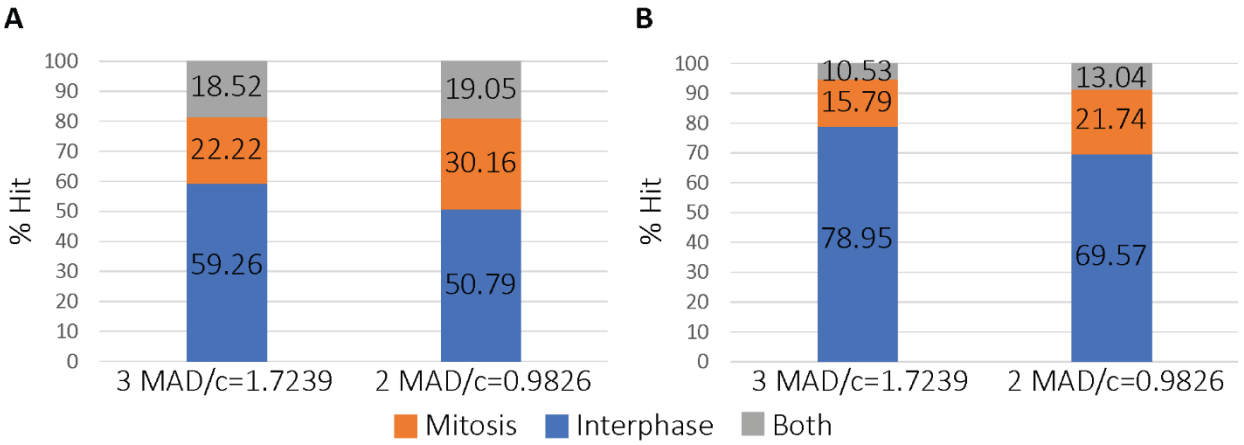

Figure 15. – Cell Cycle Specificity of Hits. A) Cell Cycle Specificity of Hits Before Quality Filtering. B) Cell Cycle Specificity of Hits After Quality Filtering. Quality filtering includes verification of quality control metrics and minimum processed cell number. Most hits were interphase specific, regardless of analysis stringency.

Additional ribosomal proteins were identified: RpL28 (Interphase specific), RpLP0 (Mitosis specific), RpS14a (Non cell cycle specific without quality filtering). Note that RpS14a, RpS27 and RpS3A are non cell cycle specific at lower stringency and without quality filtering. Without quality filtering additional members of the mediator complex identified were MED23, MED14, MED11, MED10, Cdk8 and MED24 at lower stringency, with most of them being increased binding hits. However, no cell cycle specificity class was enriched for members of the mediator complex. Bap60 and Snr1 decreased binding hits were part of both the "Polybromo-containing brahma associated proteins complex" gene group and the "Brahma associated proteins complex" gene group. Their cell cycle specificity differed, however. E(spl)me3-HLH and sima are Basic helix-loop-helix transcription factors, meaning that they contain a DNA binding domain neighbouring a helix-loop-helix motif. E(spl)me3-HLH (increased binding, interphase specific) and sima (decreased binding, mitosis specific) were opposite type of hits. Two additional signaling pathway were revealed by the gene group analysis of lower stringency hits: the Hedgehog signaling pathway (wdb, nej: both interphase specific and increased binding hits) and the insulin-like receptor signaling pathway (wdb, gig: both interphase specific hits). Finally, interphase specific hits aurA (increased binding) and Gcn2 (decreased binding) are both protein kinases (Table 10, p.119).

After quality filtering however, only MED23, MED11 and Cdk8 were identified; all of them being interphase specific hits. Equal number of increased and decreased binding hits were identified among the mediator complex members. The number of gene groups shared by 2 or more quality filtered hits was also lower (Table 10, p.119).

Table 10. – Flybase Gene Group Analysis (2MAD/c=0.9826). * = hits with at least one replicate with less than 10 processed cells or from a plate that did not pass QC.

FlyBase Group Name	Hit Member Count	Members
A-T Rich Interaction Domain Transcription Regulators	1	Jarid2
Beta Tubulins	1	betaTub56D
C2H2 Zinc Finger Transcription Factors	1	Spps
Chromodomain Helicases	1	Chd3
Compass Complex	1	Dpy-30L1
Cut Homeobox Transcription Factors	1	ct*
Cyclin Dependent Kinases	1	Cdk8
Cytoplasmic Translation Elongation Factors	1	eEF1alpha1
Cytoplasmic Translation Initiation Factors	1	eIF4A
DNA-(Apurinic Or Apyrimidinic Site) Lyases	1	RpS3
Dual Specificity Phosphatases	1	Sbf
Enhancer of Split Gene Complex	1	E(spl)m3-HLH*
Enok Complex	1	Eaf6
Heat Shock Protein 90 Chaperones	1	Gp93
Hypoxia-Inducible Factor	1	sima
Insulin-Like Receptor Signaling Pathway Core Components	1	sima
Jumonji C Domain-Containing Lysine Demethylases	1	Jarid2
Lysine Acetyltransferases	1	nej*
Negative Regulators of Hedgehog Signaling Pathway	1	wdb
Nuclear Pore Complex	1	Nup50
Nucleosome Remodeling Deacetylase Complex	1	MEP-1*
Nucleosome Remodeling Factor	1	Nurf-38*
Other CH-OH Oxidoreductases, NAD Or NADP As Acceptor	1	CtBP*
Other Paired Donor Oxidoreductases, Incorporation of Molecular Oxygen, 2-Oxoglutarate As Donor	1	Tet
Oxidoreductases Acting on Single Donors with Incorporation of Two Atoms Of Oxygen	1	PH4alphaEFB
Paired Donor Oxidoreductases, Incorporation of Molecular Oxygen, Ascorbate as Donor	1	Phm
Peptidyl-Proline Dioxygenases	1	PH4alphaEFB
Polycomb Repressive Complex 1 (Core Subunits)	1	ph-p
Rab GTPases	1	Rab5
Rab Guanine Nucleotide Exchange Factors - Denn Domain	1	Sbf
Rap-Like GTPase Activating Proteins	1	gig
Ring Finger Domain Proteins	1	unk
Set Domain Lysine Methyltransferases	1	PR-Set7*

Sp1/Klf Transcription Factors	1	Spps
Tip60 Complex	1	Eaf6
TORC Complex	1	CtBP*
Transcription Factor II D	1	bip2
Trr Complex	1	Dpy-30L1
Trx Complex	1	Dpy-30L1
Tsc1-Tsc2 Complex	1	gig
Wdb-Protein Phosphatase 2a Complex	1	wdb
Basic Helix-Loop-Helix Transcription Factors	2	E(spl)m3-HLH*, sima
Brahma Associated Proteins Complex	2	Bap60, Snr1*
Negative Regulators Of Insulin-Like Receptor Signaling Pathway	2	wdb, gig
Negative Regulators Of Wnt-TCF Signaling Pathway	2	nej*, CtBP*
Nuclear Factor - Kappa B	2	Rel*, dl*
Other Conventional Protein Kinase Domain Kinases	2	aurA, Gcn2
Polybromo-Containing Brahma Associated Proteins Complex	2	Bap60, Snr1*
Positive Regulators Of Hedgehog Signaling Pathway	2	wdb, nej*
Positive Regulators Of Wnt-TCF Signaling Pathway	2	nej*, CtBP*
Trithorax Acetylation Complex 1	2	Sbf, nej*
Cytoplasmic Large Ribosomal Proteins	3	RpL10, RpL28, RpLP0*
Cytoplasmic Small Ribosomal Proteins	5	RpS3, RpS3A, RpS17, RpS27, RpS14a
Mediator Complex	7	MED23, MED14*, MED11, MED10*, Cdk8, MED24*, MED30

3.2. Analysis of Total Ph Levels in dsRNA-Treated Cells

To determine whether changes in Ph binding to chromatin reflect changes in total Ph levels in cells, we carried out quantitative Western blot analysis of dsRNA-treated cells for the high stringency hits. No significant changes in Ph levels were observed after dsRNA treatments (Figure 16, p.122).

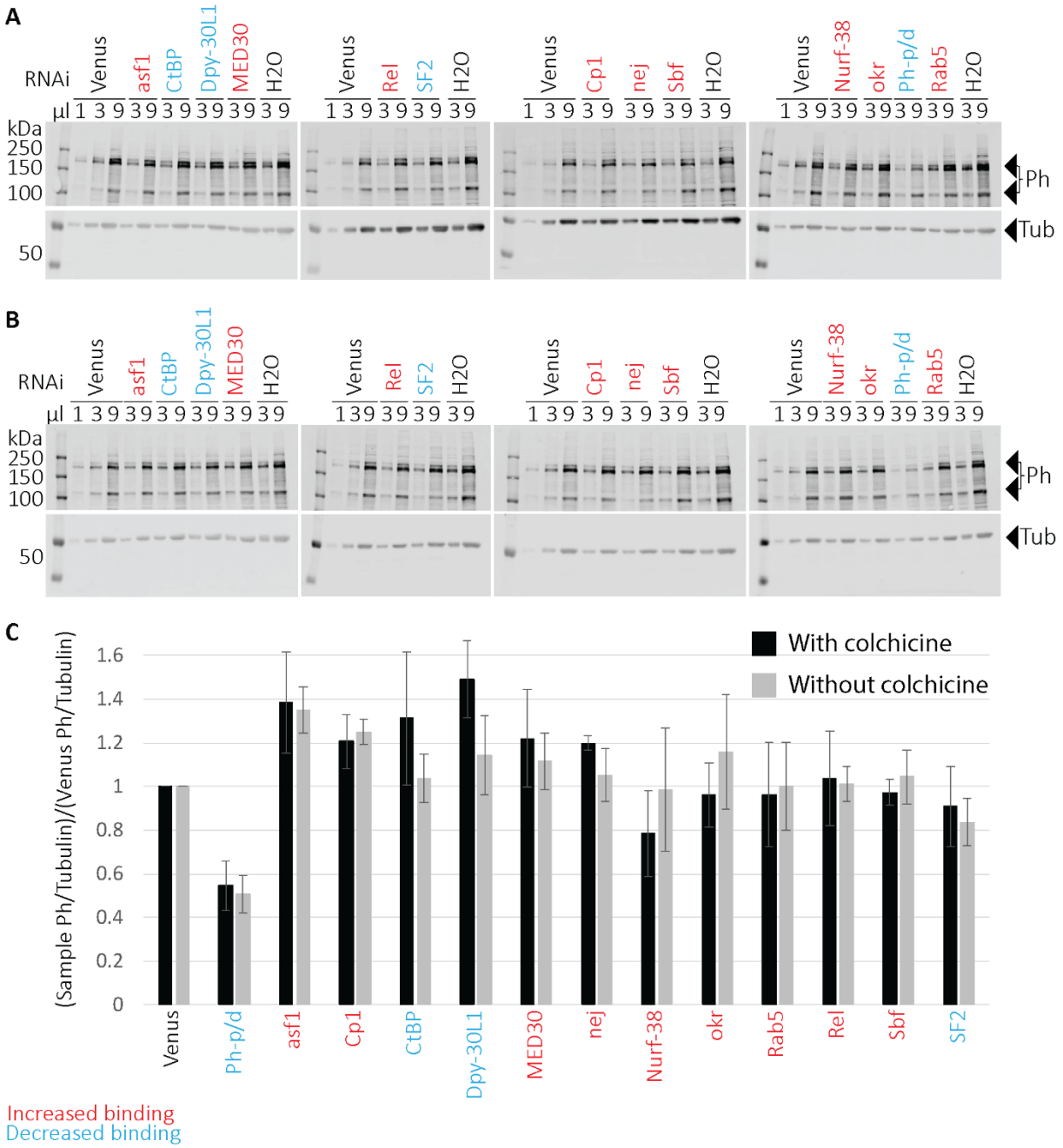

Figure 16. – Quantitative Analysis of dsRNA-Treated Cells. A) Samples Treated with Colchicine. B) Samples Treated Without Colchicine. C) Average values of RNAi treatment with standard errors of the mean. Samples of 3µl were quantified and analyzed using a one-way ANOVA test (α=0.05). Dunnett's test was used to account for multiple comparisons. No significant differences Ph levels were observed. "RNAi"=RNA interference, "kDA"= Kilodalton, "Tub"=Tubulin, n=3. Author contribution: Vincent Lapointe-Roberge and Aurélie Huang Sung.

3.3. Hit Confirmation Attempt

In an attempt to confirm identified screen hits, several experiments were performed. However, as outlined below, these methods did not succeed in confirming the hits.

3.3.1. Cell Fractionation

A scaled down cell fractionation protocol was performed to measure Ph levels in the chromatin fraction by quantitative Western blot analysis (Follmer et al., 2012). However, variation between replicates and unexpected control results led to inconsistent results so that screen hits could not be confirmed (or invalidated).

Although the cell fractionation protocol tested could not be scaled down and led to inconclusive results, we tested another protocol which seemed to work for lower amounts of cells (Shiomi et al., 2012). Preliminary results from this protocol showed expected values for control samples (treated with dsRNA against Venus as a negative control or Ph as a positive control). Indeed: Ph knockdown led to lower Ph level in every fraction compared to Venus knockdown (Figure 17, p.124).

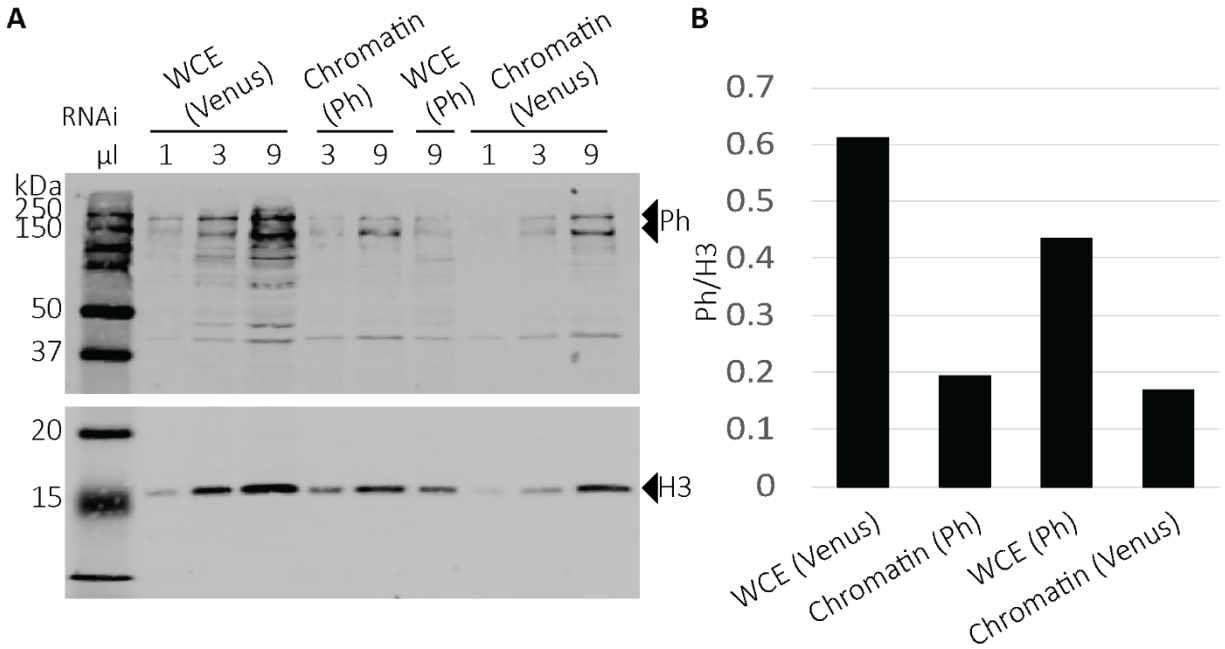

Figure 17. – Quantitative Western Blot Analysis of Whole Cell Extracts and Chromatin Fraction. A) Western Blot of Whole Cell Extracts and Chromatin Fraction from Cells Treated With dsRNA Against Ph and Venus. B) Quantitative Analysis of Fractions from dsRNA-Treated Cells. As expected, Ph knockdown led to lower Ph level both in the whole cell and in the chromatin fraction. Samples of 3µl were quantified. "RNAi"=RNA interference, "kDa"= Kilodalton.

3.3.2. Flow Cytometry of Extracted Cells

Another attempt at confirming screening hits was to use a flow cytometry-based assay (Forment & Jackson, 2015). Briefly, cytoplasmic proteins were detergent-extracted from cells prior to fixation and processing for immunofluorescence with antibodies against H3S10p (mitotic cell marker) and Ph. Samples were then analyzed by flow cytometry. This should allow quantification of the chromatin-associated signal. Again, control samples were inconsistent and had unexpected values which led to inconclusive results.

3.3.3. ChIP for Ph in dsRNA Treated cells

ChIP of dsRNA-treated cells was also performed. Ph dsRNA treated cells had low signal at expected Ph binding sites compared to Venus dsRNA treated cells. However, the number of cells required for a single ChIP experiments is high and limited the feasibility of using this method to confirm the 27 identified factors of interest in the screen.

3.3.4. Cleavage Under Targets & Release Under Nuclease

Cleavage Under Targets & Release Under Nuclease (CUT&RUN), a recently developed method overcomes the ChIP requirement for large amounts of cells, and is also a shorter protocol. In a CUT&RUN experiment, unfixed cells or nuclei are immobilized on Concanavalin A-coated beads, extracted, and incubated with an antibody against the protein of interest. Cells are subsequently incubated with a modified micrococcal nuclease (MNase), which is fused to the protein A and G immunoglobulin G domains. This targets the MNase to the antibody and thereby to binding sites for the protein of interest. Once MNase is bound, the MNase cleavage reaction is initiated by incubation with calcium and stopped by chelation. MNase cleaves DNA between nucleosomes (or other bound factors). The cleaved chromatin fragments (which should correspond to chromatin sites where the protein of interest is bound) are then release from the extracted cells. Finally, the released DNA is purified for further analysis (Meers et al., 2019; Skene & Henikoff, 2017). CUT&RUN-quantitative PCR was tested for S2R+ cells but the signal to noise ratio was poor in preliminary experiments, suggesting additional optimization is required.

4. Chapter 4 – Discussion

4.1 Factors Involved PcG Protein Binding to Chromatin Across the Cell Cycle

PcG proteins are epigenetic regulators involved in the maintenance of gene repression pattern through mitosis, which act on chromatin. How PcG protein binding to chromatin is regulated in interphase and mitosis is not completely understood. The present RNAi screen sheds light into PcG protein binding by identifying candidate factors that may control it. In total, 541 candidate genes were tested and with high stringency parameters, 19 hits (increased or decreased Ph binding to chromatin) were identified, of which 12 (63%) were previously shown to co-purify with Ph in the chromatin fraction of cells. More than half of the remaining hits (21%) are either genetic or physical interactors of TrxG genes/proteins, which counteract PcG function. With lower stringency parameters, 46 hits were identified. Among those, 19 (41%) co-purify with Ph in the chromatin fraction and 15 (30%) are TrxG-related. Quantitative Western blot analysis of whole cell extracts after RNAi treatment showed no significant change in Ph level for any of the high stringency hits. This suggests that the changes in Ph levels on chromatin measured in the RNAi screen reflect changes in Ph distribution (i.e. in partitioning between chromatin bound and unbound).

4.2. Technical Limitations

RNAi screens, including the one conducted here, are expected to contain both false positive and false negative results. A major source of false results is off-target effects—when the dsRNA targets (an)other gene(s) in addition to its intended one. The RNAi template library used was not screened for off-target effects. Thus, hits identified in the screen might result from the effect of these off-target sequences and lead to the identification of false positives (Ramadan et al., 2007). Off-target effects could also affect dsRNA treatment efficiency, as can the frequency of dsRNA treatment, the target genes and the length of treatment (Zhou et al., 2013).

4.3. Perspective

For most of the identified hits, knockdown leads to more Ph at the chromatin ("increased binding hits"). This imbalance between increased and decreased binding hits could be explained by a bias in the dynamic range of intensity detected by the microscope or by a high background value. Alternatively, it could indicate that the "default" state of PcG proteins is chromatin binding, and restricting this binding is an important regulatory step. This is particularly interesting because of the strong signature of TrxG related genes in the hit list. The TrxG antagonizes PcG function, through incompletely understood mechanisms. A hypothesis from the RNAi screen is that TrxG proteins antagonize PcG proteins by antagonizing their binding, either through competition for the same binding site or recruitment factors, or by making PcG protein-chromatin interactions more dynamic. It would be interesting to test whether increased binding hits are related to TrxG proteins, for those which have not been linked so far.

Although the goal of the screen was to identify regulators of PcG protein binding to mitotic chromosomes, mitosis specific hits were less numerous than interphase specific hits. This may be due to technical limitations, since mitotic cells displayed a narrower dynamic range of intensity parameters than interphase cells, as illustrated by the poorer quality metrics values for mitotic cells (Table 6, p.98). The number of processed mitotic cells was also lower than the number of processed interphase cells, which means that statistical analyses for hit selection performed on mitotic cell data were less precise compared to those performed on interphase cell data. Finally, cells in the RNAi screen were fixed, and it is possible that this obscures some effects, particularly very dynamic binding.

4.3.1. nej and Sbf Knockdown Have Expected Results

Sbf and nej are both interphase specific and increased binding hits. Although nej was identified based on a low number of processed cells, results from the screen correlate with the current knowledge associated with both proteins. Sbf and nej are both TrxG proteins and part of TAC1 (Petruk et al., 2001). The last component of the complex, trx was also tested in the screen, but it did not score as a hit. The dsRNA reagent used to test it did not contain any off-target region, but it is possible that the RNAi treatment used in the screen was not optimal for this reagent (Zhou

et al., 2013). The main function of TAC1 complexes is to acetylate H3K27 (note that nej is the homologue of the major histone acetyltransferase CBP) which prevents its methylation by PcG proteins (Petruk et al., 2001; Steffen & Ringrose, 2014). Thus, in the absence of TAC1 complex members, H3K27 is more likely to be trimethylated, which should promote PcG chromatin binding. This correlates with results from the screen. It should also be pointed out that Sbf (but not nej or trx) was identified as a PRC1-co-purifying protein in the original stringent purification of PRC1 (Saurin et al., 2001).

4.3.2. Cp1 Was Previously Linked to Pc

One interesting factor identified was Cp1 (Cysteine proteinase-1): an increased binding hit that is non cell cycle specific at lower stringency analysis settings but interphase specific at higher stringency setting. This suggests that Cp1 prevents the binding of Ph to chromatin (either directly or indirectly). Cp1 was initially selected as a candidate gene because it co-purified with Ph in chromatin extracts. In *Drosophila*, Cp1 has been shown to cleave a homeotic transcription factor (Lyons et al., 2014). One study on mouse embryonic stem cells also showed that the homologue of Cp1, Cathepsin L, can cleave the N-terminal tail of histone H3. While cleavage does not remove H3K27, a cleaved peptide including H3K27me2 bound less well to a Pc homologue than the uncleaved peptide (E. M. Duncan et al., 2008). This correlates well with our screening results which shows that Cp1 knockdown increased Ph presence at the chromatin, since Ph and Pc are both members of PRC1. In another RNAi screen aiming at identifying genes that control the formation of PcG bodies, Cp1 knockdown reduced Pc foci which seems to contradict results from both the present screen and the study (Gonzalez et al., 2014). Alternatively, it is possible that Cp1 promotes the formation of PcG foci but not chromatin binding.

4.3.3. Helicases Might be Involved in PcG Chromatin Binding Behaviour

Seven helicases were identified as hits including tst, Chd3 and eIF4A with high stringency analysis settings (although tst qualified as a hit based on a low number of cells), as well as bel, Rm62, Ddx1 and obe at lower stringency settings. All helicases identified were interphase specific hits except for obe, and all but Ddx1 were increased binding hits. Helicases are enzymes capable of unwinding DNA and/or RNA. A recent paper showed that PRC2 and PRC1 can be recruited to chromatin by

recognizing R-loops. The authors also suggested that RNA-DNA helicases could switch the repressed state of R-loop containing PREs to the active state by resolving R-loops (Alecki et al., 2020). This means that in the absence of such helicases, R-loops will not be resolved, which might promote the binding of PRC1 and/or PRC2 to the chromatin. Thus, helicases that are increased binding hits and interphase specific could be interesting to pursue as these might fit this recently proposed model. A study on Rm62 mammalian homologue, DDX5, which is also an RNA-DNA helicase, showed that it was implicated in R-loop resolution *in vivo* (Mersaoui et al., 2019). Rm62 was initially selected as a screening candidate because it co-purified with Ph and a study showed that it also genetically interacts with Pc and binds Dsp1, a PRE binding protein (Lamiable et al., 2010). Helicases may have other functions in regulating PcG protein binding, through either RNA or DNA substrates. Chd3, while it has an SF2 helicase like domain, is an ATP-dependent nucleosome remodeling factor (Murawska et al., 2008).

4.3.4. Ribosomal Proteins Might Compete for PcG Protein Binding

A large number of ribosomal proteins scored as hits in the screen: 5 at high stringency analysis settings and 7 at lower stringency settings or 8 without quality filtering. All of the ribosomal protein hits are increased binding hits, and all are interphase specific. However, there is a possibility that ribosomal proteins are false positives since these are frequent hits in RNAi screens (Booker et al., 2011). The RNAi screen results might be directly related to the translation of Ph. Quantitative Western blot analysis of dsRNA treated cells, similar to what was done in figure 16 (p.122), could help confirm or exclude this possibility. Nevertheless, ribosomal proteins are known to have extra-ribosomal functions (Warner & McIntosh, 2009). Besides, ribosomal proteins were selected as candidates for the screen because they co-purify with Ph in the chromatin fraction in the AP-MS experiment. RNAi screen results suggests that they prevent PcG protein binding to chromatin. Considering the RNAi screen and the AP-MS results, one of the extra-ribosomal functions could be mediated by physical interactions with Ph or PRC1, which may interfere with binding to chromatin.

4.3.5. SF2

SF2 (Splicing factor 2) is one of the few decreased binding hits. With the higher stringency analysis settings, SF2 is mitosis specific, but it is also a hit in interphase cells when the lower stringency settings are used. The finding that knockdown of SF2 decreases Ph binding suggests it may be involved in Ph recruitment, and that this role may be especially important during mitosis. SF2 was initially selected as a candidate gene because of its associated GO term: "DNA binding", however SF2 is a splicing factor. A study on SF2 homologue in DT40 cells showed that its knockdown increased genomic instability via increasing the number of R-loops (Li & Manley, 2005). If knockdown of SF2 in *Drosophila* cells increases R-loops, this might be expected to increase recruitment of PRC1 and PRC2, which is the opposite of what is observed (Alecki et al., 2020). This could suggest that SF2 is a false positive. However, it is also possible that knockdown of SF2 does not increase R-loops in *Drosophila* cells, or that R-loops formed at PcG binding sites are distinct from those regulated by SF2. The effect of SF2 on Ph binding could also be the result of another function of SF2, including one related to splicing.

4.3.6. PcG Protein Binding to Chromatin in Mitosis

Among mitosis specific hits at higher stringency analysis settings, none were reported in protein-protein interaction experiments with any PcG proteins. At lower stringency, only 2 out of 8 were. It is possible that Ph and maybe other PcG protein chromatin binding behaviour is mostly controlled passively during mitosis (without direct protein-protein interactions). One interesting fact about mitosis specific hits is the high proportion of them that are TrxG-related (1/2 at higher stringency settings and 6/8 at lower stringency). The behaviour of TrxG proteins during mitosis is poorly understood. Several were shown to persist on mitotic chromosomes including Ash1. One study showed that Ash1 switches its antagonistic relationship to Pc in interphase to a cooperative relationship during mitosis. The knockdown of Ash1 led to an increased residence time of Pc in interphase but a decreased residence time in mitosis (Steffen et al., 2013). Since samples are fixed in our study, a decreased residence time should translate into a decreased binding. This report is thus consistent with the only mitosis specific TrxG protein: Dpy30-L1, of which the knockdown also led to a decreased chromatin binding of Ph.

4.4. Confirmation Attempts

Since RNAi screens are known to identify a certain number of false positives, several experiments were tested in an attempt to confirm hits by secondary screening using an alternative assay (Malo et al., 2006; Sharma & Rao, 2009). These included cellular fractionation followed by quantitative Western blot analysis and cytoplasmic protein extraction followed by flow cytometry analysis of mitotic chromosomes. Based on initial results cellular fractionation seems to be a promising way of confirming the hits.

ChIP was also tested, and control experiments were promising. However, a high number of (dsRNA-treated) cells is required for each experiment. I therefore tried to establish the CUT&RUN methodology, which is an alternative to ChIP that can be done with small numbers of cells. I prepared the Protein A/G-MNase fusion protein used in CUT&RUN experiments, and this reagent worked well for other groups. However, for the samples used here, the protocol requires further optimization, including the cell permeabilization step, the amount of cells per sample, and the MNase digestion.

4.5. Prospective Work

4.5.1. Confirmation of Hits by Secondary Screening

Because RNAi screens can identify false positives, hits are usually confirmed by secondary screening using an alternative assay (Malo et al., 2006; Sharma & Rao, 2009). In the present work, one simple secondary screening experiment would be to perform cellular fractionation of dsRNA treated cells followed by quantitative Western blot analysis of the chromatin fraction. This method has been tested once with Ph and seemed to be working. A second important aspect of secondary screening will be the use of dsRNAs with minimal off-target effects, to prevent the confirmation of false positives.

4.5.2. Systematic Mechanistic Study of Confirmed Hits

In light of the model proposed by Follmer et al., it would be interesting to systematically determine how the distribution of Ph and other PcG proteins on chromatin in interphase and

mitosis is affected by dsRNA against confirmed hits. Either ChIP or CUT&RUN could be used for this. As discussed above, CUT&RUN is a recently developed method that is shorter and less expensive, can analyze samples in native condition (which would add another confidence level to the hit confirmation), is suitable for small cell numbers, can be high throughput and is reportedly highly reproducible and efficient (Meers et al., 2019; Skene & Henikoff, 2017). In addition to the ChIP or CUT&RUN experiments, further mechanistic work would include RT-PCR analysis of dsRNA treated cells to test for changes in gene expression. Together, these two experiments would determine whether changes in Ph binding observed by microscopy are global or locus specific, and whether changes in binding impact gene regulation.

The *Drosophila* experiment system is a powerful tool for genetic studies (Hales et al., 2015). Additionally, mutations impairing PcG proteins function lead to dramatic phenotypes (Kassis et al., 2017). Thus, studying the effect of hits' loss of function during fly development would also be interesting (Gonzalez et al., 2014). One way to proceed would be by injecting vectors cloned with shRNAs targeting hits into embryos of a *Drosophila* line that makes use of an integrase system and observe their phenotype over the course of their development (Ni et al., 2008; Perkins et al., 2015). Knockdown of decreased binding hits, in other word, genes which knockdown lead to less Ph at the chromatin could lead to flies with PcG mutant phenotype, where Hox genes would be ectopically expressed, leading to anterior segment becoming more posterior segments (Gonzalez et al., 2014). Knockdown of decreased binding hits could also lead to flies with TrxG mutant phenotypes if hits are TrxG proteins.

4.5.3. Mechanistic Study of Rm62

Because the homologue of Rm62 is implicated in resolving R-loops, and because R-loops were recently connected to PcG binding and function, Rm62 is an especially interesting candidate for detailed analysis. If Rm62 is confirmed as a hit, ChIP or CUT&RUN experiments on RNAi treated cells would indicate if PRC1 binding is increased at PREs upon Rm62 knockdown. ChIP or CUT&RUN experiments using antibodies against Rm62 would test whether Rm62 localizes to PREs. On the other hand, DRIP (DNA-RNA immunoprecipitation) experiments on RNAi treated cells would indicate if Rm62 knockdown increases R-loop formation at PREs. However, there are

limitations to DRIP experiment related to the high number of cell required for genomic DNA isolation, particularly for analysis of mitotic cells, which need to be isolated by fluorescence-activated cell sorting. MapR, a recently developed method could overcome these limitations. MapR combines the specificity of RNase H for DNA-RNA hybrids and the speed, convenience and sensitivity of CUT&RUN (Yan et al., 2019). *In vitro* assays could also be used to first verify that Rm62, like its mammalian homologue (DDX5), can resolve R-loops. This assay involves purifying Rm62, and preparing R-loop and D-loop templates. Unwinding of nucleic acid templates after incubation with Rm62 is then analyzed on native PAGE gels (Mersaoui et al., 2019, p. 5). It would also be interesting to test whether PRC1 or PRC2 affect Rm62 activity *in vitro*.

4.6. Conclusion

The fact that hits encoding proteins sharing common complexes with the same effect on Ph chromatin binding were identified and that some of the hits correlate with the literature provides confidence that *bona fide* hits were identified. Thus, hits with currently unknown links to Ph or PcG proteins are worth further investigation. Another factor contributing to the confidence in the results from the screen stems from the non-negligible overlap of the identified hits with unpublished results from an AP-MS experiment available in the lab. The latter experiment aimed at identifying proteins co-purifying with Ph in the chromatin fraction.

How chromatin-based information is propagated through mitosis is not known but is fundamental to epigenetic inheritance. The present work provides an insight on potential actors of epigenetic memory and can help uncover new links between PcG proteins and the cell cycle. This may reveal how mitotic bookmarking occurs, how (and why) most PcG proteins are released from chromosomes in mitosis, and other mechanisms involved in transmission of epigenetic information through mitosis. PcG proteins and their epigenetic functions are widely conserved and implicated in both development and disease (cancer). Understanding basic mechanisms of epigenetic inheritance thus has long term implications for human health (Bracken & Helin, 2009; Francis & Kingston, 2001; Sparmann & van Lohuizen, 2006; Thiagalingam, 2020).

References

Alecki, C., Chiwara, V., Sanz, L. A., Grau, D., Pérez, O. A., Boulier, E. L., Armache, K.-J., Chédin, F., & Francis, N. J. (2020). RNA-DNA strand exchange by the Drosophila Polycomb complex PRC2. *Nature Communications*, *11*(1), 1–14. https://doi.org/10.1038/s41467-020-15609-x

Antonova, S. V., Boeren, J., Timmers, H. T. M., & Snel, B. (2019). Epigenetics and transcription regulation during eukaryotic diversification: The saga of TFIID. *Genes & Development*, *33*(15–16), 888–902. https://doi.org/10.1101/gad.300475.117

Ashburner, M., Ball, C. A., Blake, J. A., Botstein, D., Butler, H., Cherry, J. M., Davis, A. P., Dolinski, K., Dwight, S. S., Eppig, J. T., Harris, M. A., Hill, D. P., Issel-Tarver, L., Kasarskis, A., Lewis, S., Matese, J. C., Richardson, J. E., Ringwald, M., Rubin, G. M., & Sherlock, G. (2000). Gene ontology: Tool for the unification of biology. The Gene Ontology Consortium. *Nature Genetics*, *25*(1), 25–29. https://doi.org/10.1038/75556

Barrero, M. J., Boué, S., & Izpisúa Belmonte, J. C. (2010). Epigenetic Mechanisms that Regulate Cell Identity. *Cell Stem Cell*, *7*(5), 565–570. https://doi.org/10.1016/j.stem.2010.10.009

Bauer, M., Trupke, J., & Ringrose, L. (2016). The quest for mammalian Polycomb response elements: Are we there yet? *Chromosoma*, *125*, 471–496. https://doi.org/10.1007/s00412-015-0539-4

Beck, S. A., Falconer, E., Catching, A., Hodgson, J. W., & Brock, H. W. (2010). Cell cycle defects in polyhomeotic mutants are caused by abrogation of the DNA damage checkpoint. *Developmental Biology*, *339*(2), 320–328. https://doi.org/10.1016/j.ydbio.2009.12.031

Beh, L. Y., Colwell, L. J., & Francis, N. J. (2012). A core subunit of Polycomb repressive complex 1 is broadly conserved in function but not primary sequence. *Proceedings of the National Academy of Sciences*, *109*(18), E1063–E1071. https://doi.org/10.1073/pnas.1118678109

Bettencourt-Dias, M., Giet, R., Sinka, R., Mazumdar, A., Lock, W. G., Balloux, F., Zafiropoulos, P. J., Yamaguchi, S., Winter, S., Carthew, R. W., Cooper, M., Jones, D., Frenz, L., & Glover, D. M. (2004). Genome-wide survey of protein kinases required for cell cycle progression. *Nature*, *432*(7020), 980–987. https://doi.org/10.1038/nature03160

Birmingham, A., Selfors, L. M., Forster, T., Wrobel, D., Kennedy, C. J., Shanks, E., Santoyo-Lopez, J., Dunican, D. J., Long, A., Kelleher, D., Smith, Q., Beijersbergen, R. L., Ghazal, P., & Shamu, C. E. (2009). Statistical Methods for Analysis of High-Throughput RNA Interference Screens. *Nature Methods*, *6*(8), 569–575. https://doi.org/10.1038/nmeth.1351

Boettcher, B., & Barral, Y. (2013). The cell biology of open and closed mitosis. *Nucleus*, *4*(3), 160–165. https://doi.org/10.4161/nucl.24676

Booker, M., Samsonova, A. A., Kwon, Y., Flockhart, I., Mohr, S. E., & Perrimon, N. (2011). False negative rates in Drosophila cell-based RNAi screens: A case study. *BMC Genomics*, *12*(1), 50. https://doi.org/10.1186/1471-2164-12-50

Bornemann, D., Miller, E., & Simon, J. (1996). The Drosophila Polycomb group gene Sex comb on midleg (Scm) encodes a zinc finger protein with similarity to polyhomeotic protein. *Development*, *122*(5), 1621–1630.

Bracken, A. P., & Helin, K. (2009). Polycomb group proteins: Navigators of lineage pathways led astray in cancer. *Nature Reviews. Cancer*, *9*(11), 773–784. https://doi.org/10.1038/nrc2736

Brideau, C., Gunter, B., Pikounis, B., & Liaw, A. (2003). Improved Statistical Methods for Hit Selection in High-Throughput Screening. *Journal of Biomolecular Screening*, *8*(6), 634–647. https://doi.org/10.1177/1087057103258285

Brown, J. L., Fritsch, C., Mueller, J., & Kassis, J. A. (2003). The Drosophila pho-like gene encodes a YY1-related DNA binding protein that is redundant with pleiohomeotic in homeotic gene silencing. *Development*, *130*(2), 285–294. https://doi.org/10.1242/dev.00204

Brunelle, J. L., & Green, R. (2013). Chapter Five—In Vitro Transcription from Plasmid or PCR-amplified DNA. In J. Lorsch (Ed.), *Methods in Enzymology* (Vol. 530, pp. 101–114). Academic Press. https://doi.org/10.1016/B978-0-12-420037-1.00005-1

Buchenau, P., Hodgson, J., Strutt, H., & Arndt-Jovin, D. J. (1998). The distribution of polycomb-group proteins during cell division and development in Drosophila embryos: Impact on models for silencing. *The Journal of Cell Biology*, *141*(2), 469–481. https://doi.org/10.1083/jcb.141.2.469

Cao, R., Wang, L., Wang, H., Xia, L., Erdjument-Bromage, H., Tempst, P., Jones, R. S., & Zhang, Y. (2002). Role of Histone H3 Lysine 27 Methylation in Polycomb-Group Silencing. *Science*, *298*(5595), 1039–1043. https://doi.org/10.1126/science.1076997

Carpenter, A. E., Jones, T. R., Lamprecht, M. R., Clarke, C., Kang, I. H., Friman, O., Guertin, D. A., Chang, J. H., Lindquist, R. A., Moffat, J., Golland, P., & Sabatini, D. M. (2006). CellProfiler: Image analysis software for identifying and quantifying cell phenotypes. *Genome Biology*, *7*(10), R100. https://doi.org/10.1186/gb-2006-7-10-r100

Carter, S. D., & Sjögren, C. (2012). The SMC complexes, DNA and chromosome topology: Right or knot? *Critical Reviews in Biochemistry and Molecular Biology*, *47*(1), 1–16. https://doi.org/10.3109/10409238.2011.614593

Cavalli, G., & Paro, R. (1998). The Drosophila Fab-7 Chromosomal Element Conveys Epigenetic Inheritance during Mitosis and Meiosis. *Cell*, *93*(4), 505–518. https://doi.org/10.1016/S0092-8674(00)81181-2

Cavalli, G., & Paro, R. (1999). Epigenetic Inheritance of Active Chromatin After Removal of the Main Transactivator. *Science*, *286*(5441), 955–958. https://doi.org/10.1126/science.286.5441.955

Chen, D., Dundr, M., Wang, C., Leung, A., Lamond, A., Misteli, T., & Huang, S. (2005). Condensed mitotic chromatin is accessible to transcription factors and chromatin structural proteins. *The Journal of Cell Biology*, *168*(1), 41–54. https://doi.org/10.1083/jcb.200407182

Chen, F., Archambault, V., Kar, A., Lio', P., D'Avino, P. P., Sinka, R., Lilley, K., Laue, E. D., Deak, P., Capalbo, L., & Glover, D. M. (2007). Multiple Protein Phosphatases Are Required for Mitosis in Drosophila. *Current Biology*, *17*(4), 293–303. https://doi.org/10.1016/j.cub.2007.01.068

Chen, X., Hiller, M., Sancak, Y., & Fuller, M. T. (2005). Tissue-Specific TAFs Counteract Polycomb to Turn on Terminal Differentiation. *Science*, *310*(5749), 869–872. https://doi.org/10.1126/science.1118101

Chen, X., Lu, C., Prado, J. R. M., Eun, S. H., & Fuller, M. T. (2011). Sequential changes at differentiation gene promoters as they become active in a stem cell lineage. *Development*, *138*(12), 2441–2450. https://doi.org/10.1242/dev.056572

Cherbas, L., Willingham, A., Zhang, D., Yang, L., Zou, Y., Eads, B. D., Carlson, J. W., Landolin, J. M., Kapranov, P., Dumais, J., Samsonova, A., Choi, J.-H., Roberts, J., Davis, C. A., Tang, H., van Baren, M. J., Ghosh, S., Dobin, A., Bell, K., … Cherbas, P. (2011). The transcriptional diversity of 25 Drosophila cell lines. *Genome Research*, *21*(2), 301–314. https://doi.org/10.1101/gr.112961.110

Chung, N., Zhang, X. D., Kreamer, A., Locco, L., Kuan, P.-F., Bartz, S., Linsley, P. S., Ferrer, M., & Strulovici, B. (2008). Median Absolute Deviation to Improve Hit Selection for Genome-Scale RNAi Screens. *Journal of Biomolecular Screening*, *13*(2), 149–158. https://doi.org/10.1177/1087057107312035

Clapier, C. R., Chakravarthy, S., Petosa, C., Fernández-Tornero, C., Luger, K., & Müller, C. W. (2008). Structure of the Drosophila nucleosome core particle highlights evolutionary constraints on the H2A-H2B histone dimer. *Proteins: Structure, Function, and Bioinformatics*, *71*(1), 1–7. https://doi.org/10.1002/prot.21720

Clemens, J. C., Worby, C. A., Simonson-Leff, N., Muda, M., Maehama, T., Hemmings, B. A., & Dixon, J. E. (2000). Use of double-stranded RNA interference in Drosophila cell lines to dissect signal transduction pathways. *Proceedings of the National Academy of Sciences of the United States of America*, *97*(12), 6499–6503. https://doi.org/10.1073/pnas.110149597

Debec, A., & Marcaillou, C. (1997). Structural alterations of the mitotic apparatus induced by the heat shock response in Drosophila cells. *Biology of the Cell*, *89*(1), 67–78. https://doi.org/10.1016/S0248-4900(99)80082-3

Delest, A., Sexton, T., & Cavalli, G. (2012). Polycomb: A paradigm for genome organization from one to three dimensions. *Current Opinion in Cell Biology*, *24*(3), 405–414. https://doi.org/10.1016/j.ceb.2012.01.008

Douglas Zhang, X., Yang, X. C., Chung, N., Gates, A., Stec, E., Kunapuli, P., J Holder, D., Ferrer, M., & S Espeseth, A. (2006). Robust statistical methods for hit selection in RNA interference high-throughput screening experiments. *Pharmacogenomics*, *7*(3), 299–309. https://doi.org/10.2217/14622416.7.3.299

Dovat, S., Ronni, T., Russell, D., Ferrini, R., Cobb, B. S., & Smale, S. T. (2002). A common mechanism for mitotic inactivation of C2H2 zinc finger DNA-binding domains. *Genes & Development*, *16*(23), 2985–2990. https://doi.org/10.1101/gad.1040502

Duncan, E. M., Muratore-Schroeder, T. L., Cook, R. G., Garcia, B. A., Shabanowitz, J., Hunt, D. F., & Allis, C. D. (2008). Cathepsin L Proteolytically Processes Histone H3 During Mouse Embryonic Stem Cell Differentiation. *Cell*, *135*(2), 284–294. https://doi.org/10.1016/j.cell.2008.09.055

Duncan, I. M. (1982). Polycomblike: A gene that appears to be required for the normal expression of the bithorax and antennapedia gene complexes of Drosophila melanogaster. *Genetics*, *102*(1), 49–70.

Dura, J.-M., Brock, H. W., & Santamaria, P. (1985). Polyhomeotic: A gene of Drosophila melanogaster required for correct expression of segmental identity. *Molecular and General Genetics MGG*, *198*(2), 213–220. https://doi.org/10.1007/BF00382998

Echeverri, C. J., & Perrimon, N. (2006). High-throughput RNAi screening in cultured cells: A user's guide. *Nature Reviews Genetics*, *7*(5), 373–384. https://doi.org/10.1038/nrg1836

Fanti, L., Perrini, B., Piacentini, L., Berloco, M., Marchetti, E., Palumbo, G., & Pimpinelli, S. (2008). The trithorax group and Pc group proteins are differentially involved in heterochromatin formation in Drosophila. *Chromosoma*, *117*(1), 25–39. https://doi.org/10.1007/s00412-007-0123-7

Festuccia, N., Gonzalez, I., Owens, N., & Navarro, P. (2017). Mitotic bookmarking in development and stem cells. *Development*, *144*(20), 3633–3645. https://doi.org/10.1242/dev.146522

Filion, G. J., van Bemmel, J. G., Braunschweig, U., Talhout, W., Kind, J., Ward, L. D., Brugman, W., de Castro, I. J., Kerkhoven, R. M., Bussemaker, H. J., & van Steensel, B. (2010). Systematic Protein Location Mapping Reveals Five Principal Chromatin Types in Drosophila Cells. *Cell*, *143*(2), 212–224. https://doi.org/10.1016/j.cell.2010.09.009

Fischle, W., Tseng, B. S., Dormann, H. L., Ueberheide, B. M., Garcia, B. A., Shabanowitz, J., Hunt, D. F., Funabiki, H., & Allis, C. D. (2005). Regulation of HP1–chromatin binding by histone H3 methylation and phosphorylation. *Nature*, *438*(7071), 1116–1122. https://doi.org/10.1038/nature04219

Flockhart, I. T., Booker, M., Hu, Y., McElvany, B., Gilly, Q., Mathey-Prevot, B., Perrimon, N., & Mohr, S. E. (2012). FlyRNAi.org—the database of the Drosophila RNAi screening center: 2012 update. *Nucleic Acids Research*, *40*(Database issue), D715–D719. https://doi.org/10.1093/nar/gkr953

Follmer, N. E., Wani, A. H., & Francis, N. J. (2012). A Polycomb Group Protein Is Retained at Specific Sites on Chromatin in Mitosis. *PLOS Genetics*, *8*(12), e1003135. https://doi.org/10.1371/journal.pgen.1003135

Fonseca, J. P., Steffen, P. A., Müller, S., Lu, J., Sawicka, A., Seiser, C., & Ringrose, L. (2012). In vivo Polycomb kinetics and mitotic chromatin binding distinguish stem cells from differentiated cells. *Genes & Development*, *26*(8), 857–871. https://doi.org/10.1101/gad.184648.111

Forment, J. V., & Jackson, S. P. (2015). A flow-cytometry-based method to simplify the analysis and quantification of protein association to chromatin in mammalian cells. *Nature Protocols*, *10*(9), 1297–1307. https://doi.org/10.1038/nprot.2015.066

Francis, N. J. (2009). Mechanisms of epigenetic inheritance: Copying of Polycomb repressed chromatin. *Cell Cycle*, *8*(21), 3521–3526. https://doi.org/10.4161/cc.8.21.9876

Francis, N. J., & Kingston, R. E. (2001). Mechanisms of transcriptional memory. *Nature Reviews Molecular Cell Biology*, *2*(6), 409–421. https://doi.org/10.1038/35073039

Frey, F., Sheahan, T., Finkl, K., Stoehr, G., Mann, M., Benda, C., & Müller, J. (2016). Molecular basis of PRC1 targeting to Polycomb response elements by PhoRC. *Genes & Development*, *30*(9), 1116–1127. https://doi.org/10.1101/gad.279141.116

Friberg, A., Oddone, A., Klymenko, T., Müller, J., & Sattler, M. (2010). Structure of an atypical Tudor domain in the Drosophila Polycomblike protein. *Protein Science : A Publication of the Protein Society*, *19*(10), 1906–1916. https://doi.org/10.1002/pro.476

Gehring, W. J. (1970). *A recessive lethal [l(4)29] with a homeotic effect in D. melanogaster*. https://www.scienceopen.com/document?vid=7110acab-81a7-4f48-abf7-9fca5d8d5215

Gonzalez, I., Mateos-Langerak, J., Thomas, A., Cheutin, T., & Cavalli, G. (2014). Identification of Regulators of the Three-Dimensional Polycomb Organization by a Microscopy-Based

Genome-wide RNAi Screen. *Molecular Cell*, *54*(3), 485–499. https://doi.org/10.1016/j.molcel.2014.03.004

Goshima, G., Wollman, R., Goodwin, S. S., Zhang, N., Scholey, J. M., Vale, R. D., & Stuurman, N. (2007). Genes Required for Mitotic Spindle Assembly in Drosophila S2 Cells. *Science*, *316*(5823), 417–421. https://doi.org/10.1126/science.1141314

Gottesfeld, J. M., & Forbes, D. J. (1997). Mitotic repression of the transcriptional machinery. *Trends in Biochemical Sciences*, *22*(6), 197–202. https://doi.org/10.1016/s0968-0004(97)01045-1

Gutiérrez, L., Oktaba, K., Scheuermann, J. C., Gambetta, M. C., Ly-Hartig, N., & Müller, J. (2012). The role of the histone H2A ubiquitinase Sce in Polycomb repression. *Development (Cambridge, England)*, *139*(1), 117–127. https://doi.org/10.1242/dev.074450

Güttinger, S., Laurell, E., & Kutay, U. (2009). Orchestrating nuclear envelope disassembly and reassembly during mitosis. *Nature Reviews. Molecular Cell Biology*, *10*(3), 178–191. https://doi.org/10.1038/nrm2641

Hales, K. G., Korey, C. A., Larracuente, A. M., & Roberts, D. M. (2015). Genetics on the Fly: A Primer on the Drosophila Model System. *Genetics*, *201*(3), 815–842. https://doi.org/10.1534/genetics.115.183392

Henikoff, S., & Greally, J. M. (2016). Epigenetics, cellular memory and gene regulation. *Current Biology*, *26*(14), R644–R648. https://doi.org/10.1016/j.cub.2016.06.011

Hirota, T., Lipp, J. J., Toh, B.-H., & Peters, J.-M. (2005). Histone H3 serine 10 phosphorylation by Aurora B causes HP1 dissociation from heterochromatin. *Nature*, *438*(7071), 1176–1180. https://doi.org/10.1038/nature04254

Horn, T., Arziman, Z., Berger, J., & Boutros, M. (2007). GenomeRNAi: A database for cell-based RNAi phenotypes. *Nucleic Acids Research*, *35*(Database issue), D492-497. https://doi.org/10.1093/nar/gkl906

Hou, C., Li, L., Qin, Z. S., & Corces, V. G. (2012). Gene Density, Transcription, and Insulators Contribute to the Partition of the Drosophila Genome into Physical Domains. *Molecular Cell*, *48*(3), 471–484. https://doi.org/10.1016/j.molcel.2012.08.031

Ingham, P. W. (1984). A gene that regulates the bithorax complex differentially in larval and adult cells of Drosophila. *Cell*, *37*(3), 815–823. https://doi.org/10.1016/0092-8674(84)90416-1

Jablonka, E., & Lamb, M. J. (2002). The Changing Concept of Epigenetics. *Annals of the New York Academy of Sciences*, *981*(1), 82–96. https://doi.org/10.1111/j.1749-6632.2002.tb04913.x

Johnson, T. C., & Holland, J. J. (1965). RIBONUCLEIC ACID AND PROTEIN SYNTHESIS IN MITOTIC HELA CELLS. *Journal of Cell Biology*, *27*(3), 565–574. https://doi.org/10.1083/jcb.27.3.565

Jürgens, G. (1985). A group of genes controlling the spatial expression of the bithorax complex in Drosophila. *Nature*, *316*(6024), 153–155. https://doi.org/10.1038/316153a0

Kadauke, S., & Blobel, G. A. (2013). Mitotic bookmarking by transcription factors. *Epigenetics & Chromatin*, *6*, 6. https://doi.org/10.1186/1756-8935-6-6

Kahn, T. G., Dorafshan, E., Schultheis, D., Zare, A., Stenberg, P., Reim, I., Pirrotta, V., & Schwartz, Y. B. (2016). Interdependence of PRC1 and PRC2 for recruitment to Polycomb Response Elements. *Nucleic Acids Research*, *44*(21), 10132–10149. https://doi.org/10.1093/nar/gkw701

Kang, H., McElroy, K. A., Jung, Y. L., Alekseyenko, A. A., Zee, B. M., Park, P. J., & Kuroda, M. I. (2015). Sex comb on midleg (Scm) is a functional link between PcG-repressive complexes in Drosophila. *Genes & Development*, *29*(11), 1136–1150. https://doi.org/10.1101/gad.260562.115

Kang, X., Qi, Y., Zuo, Y., Wang, Q., Zou, Y., Schwartz, R. J., Cheng, J., & Yeh, E. T. H. (2010). SUMO-Specific Protease 2 Is Essential for Suppression of Polycomb Group Proteins Mediated Gene Silencing During Embryonic Development. *Molecular Cell*, *38*(2), 191–201. https://doi.org/10.1016/j.molcel.2010.03.005

Kassis, J. A., & Brown, J. L. (2013). Polycomb group response elements in Drosophila and vertebrates. *Advances in Genetics*, *81*, 83–118. https://doi.org/10.1016/B978-0-12-407677-8.00003-8

Kassis, J. A., Kennison, J. A., & Tamkun, J. W. (2017). Polycomb and Trithorax Group Genes in Drosophila. *Genetics*, *206*(4), 1699–1725. https://doi.org/10.1534/genetics.115.185116

Kim, C. A., Gingery, M., Pilpa, R. M., & Bowie, J. U. (2002). The SAM domain of polyhomeotic forms a helical polymer. *Nature Structural Biology*, *9*(6), 453–457. https://doi.org/10.1038/nsb802

Kim, C. A., Sawaya, M. R., Cascio, D., Kim, W., & Bowie, J. U. (2005). Structural Organization of a Sex-comb-on-midleg/Polyhomeotic Copolymer. *Journal of Biological Chemistry*, *280*(30), 27769–27775. https://doi.org/10.1074/jbc.M503055200

Klebes, A., Sustar, A., Kechris, K., Li, H., Schubiger, G., & Kornberg, T. B. (2005). Regulation of cellular plasticity in Drosophila imaginal disc cells by the Polycomb group, trithorax group and lama genes. *Development*, *132*(16), 3753–3765. https://doi.org/10.1242/dev.01927

Klymenko, T., Papp, B., Fischle, W., Köcher, T., Schelder, M., Fritsch, C., Wild, B., Wilm, M., & Müller, J. (2006). A Polycomb group protein complex with sequence-specific DNA-binding and selective methyl-lysine-binding activities. *Genes & Development*, *20*(9), 1110–1122. https://doi.org/10.1101/gad.377406

Kouzarides, T. (2007). Chromatin Modifications and Their Function. *Cell*, *128*(4), 693–705. https://doi.org/10.1016/j.cell.2007.02.005

Kulkarni, M. M., Booker, M., Silver, S. J., Friedman, A., Hong, P., Perrimon, N., & Mathey-Prevot, B. (2006). Evidence of off-target effects associated with long dsRNAs in Drosophila melanogaster cell-based assays. *Nature Methods*, *3*(10), 833–838. https://doi.org/10.1038/nmeth935

Lagarou, A., Mohd-Sarip, A., Moshkin, Y. M., Chalkley, G. E., Bezstarosti, K., Demmers, J. A. A., & Verrijzer, C. P. (2008). DKDM2 couples histone H2A ubiquitylation to histone H3 demethylation during Polycomb group silencing. *Genes & Development*, *22*(20), 2799–2810. https://doi.org/10.1101/gad.484208

Lamiable, O., Rabhi, M., Peronnet, F., Locker, D., & Decoville, M. (2010). Rm62, a DEAD-box RNA helicase, complexes with DSP1 in Drosophila embryos. *Genesis*, *48*(4), 244–253. https://doi.org/10.1002/dvg.20609

Lee, N., Maurange, C., Ringrose, L., & Paro, R. (2005). Suppression of Polycomb group proteins by JNK signalling induces transdetermination in Drosophila imaginal discs. *Nature*, *438*(7065), 234–237. https://doi.org/10.1038/nature04120

Leung, Y. Y., Yao Hui, L. L., & Kraus, V. B. (2015). Colchicine—Update on mechanisms of action and therapeutic uses. *Seminars in Arthritis and Rheumatism*, *45*(3), 341–350. https://doi.org/10.1016/j.semarthrit.2015.06.013

Lewis, E. B. (1978). A gene complex controlling segmentation in Drosophila. *Nature*, *276*, 565–570. https://doi.org/10.1038/276565a0

Lewis, P. H. (1947). Melanogaster-new mutants: Report of Pamela H. Lewis. *Drosophila Information Service*, *21*, 69.

Li, X., & Manley, J. L. (2005). Inactivation of the SR Protein Splicing Factor ASF/SF2 Results in Genomic Instability. *Cell*, *122*(3), 365–378. https://doi.org/10.1016/j.cell.2005.06.008

Lyons, G. R., Andersen, R. O., Abdi, K., Song, W.-S., & Kuo, C. T. (2014). Cysteine Proteinase-1 and Cut Protein Isoform Control Dendritic Innervation of Two Distinct Sensory Fields by a Single Neuron. *Cell Reports*, *6*(5), 783–791. https://doi.org/10.1016/j.celrep.2014.02.003

Maeda, R. K., & Karch, F. (2006). The ABC of the BX-C: The bithorax complex explained. *Development*, *133*(8), 1413–1422. https://doi.org/10.1242/dev.02323

Maiato, H., Hergert, P. J., Moutinho-Pereira, S., Dong, Y., Vandenbeldt, K. J., Rieder, C. L., & McEwen, B. F. (2006). The ultrastructure of the kinetochore and kinetochore fiber in Drosophila somatic cells. *Chromosoma*, *115*(6), 469–480. https://doi.org/10.1007/s00412-006-0076-2

Malo, N., Hanley, J. A., Cerquozzi, S., Pelletier, J., & Nadon, R. (2006). Statistical practice in high-throughput screening data analysis. *Nature Biotechnology*, *24*(2), 167–175. https://doi.org/10.1038/nbt1186

Margueron, R., & Reinberg, D. (2010). Chromatin Structure and the Inheritance of Epigenetic Information. *Nature Reviews. Genetics*, *11*(4), 285–296. https://doi.org/10.1038/nrg2752

Martinez, A.-M., & Cavalli, G. (2006). The role of polycomb group proteins in cell cycle regulation during development. *Cell Cycle (Georgetown, Tex.)*, *5*(11), 1189–1197. https://doi.org/10.4161/cc.5.11.2781

Meers, M. P., Bryson, T. D., Henikoff, J. G., & Henikoff, S. (2019). Improved CUT&RUN chromatin profiling tools. *ELife*, *8*, e46314. https://doi.org/10.7554/eLife.46314

Mersaoui, S. Y., Yu, Z., Coulombe, Y., Karam, M., Busatto, F. F., Masson, J., & Richard, S. (2019). Arginine methylation of the DDX5 helicase RGG/RG motif by PRMT5 regulates resolution of RNA:DNA hybrids. *The EMBO Journal*, *38*(15). https://doi.org/10.15252/embj.2018100986

Mohr, S., Bakal, C., & Perrimon, N. (2010). Genomic Screening with RNAi: Results and Challenges. *Annual Review of Biochemistry*, *79*, 37–64. https://doi.org/10.1146/annurev-biochem-060408-092949

Mohr, S. E., Hu, Y., Kim, K., Housden, B. E., & Perrimon, N. (2014). Resources for Functional Genomics Studies in Drosophila melanogaster. *Genetics*, *197*(1), 1–18. https://doi.org/10.1534/genetics.113.154344

Müller, J., Hart, C. M., Francis, N. J., Vargas, M. L., Sengupta, A., Wild, B., Miller, E. L., O'Connor, M. B., Kingston, R. E., & Simon, J. A. (2002). Histone Methyltransferase Activity of a Drosophila Polycomb Group Repressor Complex. *Cell*, *111*(2), 197–208. https://doi.org/10.1016/S0092-8674(02)00976-5

Murawska, M., Kunert, N., Vugt, J. van, Längst, G., Kremmer, E., Logie, C., & Brehm, A. (2008). DCHD3, a Novel ATP-Dependent Chromatin Remodeler Associated with Sites of Active Transcription. *Molecular and Cellular Biology*, *28*(8), 2745–2757. https://doi.org/10.1128/MCB.01839-07

Nekrasov, M., Klymenko, T., Fraterman, S., Papp, B., Oktaba, K., Köcher, T., Cohen, A., Stunnenberg, H. G., Wilm, M., & Müller, J. (2007). Pcl-PRC2 is needed to generate high levels of H3-K27 trimethylation at Polycomb target genes. *The EMBO Journal*, *26*(18), 4078–4088. https://doi.org/10.1038/sj.emboj.7601837

Ng, J., Hart, C. M., Morgan, K., & Simon, J. A. (2000). A Drosophila ESC-E(Z) Protein Complex Is Distinct from Other Polycomb Group Complexes and Contains Covalently Modified ESC. *Molecular and Cellular Biology*, *20*(9), 3069–3078. https://doi.org/10.1128/MCB.20.9.3069-3078.2000

Ni, J.-Q., Markstein, M., Binari, R., Pfeiffer, B., Liu, L.-P., Villalta, C., Booker, M., Perkins, L., & Perrimon, N. (2008). Vector and parameters for targeted transgenic RNA interference in

Drosophila melanogaster. *Nature Methods*, *5*(1), 49–51. https://doi.org/10.1038/nmeth1146

O'Connell, S., Wang, L., Robert, S., Jones, C. A., Saint, R., & Jones, R. S. (2001). Polycomblike PHD Fingers Mediate Conserved Interaction with Enhancer of Zeste Protein. *Journal of Biological Chemistry*, *276*(46), 43065–43073. https://doi.org/10.1074/jbc.M104294200

Orsi, G. A., Kasinathan, S., Hughes, K. T., Saminadin-Peter, S., Henikoff, S., & Ahmad, K. (2014). High-resolution mapping defines the cooperative architecture of Polycomb response elements. *Genome Research*, *24*(5), 809–820. https://doi.org/10.1101/gr.163642.113

Paro, R., & Hogness, D. S. (1991). The Polycomb protein shares a homologous domain with a heterochromatin-associated protein of Drosophila. *Proceedings of the National Academy of Sciences*, *88*(1), 263–267. https://doi.org/10.1073/pnas.88.1.263

Paro, Renato. (1990). Imprinting a determined state into the chromatin of Drosophila. *Trends in Genetics*, *6*, 416–421. https://doi.org/10.1016/0168-9525(90)90303-N

Perkins, L. A., Holderbaum, L., Tao, R., Hu, Y., Sopko, R., McCall, K., Yang-Zhou, D., Flockhart, I., Binari, R., Shim, H.-S., Miller, A., Housden, A., Foos, M., Randkelv, S., Kelley, C., Namgyal, P., Villalta, C., Liu, L.-P., Jiang, X., … Perrimon, N. (2015). The Transgenic RNAi Project at Harvard Medical School: Resources and Validation. *Genetics*, *201*(3), 843–852. https://doi.org/10.1534/genetics.115.180208

Petruk, S., Sedkov, Y., Smith, S., Tillib, S., Kraevski, V., Nakamura, T., Canaani, E., Croce, C. M., & Mazo, A. (2001). Trithorax and dCBP Acting in a Complex to Maintain Expression of a Homeotic Gene. *Science*, *294*(5545), 1331–1334. https://doi.org/10.1126/science.1065683

Prescott, D. M., & Bender, M. A. (1962). Synthesis of RNA and protein during mitosis in mammalian tissue culture cells. *Experimental Cell Research*, *26*(2), 260–268. https://doi.org/10.1016/0014-4827(62)90176-3

Probst, A. V., Dunleavy, E., & Almouzni, G. (2009). Epigenetic inheritance during the cell cycle. *Nature Reviews Molecular Cell Biology*, *10*(3), 192–206. https://doi.org/10.1038/nrm2640

Ptashne, M. (2007). On the use of the word 'epigenetic'. *Current Biology*, *17*(7), R233–R236. https://doi.org/10.1016/j.cub.2007.02.030

Ramadan, N., Flockhart, I., Booker, M., Perrimon, N., & Mathey-Prevot, B. (2007). Design and implementation of high-throughput RNAi screens in cultured Drosophila cells. *Nature Protocols*, *2*(9), 2245–2264. https://doi.org/10.1038/nprot.2007.250

Rieber, N., Knapp, B., Eils, R., & Kaderali, L. (2009). RNAither, an automated pipeline for the statistical analysis of high-throughput RNAi screens. *Bioinformatics*, *25*(5), 678–679. https://doi.org/10.1093/bioinformatics/btp014

Ringrose, L., & Paro, R. (2004). Epigenetic Regulation of Cellular Memory by the Polycomb and Trithorax Group Proteins. *Annual Review of Genetics*, *38*(1), 413–443. https://doi.org/10.1146/annurev.genet.38.072902.091907

Rogers, S. L., & Rogers, G. C. (2008). Culture of Drosophila S2 cells and their use for RNAi-mediated loss-of-function studies and immunofluorescence microscopy. *Nature Protocols*, *3*(4), 606–611. https://doi.org/10.1038/nprot.2008.18

Roskoski, R. (2019). Cyclin-dependent protein serine/threonine kinase inhibitors as anticancer drugs. *Pharmacological Research*, *139*, 471–488. https://doi.org/10.1016/j.phrs.2018.11.035

Saurin, A. J., Shao, Z., Erdjument-Bromage, H., Tempst, P., & Kingston, R. E. (2001). A Drosophila Polycomb group complex includes Zeste and dTAFII proteins. *Nature*, *412*(6847), 655–660. https://doi.org/10.1038/35088096

Savla, U., Benes, J., Zhang, J., & Jones, R. S. (2008). Recruitment of Drosophila Polycomb-group proteins by Polycomblike, a component of a novel protein complex in larvae. *Development*, *135*(5), 813–817. https://doi.org/10.1242/dev.016006

Scheuermann, J. C., de Ayala Alonso, A. G., Oktaba, K., Ly-Hartig, N., McGinty, R. K., Fraterman, S., Wilm, M., Muir, T. W., & Müller, J. (2010). Histone H2A deubiquitinase activity of the Polycomb repressive complex PR-DUB. *Nature*, *465*(7295), 243–247. https://doi.org/10.1038/nature08966

Schmidt, E. E., Pelz, O., Buhlmann, S., Kerr, G., Horn, T., & Boutros, M. (2013). GenomeRNAi: A database for cell-based and in vivo RNAi phenotypes, 2013 update. *Nucleic Acids Research*, *41*(Database issue), D1021-1026. https://doi.org/10.1093/nar/gks1170

Schneider, C. A., Rasband, W. S., & Eliceiri, K. W. (2012). NIH Image to ImageJ: 25 years of image analysis. *Nature Methods*, *9*(7), 671–675. https://doi.org/10.1038/nmeth.2089

Schneider, I. (1972). Cell lines derived from late embryonic stages of Drosophila melanogaster. *Development*, *27*(2), 353–365.

Schuettengruber, B., Bourbon, H.-M., Di Croce, L., & Cavalli, G. (2017). Genome Regulation by Polycomb and Trithorax: 70 Years and Counting. *Cell*, *171*(1), 34–57. https://doi.org/10.1016/j.cell.2017.08.002

Schwartz, Y. B., & Pirrotta, V. (2007). Polycomb silencing mechanisms and the management of genomic programmes. *Nature Reviews Genetics*, *8*(1), 9–22. https://doi.org/10.1038/nrg1981

Sexton, T., Yaffe, E., Kenigsberg, E., Bantignies, F., Leblanc, B., Hoichman, M., Parrinello, H., Tanay, A., & Cavalli, G. (2012). Three-Dimensional Folding and Functional Organization Principles of the Drosophila Genome. *Cell*, *148*(3), 458–472. https://doi.org/10.1016/j.cell.2012.01.010

Shao, Z., Raible, F., Mollaaghababa, R., Guyon, J. R., Wu, C., Bender, W., & Kingston, R. E. (1999). Stabilization of Chromatin Structure by PRC1, a Polycomb Complex. *Cell*, *98*(1), 37–46. https://doi.org/10.1016/S0092-8674(00)80604-2

Sharma, S., & Rao, A. (2009). RNAi screening: Tips and techniques. *Nature Immunology*, *10*(8), 799–804. https://doi.org/10.1038/ni0809-799

Shearn, A., Hersperger, G., & Hersperger, E. (1978). Genetic Analysis of Two Allelic Temperature-Sensitive Mutants of Drosophila Melanogaster Both of Which Are Zygotic and Maternal-Effect Lethals. *Genetics*, *89*(2), 341–353.

Shiomi, Y., Hayashi, A., Ishii, T., Shinmyozu, K., Nakayama, J., Sugasawa, K., & Nishitani, H. (2012). Two different replication factor C proteins, Ctf18 and RFC1, separately control PCNA-CRL4Cdt2-mediated Cdt1 proteolysis during S phase and following UV irradiation. *Molecular and Cellular Biology*, *32*(12), 2279–2288. https://doi.org/10.1128/MCB.06506-11

Sif, S., Stukenberg, P. T., Kirschner, M. W., & Kingston, R. E. (1998). Mitotic inactivation of a human SWI/SNF chromatin remodeling complex. *Genes & Development*, *12*(18), 2842–2851. https://doi.org/10.1101/gad.12.18.2842

Skene, P. J., & Henikoff, S. (2017). An efficient targeted nuclease strategy for high-resolution mapping of DNA binding sites. *ELife*, *6*, e21856. https://doi.org/10.7554/eLife.21856

Skourti-Stathaki, K., Torlai Triglia, E., Warburton, M., Voigt, P., Bird, A., & Pombo, A. (2019). R-Loops Enhance Polycomb Repression at a Subset of Developmental Regulator Genes. *Molecular Cell*, *73*(5), 930-945.e4. https://doi.org/10.1016/j.molcel.2018.12.016

Slifer, E. H. (1942). A mutant stock of Drosophila with extra sex-combs. *Journal of Experimental Zoology*, *90*(1), 31–40. https://doi.org/10.1002/jez.1400900103

Somma, M. P., Ceprani, F., Bucciarelli, E., Naim, V., Arcangelis, V. D., Piergentili, R., Palena, A., Ciapponi, L., Giansanti, M. G., Pellacani, C., Petrucci, R., Cenci, G., Vernì, F., Fasulo, B., Goldberg, M. L., Cunto, F. D., & Gatti, M. (2008). Identification of Drosophila Mitotic Genes by Combining Co-Expression Analysis and RNA Interference. *PLOS Genetics*, *4*(7), e1000126. https://doi.org/10.1371/journal.pgen.1000126

Sparmann, A., & van Lohuizen, M. (2006). Polycomb silencers control cell fate, development and cancer. *Nature Reviews. Cancer*, *6*(11), 846–856. https://doi.org/10.1038/nrc1991

Steffen, P. A., Fonseca, J. P., Gänger, C., Dworschak, E., Kockmann, T., Beisel, C., & Ringrose, L. (2013). Quantitative in vivo analysis of chromatin binding of Polycomb and Trithorax group proteins reveals retention of ASH1 on mitotic chromatin. *Nucleic Acids Research*, *41*(10), 5235–5250. https://doi.org/10.1093/nar/gkt217

Steffen, P. A., & Ringrose, L. (2014). What are memories made of? How Polycomb and Trithorax proteins mediate epigenetic memory. *Nature Reviews Molecular Cell Biology*, *15*(5), 340–356. https://doi.org/10.1038/nrm3789

Swenson, J. M., Colmenares, S. U., Strom, A. R., Costes, S. V., & Karpen, G. H. (2016). The composition and organization of Drosophila heterochromatin are heterogeneous and dynamic. *ELife*, *5*, e16096. https://doi.org/10.7554/eLife.16096

Teves, S. S., An, L., Hansen, A. S., Xie, L., Darzacq, X., & Tjian, R. (2016). A dynamic mode of mitotic bookmarking by transcription factors. *ELife*, *5*, e22280. https://doi.org/10.7554/eLife.22280

The Gene Ontology Consortium. (2019). The Gene Ontology Resource: 20 years and still GOing strong. *Nucleic Acids Research*, *47*(D1), D330–D338. https://doi.org/10.1093/nar/gky1055

Thiagalingam, S. (2020). Epigenetic memory in development and disease: Unraveling the mechanism. *Biochimica et Biophysica Acta (BBA) - Reviews on Cancer*, 188349. https://doi.org/10.1016/j.bbcan.2020.188349

Thurmond, J., Goodman, J. L., Strelets, V. B., Attrill, H., Gramates, L. S., Marygold, S. J., Matthews, B. B., Millburn, G., Antonazzo, G., Trovisco, V., Kaufman, T. C., Calvi, B. R., Perrimon, N., Gelbart, S. R., Agapite, J., Broll, K., Crosby, L., Santos, G. dos, Emmert, D., … Baker, P. (2019). FlyBase 2.0: The next generation. *Nucleic Acids Research*, *47*(D1), D759–D765. https://doi.org/10.1093/nar/gky1003

Tie, F., Furuyama, T., Prasad-Sinha, J., Jane, E., & Harte, P. J. (2001). The Drosophila Polycomb Group proteins ESC and E(Z) are present in a complex containing the histone-binding protein p55 and the histone deacetylase RPD3. *Development*, *128*(2), 275–286.

Tomari, Y., & Zamore, P. D. (2005). Perspective: Machines for RNAi. *Genes & Development*, *19*(5), 517–529. https://doi.org/10.1101/gad.1284105

Van Bortle, K., Nichols, M. H., Li, L., Ong, C.-T., Takenaka, N., Qin, Z. S., & Corces, V. G. (2014). Insulator function and topological domain border strength scale with architectural protein occupancy. *Genome Biology*, *15*(5), R82. https://doi.org/10.1186/gb-2014-15-5-r82

Varier, R. A., Outchkourov, N. S., de Graaf, P., van Schaik, F. M. A., Ensing, H. J. L., Wang, F., Higgins, J. M. G., Kops, G. J. P. L., & Timmers, Ht. M. (2010). A phospho/methyl switch at histone H3 regulates TFIID association with mitotic chromosomes. *The EMBO Journal*, *29*(23), 3967–3978. https://doi.org/10.1038/emboj.2010.261

Waddington, C. H. (2012). The epigenotype. 1942. *International Journal of Epidemiology*, *41*(1), 10–13. https://doi.org/10.1093/ije/dyr184

Wang, F., & Higgins, J. M. G. (2013). Histone modifications and mitosis: Countermarks, landmarks, and bookmarks. *Trends in Cell Biology*, *23*(4), 175–184. https://doi.org/10.1016/j.tcb.2012.11.005

Wang, L., Brown, J. L., Cao, R., Zhang, Y., Kassis, J. A., & Jones, R. S. (2004). Hierarchical recruitment of polycomb group silencing complexes. *Molecular Cell*, *14*(5), 637–646. https://doi.org/10.1016/j.molcel.2004.05.009

Wang, L., Jahren, N., Vargas, M. L., Andersen, E. F., Benes, J., Zhang, J., Miller, E. L., Jones, R. S., & Simon, J. A. (2006). Alternative ESC and ESC-Like Subunits of a Polycomb Group Histone Methyltransferase Complex Are Differentially Deployed during Drosophila Development. *Molecular and Cellular Biology*, *26*(7), 2637–2647. https://doi.org/10.1128/MCB.26.7.2637-2647.2006

Wani, A. H., Boettiger, A. N., Schorderet, P., Ergun, A., Münger, C., Sadreyev, R. I., Zhuang, X., Kingston, R. E., & Francis, N. J. (2016). Chromatin topology is coupled to Polycomb group protein subnuclear organization. *Nature Communications*, *7*, 10291. https://doi.org/10.1038/ncomms10291

Warner, J. R., & McIntosh, K. B. (2009). How common are extraribosomal functions of ribosomal proteins? *Molecular Cell*, *34*(1), 3–11. https://doi.org/10.1016/j.molcel.2009.03.006

Wei, G. H., Liu, D. P., & Liang, C. C. (2005). Chromatin domain boundaries: Insulators and beyond. *Cell Research*, *15*(4), 292–300. https://doi.org/10.1038/sj.cr.7290298

Whitcomb, S. J., Basu, A., Allis, C. D., & Bernstein, E. (2007). Polycomb Group proteins: An evolutionary perspective. *Trends in Genetics*, *23*(10), 494–502. https://doi.org/10.1016/j.tig.2007.08.006

Wiles, A. M., Ravi, D., Bhavani, S., & Bishop, A. J. R. (2008). An Analysis of Normalization Methods for Drosophila RNAi Genomic Screens and Development of a Robust Validation Scheme. *Journal of Biomolecular Screening*, *13*(8), 777–784. https://doi.org/10.1177/1087057108323125

Wu, J., Liu, T., Rios, Z., Mei, Q., Lin, X., & Cao, S. (2017). Heat Shock Proteins and Cancer. *Trends in Pharmacological Sciences*, *38*(3), 226–256. https://doi.org/10.1016/j.tips.2016.11.009

Yan, Q., Shields, E. J., Bonasio, R., & Sarma, K. (2019). Mapping Native R-Loops Genome-wide Using a Targeted Nuclease Approach. *Cell Reports*, *29*(5), 1369-1380.e5. https://doi.org/10.1016/j.celrep.2019.09.052

Yanagawa, S., Lee, J.-S., & Ishimoto, A. (1998). Identification and Characterization of a Novel Line of Drosophila Schneider S2 Cells That Respond to Wingless Signaling. *Journal of Biological Chemistry*, *273*(48), 32353–32359. https://doi.org/10.1074/jbc.273.48.32353

Zhang, X. D. (2007). A pair of new statistical parameters for quality control in RNA interference high-throughput screening assays. *Genomics*, *89*(4), 552–561. https://doi.org/10.1016/j.ygeno.2006.12.014

Zhang, X. D. (2008). Novel analytic criteria and effective plate designs for quality control in genome-scale RNAi screens. *Journal of Biomolecular Screening*, *13*(5), 363–377. https://doi.org/10.1177/1087057108317062

Zhang, X. D. (2011, February). *Optimal High-Throughput Screening: Practical Experimental Design and Data Analysis for Genome-Scale RNAi Research*. Cambridge Core. https://doi.org/10.1017/CBO9780511973888

Zhao, H., Zhu, M., Limbo, O., & Russell, P. (2018). RNase H eliminates R-loops that disrupt DNA replication but is nonessential for efficient DSB repair. *EMBO Reports*, *19*(5). https://doi.org/10.15252/embr.201745335

Zhao, Y., & Garcia, B. A. (2015). Comprehensive Catalog of Currently Documented Histone Modifications. *Cold Spring Harbor Perspectives in Biology*, *7*(9), a025064. https://doi.org/10.1101/cshperspect.a025064

Zhou, R., Mohr, S., Hannon, G. J., & Perrimon, N. (2013). Inducing RNAi in Drosophila Cells by Transfection with dsRNA. *Cold Spring Harbor Protocols*, *2013*(5), 461–463. https://doi.org/10.1101/pdb.prot074351

Annex 1- Interphase Cell Analysis Pipeline Comments

[1] [Images]
To begin creating your project, use the Images module to compile a list of files and/or folders that you want to analyze. You can also specify a set of rules to include only the desired files in your selected folders.

Pipeline comment: module 1
Images from MetaXpress are loaded here.
With MetaXpress, thumbnails and non TIF files are exported with images of interest in a common folder.
Those are filtered out of the analysis pipeline with a set of rules.

[2] [Metadata]
The Metadata module optionally allows you to extract information describing your images (i.e, metadata) which will be stored along with your measurements. This information can be contained in the file name and/or location, or in an external file.

Pipeline comment: module 2
Images exported from MetaXpress contain plate/experiment, well, site and channel information and thus were extracted with a regular expression string.

[3] [NamesAndTypes]
The NamesAndTypes module allows you to assign a meaningful name to each image by which other modules will refer to it.

Pipeline comment: module 3
Meaningful names were assigned to automatic channel names given by MetaXpress.
To prevent any loss of information, intensity range was determined by image bit-depth.

[4] [Groups]
The Groups module optionally allows you to split your list of images into image subsets (groups) which will be processed independently of each other. Examples of groupings include screening batches, microtiter plates, time-lapse movies, etc.

Pipeline comment: module 4
This module was not used.

[5] [IdentifyPrimaryObjects]
Pipeline comment: module 5
The output from this module will be used in the next module (module 6) to identify cells.
The aim is to identify 1 object/cell as assumed by the next module.

In the case of our images, both interphase and mitotic cells are present.
Interphase cells had 1 nucleus/cell, whereas mitotic cells had several mitotic chromosomes per cell.
However, this pipeline only focuses on interphase cells.
Thus, nucleus staining (Hoechst) images (rawDNA) were used to obtain 1 object/cell.
These objects were named "CellIdentifier" and roughly represent the nucleus for interphase cells.

[6] [IdentifySecondaryObjects]
Pipeline comment: module 6
Secondary objects are identified on the basis of 1 primary object per secondary object.
In other words: "Cell" objects were identified on the basis of 1 "CellIdentifier" per "Cell".
Images from the tubulin staining were used (rawCy5).
"Cell" objects overlapping with image borders were discarded.
"Cell" objects are filtered later in the pipeline in order to only keep interphase cells in the data output (see module 20).

[7] [IdentifyPrimaryObjects]
Pipeline comment: module 7
This module aims at identifying objects corresponding to interphase nuclei.
These objects were named "InterphaseNucleus".

[8] [IdentifyTertiaryObjects]
Pipeline: module 8
"InterphaseCytoplasm" objects, corresponding to cell cytoplasmic areas, were created by removing the previously defined "InterphaseNucleus" object from corresponding "Cell" object.

[9] [MeasureObjectSizeShape]
Pipeline comment: module 9
Multiple measurements of "CellIdentifier" and "InterphaseCytoplasm" objects from module 5 and 8 were made.
A subset of these are used later in the pipeline (see module 10 and 17).

[10] [FilterObjects]
Pipeline comment: module 10
"CellIdentifier" objects were filtered by size in order to minimize objects identified on the basis of an artifact.
These objects were named "FilterCellIdentifier".

[11] [RelateObjects]
Pipeline Comment: module 11
"FilterCellIdentifier" objects were assigned to corresponding "Cell" objects (previously identified) for filtering purposes (see module 20).

[12] [IdentifyPrimaryObjects]
Pipeline comment: module 12
To filter out mitotic cells, "MitoticIdentifier" objects were created.
Those roughly correspond to mitotic chromosomes but are precise enough to help filter out mitotic cells in the following modules.

[13] [RelateObjects]
Pipeline comment: module 13
"MitoticIdentifier" objects were assigned to corresponding "Cell" objects (previously identified) for filtering purposes (see module 20).

[14] [MeasureObjectIntensityDistribution]
Pipeline comment: module 14
Each "Cell" is fractionated into 3 ring-shaped areas.
Measurements for each ring of each "Cell" are taken.
A subset of theses measurements will be used to assess the tubulin staining (rawCy5) distribution across cells and discriminate interphase cells from mitotic cells.

[15] [CalculateMath]
Pipeline comment: module 15
The inner ring's mean tubulin intensity of each cell was divided by the corresponding outer ring's mean tubulin intensity.
This value was named "InnerOnOuter"
If the intensity of cell for tubulin staining is uniform across the cell, this value would be 1.
For an interphase cell, the tubulin staining should be absent from the nucleus which is located in ring 1 and might overlap with ring 2 but not ring 3. Thus, an InnerOnOuter value for an interphase cell should be lower than 1.
For a mitotic cell, there is no nuclear membrane which should allow a more uniform tubulin staining across the cell (from ring 1 to 3) compared to interphase cells. Thus, an InnerOnOuter value for a mitotic cell should be higher than or equal to 1.
This value will be used to discriminate between interphase and mitotic cells (see module 20).

[16] [MeasureObjectIntensity]
Pipeline comment: module 16
Measurement of tubulin staining intensity for "InterphaseCytoplasm" objects.
Data from this module will be used for module 17.

[17] [FilterObjects]
Pipeline comment: module 17
Colchicine treatment give interphase cell a uniform tubulin staining in the cytoplasm.
"InterphaseCytoplasm" objects were filtered using area size and standard deviation value of assigned pixel intensity to avoid misidentification of "Cell" based on artifacts.
These filtered objects were named "FInterphaseCytoplasm" and are used in module 20.

[18] [RelateObjects]
Pipeline comment: module 18
"FInterphaseCytoplasm" objects (Filtered "InterphaseCytoplasm") were assigned to corresponding "Cell" objects for filtering purposes (see module 20).

[19] [RelateObjects]
Pipeline comment: module 19
"InterphaseNucleus" objects were assigned to corresponding "Cell" objects for filtering purposes (see module 20).

[20] [FilterObjects]
Pipeline comment: module 20
"Cell" objects initially identified in module 6 were filtered based on:
- the number "FilterCellIdentifier" object to minimize misidentified "Cell" objects (see module 10),
- the "Cell" object number: a "Cell" overlapping an image border is usually assigned an object number value of 0, to avoid such objects in the analysis, a minimum object number of 1 was set,
- the number of "MitoticIdentifier" object per cell: the more "MitoticIdentifier" a cell has the more likely it is a mitotic cell thus a maximum value of 2 was set based on empirical evidence to filter out mitotic cells (see module 12),
- the InnerOnOuter value to filter out mitotic cells (see module 15),
- the number of "FInterphaseCytoplasm" object to minimize misidentified "Cell" objects (see module 17),
- the number of "InterphaseNucleus" object to minimize misidentified "Cell" objects (see module 7).

[21] [RelateObjects]
Pipeline comment: module 21
"InterphaseNucleus" objects were assigned to corresponding "FilterCell" object for filtering purposes (see module 22).

[22] [FilterObjects]
Pipeline comment: module 22
"InterphaseNucleus" objects were filtered by number of parent "FilterCell" object for analysis purposes.

[23] [RelateObjects]
Pipeline comment: module 23
Filtered interphase cytoplasm ("FInterphaseCytoplasm" objects) were assigned to corresponding "FilterCell" object for filtering purposes (see module 24).

[24] [FilterObjects]
Pipeline comment: 24

Previously filtered interphase cytoplasm ("FInterphaseCytoplasm") were filtered again by number of parent "FilterCell" object for analysis purposes.

[25] [MeasureObjectIntensity]
Pipeline comment: 25
Intensity measurements of Ph staining were made for "FilterInterphaseNucleus" objects, "FilterInterphaseCytoplasm" and "FilterCell" objects for analysis purposes.

[26] [CalculateMath]
Pipeline comment: module 26
Median Ph staining pixel intensity in ''FilterInterphaseNucleus'' objects was divided by the median Ph staining pixel intensity in ''FilterInterphaseCytoplasm'' objects for analysis purposes.

[27] [ExportToSpreadsheet]
Pipeline comment: module 27
This module was used to export values of interest for analysis in the form of CSV files.

Annex 2- Mitotic Cell Analysis Pipeline Comments

[1] [Images]
To begin creating your project, use the Images module to compile a list of files and/or folders that you want to analyze. You can also specify a set of rules to include only the desired files in your selected folders.

Pipeline comment: module 1
Images from MetaXpress are loaded here.
With MetaXpress, thumbnails and non TIF files are exported with images of interest in a common folder.
Those are filtered out of the analysis pipeline with a set of rules

[2] [Metadata]
The Metadata module optionally allows you to extract information describing your images (i.e, metadata) which will be stored along with your measurements. This information can be contained in the file name and/or location, or in an external file.

Pipeline comment: module 2
Images exported from MetaXpress contain plate/experiment, well, site and channel information and thus were extracted with a regular expression string.

[3] [NamesAndTypes]
The NamesAndTypes module allows you to assign a meaningful name to each image by which other modules will refer to it.

Pipeline comment: module 3
Meaningful names were assigned to automatic channel names given by MetaXpress.
To avoid any loss of information, intensity range was determined by image bit-depth.

[4] [Groups]
The Groups module optionally allows you to split your list of images into image subsets (groups) which will be processed independently of each other. Examples of groupings include screening batches, microtiter plates, time-lapse movies, etc.

Pipeline comment: module 4
This module was not used.

[5] [IdentifyPrimaryObjects]
Pipeline comment: module 5
The output from this module will be used in the next module (module 6) to identify cells.
The aim is to identify 1 object/cell as assumed by the next module.

In the case of our images, both interphase and mitotic cells are present.
Interphase cells had 1 nucleus/cell, whereas mitotic cells had several mitotic chromosomes per cell or 1 set of mitotic chromosomes per cell.
Each mitotic chromosome from the same set would be closer to each other than 2 mitotic chromosomes from 2 different sets. Thus, manipulating typical diameter of objects to find in the image was enough to identify one single object (a chromosome set) per mitotic cell, which this pipeline focuses on.
Nucleus staining (Hoechst) images (rawDNA) were used to obtain 1 object/cell.
These objects were named "CellIdentifier" and roughly represent the nucleus for interphase cells and the chromosome set for mitotic cells.
Interphase cells are filtered out later in the pipeline (see module 20).

[6] [IdentifySecondaryObjects]
Pipeline comment: module 6
Secondary objects are identified on the basis of 1 primary object per secondary object.
In other words: "Cell" objects were identified on the basis of 1 "CellIdentifier" per "Cell".
Images from the tubulin staining were used (rawCy5).
"Cell" objects overlapping with image borders were discarded.
"Cell" objects are filtered later in the pipeline (see module 20).

[7] [IdentifyPrimaryObjects]
Pipeline comment: module 7
To isolate mitotic cells, "MitoticIdentifier" objects were created.
Those roughly correspond to mitotic chromosomes but are precise enough to help isolate mitotic cells in the following modules.

[8] [IdentifyPrimaryObjects]
Pipeline comment: module 8
This module aims at identifying objects corresponding to mitotic chromatin.
These objects were named "MitoticChromatin".

[9] [RelateObjects]
Pipeline comment: module 9
"MitoticChromatin" objects were assigned to corresponding "Cell" objects (previously identified) for merging purposes (see module 10).

[10] [SplitOrMergeObjects]
Pipeline comment: module 10
In order to have a set of chromosomes ("Mitotic chromatin" objects) as a unified object (for example: to calculate the median pixel intensity of the chromatin area of a cell), "MitoticChromatin" objects were merged as a single object on the basis of their corresponding parent "Cell" object.
These objects were named "RelabeledMitoticChromatin".

[11] [IdentifyTertiaryObjects]
Pipeline comment: module 11
"MitoticCytoplasm" objects, corresponding to cell cytoplasmic area, were created by removing the previously defined "RelabeledMitoticChromatin" object from corresponding "Cell" object.

[12] [RelateObjects]
Pipeline comment: module 12
"CellIdentifier" objects were assigned to corresponding "Cell" objects (previously identified) for filtering purposes (see module 14).

[13] [MeasureObjectSizeShape]
Pipeline comment: module 13
Multiple measurements of "CellIdentifier" objects from module 5 were made.
A subset of these are used later in the pipeline (see module 14).

[14] [FilterObjects]
Pipeline comment: module 14
"CellIdentifier" objects were filtered by size to minimize objects identified on the basis of an artifact.
The number of parent "Cell" object was also used in order to, later in module 20, exclude cells overlapping with image borders respectively.
These objects were named "FilterCellIdentifier".

[15] [RelateObjects]
Pipeline comment: module 15
"FilterCellIdentifier" objects were assigned to corresponding "Cell" objects (previously identified) for filtering purposes (see module 20).

[16] [RelateObjects]
Pipeline comment: module 16
"MitoticIdentifier" objects were assigned to corresponding "Cell" objects (previously identified) for filtering purposes (see module 20).

[17] [MeasureObjectIntensityDistribution]
Pipeline comment: module 17
Each "Cell" is fractionated into 3 ring-shaped areas.
Measurements for each ring of each "Cell" are taken.
A subset of theses measurements will be used to assess the tubulin staining (rawCy5) distribution across cells and discriminate interphase cells from mitotic cells.

[18] [CalculateMath]
Pipeline comment: module 18
The inner ring's mean tubulin intensity of each cell was divided by the corresponding outer ring's mean tubulin intensity.

This value was named "InnerOnOuter"

If the intensity of cell for tubulin staining is uniform across the cell, this value would be 1.

For an interphase cell, the tubulin staining should be absent from the nucleus which is located in ring 1 and might overlap with ring 2 but not ring 3. Thus, an InnerOnOuter value for an interphase cell should be lower than 1.

For a mitotic cell, there is no nuclear membrane which should allow a more uniform tubulin staining across the cell (from ring 1 to 3) compared to interphase cells. Thus, an InnerOnOuter value for a mitotic cell should be higher than or equal to 1.

This value will be used to discriminate between interphase and mitotic cells (see module 20).

[19] [MeasureObjectIntensity]

Pipeline comment: module 19

Measurements of tubulin staining intensity (rawCy5) for "Cell" objects were made.

Data from this module will be used for module 20.

[20] [FilterObjects]

Pipeline comment: module 20

"Cell" objects initially identified in module 6 were filtered based on:

- the number of "FilterCellIdentifier" object to minimize misidentified "Cell" objects (see module 14),
- the number of "MitoticIdentifier" object per "Cell": the more "MitoticIdentifier" a "Cell" has the more likely it is a mitotic cell thus a minimum value of 3 was set based on empirical evidence to filter out interphase cells (see module 7),
- the InnerOnOuter value to filter out interphase cells (see module 18),
- the standard deviation of pixel intensity for tubulin staining (rawCy5): mitotic cells should have a uniform tubulin staining across the cell (given the absence of nuclear membrane and the presence of colchicine) (see module 19).

These filtered objects were named "FilterCell".

[21] [RelateObjects]

Pipeline comment: module 21:

"MitoticCytoplasm" objects were assigned to corresponding "FilterCell" objects for filtering purposes (see module 22).

[22] [FilterObjects]

Pipeline comment: module 22

"MitoticCytoplasm" were filtered by number of parent "FilterCell" object for analysis purposes.

These filtered objects were named "FilterMitoticCytoplasm".

[23] [RelateObjects]

Pipeline comment: module 23

"RelabeledMitoticChromatin" objects were assigned to corresponding "FilterCell" object for filtering purposes (see module 24).

[24] [FilterObjects]
Pipeline comment: module 24
"RelabeledMitoticChromatin" objects were filtered by number of parent "FilterCell" object for analysis purposes.
These filtered objects were named "FilterMitoticChromatin".

[25] [MeasureObjectIntensity]
Pipeline comment: module 25
Intensity measurements of Ph staining were made for "FilterMitoticChromatin" objects, "FilterMitoticCytoplasm" and "FilterCell" objects for analysis purposes.

[26] [CalculateMath]
Pipeline comment: module 26
Median Ph staining pixel intensity in "FilterMitoticChromatin" objects was divided by the median Ph staining pixel intensity in "FilterMitoticCytoplasm" objects for analysis purposes.

[27] [MeasureImageAreaOccupied]
Pipeline comment: module 27
Data output form this module was not used for the analysis.

[28] [ExportToSpreadsheet]
Pipeline comment: module 28
This module was used to export values of interest for analysis in the form of CSV files.

Annex 3- Reagents

Reagent	Company/Source	Reference	Concentration
2-Propanol (Certified ACS)	Fisher Chemical	A4164	≥99.5%
Acetic Acid, Glacial (CH3COOH)	Fisher Scientific Company	351271212	≥99.7%
Acrylamide/Bis-acrylamide, 40% Solution 37.5:1	BioShop	ACR005	0.4
Agarose A	Bio Basic	D0012	-
Albumin, bovine serum (BSA)	BioShop	ALB001	≥98%
Ammonium persulfate (APS)	Sigma-Aldrich	A3678	≥98%
Bacto™ Peptone	BD Biosciences	211677	-
Beta-Mercaptoethanol	Sigma-Aldrich	M6250	≥99%
BioTrace® NT Nitrocellulose Transfer Membranes	Canadawide Scientific	615040	-
Bromophenol Blue sodium salt	Sigma-Aldrich	B8026	-
Colchicine	Sigma-Aldrich	C3915	≥95%
Corning® 96 Well CellBIND® Microplates	Corning	3340	-
DMSO	Sigma-Aldrich	D2650	≥99.7%
dNTP	New England BioLabs	N0447	10mM each
Drosophila RNAi Library	Open Biosystems, gift from the Lécuyer lab	RDM4339	-
DTT	BioShop	DTT001	≥99.5%
EDTA, Disodium Dihydrate, Reagent Grade	BioShop	EDT002	≥99%
Ethidium bromide solution	Sigma-Aldrich	E1510	10 mg/ml
Filtropur V100, 1000ml, 0.2µm	Sarstedt	833942001	-
Formaldehyde	Sigma-Aldrich	F1635	0.37
Gibco™ Fetal Bovine Serum, Qualified, Heat Inactivated	Gibco™	16140089	-
Glycerol, Biotechnology Grade	BioShop	GLY001	≥99.7%
Glycine, Reagent Grade	BioShop	GLN002	≥99%
Goat anti-Mouse IgG (H+L) Cross-Adsorbed Secondary Antibody, Alexa Fluor 680	Invitrogen	A21057	2 mg/ml
Goat anti-Mouse IgG (H+L) Highly Cross-Adsorbed Secondary Antibody, Alexa Fluor Plus 647	Invitrogen	A32728	2 mg/mL
Goat anti-Rabbit IgG (H+L) Cross-Adsorbed Secondary Antibody, Alexa Fluor 488	Invitrogen	A11008	2 mg/ml
Goat anti-Rabbit IgG (H+L) Cross-Adsorbed Secondary Antibody, Alexa Fluor 680	Invitrogen	A21076	2 mg/ml
Grade 3MM Chr Cellulose Chromatography Papers	GE Healthcare Life Sciences	3030917	-
Hoechst	Sigma-Aldrich	B1155	≥98%
Methanol (MeOH, CH3OH)	Sigma-Aldrich	179337	≥99.8%
Methanol (MeOH, CH3OH)	BioShop	MET302	≥99.8%

MgCl2	Invitrogen	18038042	50mM
Monoclonal mouse anti-α-tubulin, clone B-5-1-2	Sigma-Aldrich	T5168	-
NucleoSpin Gel and PCR Clean-up	Macherey-Nagel	740609	-
PCR Buffer	Invitrogen	18038042	10X
Ph75I	Homemade antibody	-	-
Potassium bicarbonate (KHCO3)	Sigma-Aldrich	P7682	-
Potassium Chloride (KCl)	BioShop	POC308	≥99%
Potassium phosphate monobasic (KH2PO4)	American Bioanalytical	AB01660	≥99%
Precision Plus Protein™ Standard	Bio-Rad	1610394	-
RNAPol Reaction Buffer	New England BioLabs	M0251	10X
RNAPol Reaction Buffer	New England BioLabs	M0378S	10X
Rnase inhibitor murine	New England BioLabs	M0314	40,000 U/ml
rNTP	New England BioLabs	N0466	25mM each
S2R+ Cells	Gift from the Lécuyer lab	-	-
Select Yeast Extract	Sigma-Aldrich	Y1000	-
Shields and Sang M3 Insect Medium	Sigma-Aldrich	S8398	-
Sodium Azide (NaN3)	Sigma-Aldrich	S2002	≥99.5%
Sodium Chloride (NaCl)	BioShop	SOD002	≥99%
Sodium citrate (Na3C6H5O7)	BioShop	CIT001	≥99.5%
Sodium Dodecyl Sulfate (SDS)	BioShop	SDS003	>99%
Sodium phosphate dibasic heptahydrate (Na2HPO4-7H2O)	Sigma-Aldrich	S9390	≥98%
T3 RNA polymerase	New England BioLabs	M0378S	50,000 U/ml
T7 RNA polymerase	New England BioLabs	M0251	50,000 U/ml
T7/T3 Oligo primer	Integrated DNA Technologies	-	-
Taq Enzyme	Invitrogen	18038042	5U/ul
TEMED, Electrophoresis Grade	BioShop	TEM001	≥99%
TRIS (Base), Ultra Pure	BioShop	TRS001	≥99.9%
Triton™ X-100	Sigma-Aldrich	T8787	-
TWEEN® 20	BioShop	TWN508	≥97%
UltraPure™ DNase/RNase-Free Distilled Water	Invitrogen	10977-015	-
Xylene Cyanol FF	Sigma-Aldrich	X4126	-